

# 具有宽占空比范围的 LM5146 100V 同步降压直流/直流控制器

## 1 特性

- 提供功能安全型
  - 可帮助进行功能安全系统设计的文档
- 多功能同步降压直流/直流控制器
  - 宽输入电压范围为 5.5V 至 100V
  - 150°C 最大结温
  - 具有  $\pm 1\%$  反馈精度的 0.8V 基准
  - 可调输出电压范围为 0.8V 至 60V
  - 40ns  $t_{ON(min)}$ , 可实现高  $V_{IN}/V_{OUT}$  比
  - 140ns  $t_{OFF(min)}$ , 可实现低压降
  - 无损  $R_{DS(on)}$  或分流电流感应
  - 针对 CISPR 11 和 CISPR 32 B 类 EMI 要求进行了优化
- 开关频率范围为 100kHz 至 1MHz
  - 同步输入和同步输出功能
  - 可选二极管仿真或 FPWM
- 适用于标准  $V_{TH}$  MOSFET 的 7.5V 栅极驱动器
  - 14ns 自适应死区时间控制
  - 2.3A 拉电流和 3.5A 灌电流能力
- 快速线路和负载瞬态响应
  - 具有线路前馈的电压模式控制
  - 高增益带宽误差放大器
- 固有保护特性, 可实现稳健设计
  - 可调节输出电压软启动
  - 断续模式过流保护
  - 具有迟滞功能的输入 UVLO
  - VCC 和栅极驱动 UVLO 保护
  - 精密使能输入和漏极开路 PGOOD 指示器 (用于时序和控制)
  - 具有迟滞功能的热关断保护
- 具有可湿性侧面的 20 引脚 VQFN 封装
- 使用 LM5146 并借助 WEBENCH® Power Designer 创建定制设计方案

## 2 应用

- 无线基础设施、云计算
- 工业电机驱动、测试和测量
- 个人交通工具：电动自行车
- 资产跟踪和机群管理系统
- 非隔离式 PoE、IP 摄像头
- 反相降压/升压稳压器

## 3 说明

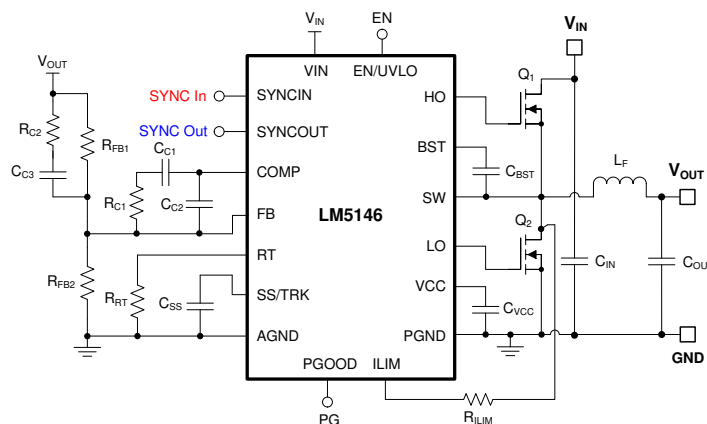
LM5146 100V 同步降压控制器旨在对高输入电压源或会发生高电压瞬变的输入电源轨进行电压调节, 从而尽可能地减少对外部浪涌抑制组件的需求。40ns 的高侧开关超短导通时间有助于获得较大的降压比, 支持从 48V 标称输入到低电压轨的直接降压转换, 从而降低系统的复杂性并减少解决方案成本。LM5146 在输入电压突降至 5.5V 时, 仍能根据需要以接近 100% 的占空比继续工作, 因此非常适用于高性能工业控制、机器人、数据通信和射频应用。

强制 PWM (FPWM) 模式运行可以消除开关频率变化从而尽可能地降低 EMI, 而用户可选的二极管仿真功能则可以降低轻负载条件下的电流消耗。高达 1MHz 的可调开关频率可同步至外部时钟源, 从而消除噪声敏感应用中的拍频。

### 器件信息

器件型号	封装 <sup>(1)</sup>	封装尺寸 (标称值)
LM5146	VQFN (20)	4.50mm × 3.50mm

(1) 如需了解所有可用封装, 请参阅数据表末尾的可订购产品附录。



典型应用电路和能效,  $V_{OUT} = 12V$ ,  $F_{SW} = 400kHz$

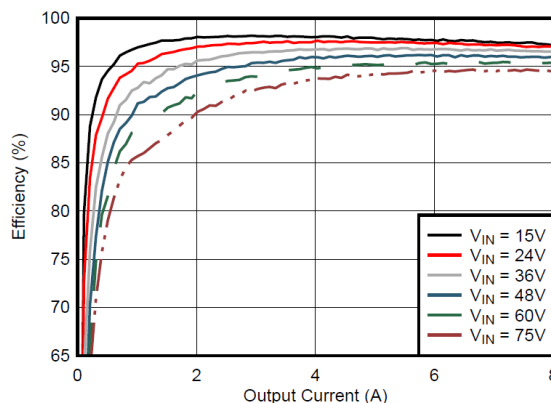


## Table of Contents

<b>1 特性</b> .....	<b>1</b>	8.4 Device Functional Modes.....	<b>25</b>
<b>2 应用</b> .....	<b>1</b>	<b>9 Application and Implementation</b> .....	<b>27</b>
<b>3 说明</b> .....	<b>1</b>	9.1 Application Information.....	27
<b>4 Revision History</b> .....	<b>2</b>	9.2 Typical Applications.....	36
<b>5 说明 (续)</b> .....	<b>3</b>	<b>10 Power Supply Recommendations</b> .....	<b>46</b>
<b>6 Pin Configuration and Functions</b> .....	<b>4</b>	<b>11 Layout</b> .....	<b>47</b>
6.1 Wettable Flanks.....	5	11.1 Layout Guidelines.....	47
<b>7 Specifications</b> .....	<b>6</b>	11.2 Layout Example.....	50
7.1 Absolute Maximum Ratings .....	6	<b>12 Device and Documentation Support</b> .....	<b>51</b>
7.2 ESD Ratings .....	6	12.1 Device Support.....	51
7.3 Recommended Operating Conditions .....	7	12.2 Documentation Support.....	52
7.4 Thermal Information .....	7	12.3 接收文档更新通知.....	52
7.5 Electrical Characteristics .....	8	12.4 支持资源.....	52
7.6 Switching Characteristics .....	10	12.5 Trademarks.....	53
7.7 Typical Characteristics.....	11	12.6 Electrostatic Discharge Caution.....	53
<b>8 Detailed Description</b> .....	<b>16</b>	12.7 Glossary.....	53
8.1 Overview.....	16	<b>13 Mechanical, Packaging, and Orderable Information</b> .....	<b>54</b>
8.2 Functional Block Diagram.....	16		
8.3 Feature Description.....	17		

## 4 Revision History

注：以前版本的页码可能与当前版本的页码不同

Changes from Revision * (June 2021) to Revision A (June 2021)	Page
• 从标题中删除了“6V 至”.....	1
• 更新了功能安全链接.....	1
• 首次发布量产数据数据表.....	1

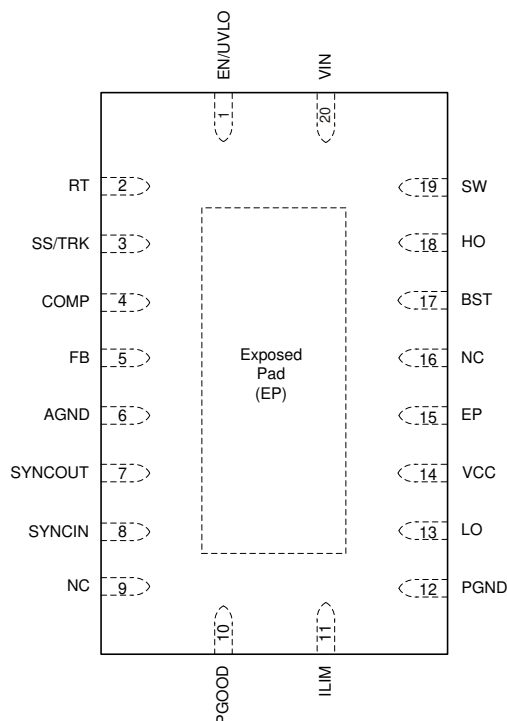
## 5 说明 (续)

具有线路前馈的 LM5146 电压模式控制器使用适用于标准阈值 MOSFET 的可靠的 7.5V 栅极驱动器驱动外部高侧和低侧 N 沟道电源开关。具有 2.3A 拉电流和 3.5A 灌电流能力的自适应定时栅极驱动器可在开关切换期间尽可能地减少体二极管导通，从而降低在以高输入电压和高频率驱动 MOSFET 时的开关损耗并提高热性能。LM5146 可从开关稳压器的输出或其他可用的源供电，从而进一步提高效率。

180° 异相时钟输出（相对于内部振荡器的同步输出）非常适用于级联或多通道电源，可降低输入电容器纹波电流和 EMI 滤波器尺寸。LM5146 的附加功能包括可配置软启动、用于故障报告和输出监控的漏极开路电源正常监视器、单调启动至预偏置负载、集成 VCC 偏置电源稳压器和自举二极管、外部电源跟踪、针对可调线路欠压锁定 (UVLO) 且具有迟滞的精密使能输入、断续模式过载保护和带自动恢复的热关断保护。

LM5146 控制器采用 4.5mm × 3.5mm 热增强型 20 引脚 VQFN 封装，并为高电压引脚和可湿性侧面留出额外空间，以便对焊锡接点填角焊缝进行光学检测。

## 6 Pin Configuration and Functions



Connect Exposed Pad on bottom to AGND and PGND on the PCB.

**图 6-1. 20-Pin VQFN With Wettable Flanks in RGY Package (Top View)**

**表 6-1. Pin Functions**

PIN		I/O <sup>(1)</sup>	DESCRIPTION
NO.	NAME		
1	EN/UVLO	I	Enable input and undervoltage lockout programming pin. If the EN/UVLO voltage is below 0.4 V, the controller is in shutdown mode with all functions disabled. If the EN/UVLO voltage is greater than 0.4 V and less than 1.2 V, the regulator is in standby mode with the VCC regulator operational, the SS pin grounded, and no switching at the HO and LO outputs. If the EN/UVLO voltage is above 1.2 V, the SS/TRK voltage can ramp and pulse-width modulated gate-drive signals are delivered to the HO and LO pins. A 10- $\mu$ A current source is enabled when EN/UVLO exceeds 1.2 V and flows through the external UVLO resistor divider to provide hysteresis. Hysteresis can be adjusted by varying the resistance of the external divider.
2	RT	I	Oscillator frequency adjust pin. The internal oscillator is programmed with a single resistor between RT and the AGND. TI recommends a maximum oscillator frequency of 1 MHz. An RT pin resistor is required even when using the SYNCIN pin to synchronize to an external clock.
3	SS/TRK	I	Soft start and voltage-tracking pin. An external capacitor and an internal 10- $\mu$ A current source set the ramp rate of the error amplifier reference during start-up. When the SS/TRK pin voltage is less than 0.8 V, the SS/TRK voltage controls the noninverting input of the error amp. When the SS/TRK voltage exceeds 0.8 V, the amplifier is controlled by the internal 0.8-V reference. SS/TRK is discharged to ground during standby and fault conditions. After start-up, the SS/TRK voltage is clamped 115 mV above the FB pin voltage. If FB falls due to a load fault, SS/TRK is discharged to a level 115 mV above FB to provide a controlled recovery when the fault is removed. Voltage tracking can be implemented by connecting a low impedance reference between 0 V and 0.8 V to the SS/TRK pin. The 10- $\mu$ A SS/TRK charging current flows into the reference and produces a voltage error if the impedance is not low. Connect a minimum capacitance from SS/TRK to AGND of 2.2 nF.
4	COMP	O	Low impedance output of the internal error amplifier. Connect the loop compensation network between the COMP pin and the FB pin.
5	FB	I	Feedback connection to the inverting input of the internal error amplifier. A resistor divider from the output to this pin sets the output voltage level. The regulation threshold at the FB pin is nominally 0.8 V.
6	AGND	P	Analog ground. Return for the internal 0.8-V voltage reference and analog circuits.

**表 6-1. Pin Functions (continued)**

PIN		I/O <sup>(1)</sup>	DESCRIPTION
NO.	NAME		
7	SYNCOUT	O	Synchronization output. Logic output that provides a clock signal that is 180° out-of-phase with the high-side FET gate drive. Connect SYNCOUT of the master LM5146 to the SYNCIN pin of a second LM5146 to operate two controllers at the same frequency with 180° interleaved high-side FET switch turn-on transitions. Note that the SYNCOUT pin does not provide 180° interleaving when the controller is operating from an external clock that is different from the free-running frequency set by the RT resistor.
8	SYNCIN	I	Dual function pin to provide an optional clock input and enable diode emulation by the low-side MOSFET. Connecting a clock signal to the SYNCIN pin synchronizes switching to the external clock. Diode emulation by the low-side MOSFET is disabled when the controller is synchronized to an external clock, and negative inductor current can flow in the low-side MOSFET with light loads. A continuous logic low state at the SYNCIN pin enables diode emulation to prevent reverse current flow in the inductor. Diode emulation results in discontinuous mode operation (DCM) at light loads, which improves efficiency. A logic high state at the SYNCIN pin disables diode emulation, producing forced-PWM (FPWM) operation. During soft start when SYNCIN is high or a clock signal is present, the LM5146 operates in diode emulation mode until the output is in regulation, then gradually increases the SW zero-cross threshold, resulting in a gradual transition from DCM to FPWM.
9	NC	—	No electrical connection
10	PGOOD	O	Power-good indicator. This pin is an open-drain output. A high state indicates that the voltage at the FB pin is within a specified tolerance window centered at 0.8 V.
11	ILIM	I	Current limit adjust and current sense comparator input. A current sourced from the ILIM pin through an external resistor programs the threshold voltage for valley current limiting. The opposite end of the threshold adjust resistor can be connected to either the drain of the low-side MOSFET for $R_{DS(on)}$ sensing or to a current sense resistor connected to the source of the low-side FET.
12	PGND	P	Power ground return pin for the low-side MOSFET gate driver. Connect directly to the source of the low-side MOSFET or the ground side of a shunt resistor.
13	LO	P	Low-side MOSFET gate drive output. Connect to the gate of the low-side synchronous rectifier FET through a short, low inductance path.
14	VCC	O	Output of the 7.5-V bias regulator. Locally decouple to PGND using a low-ESR/ESL capacitor located as close as possible to the controller. Controller bias can be supplied from an external supply that is greater than the internal VCC regulation voltage. Use caution when applying external bias to ensure that the applied voltage is not greater than the minimum $V_{IN}$ voltage and does not exceed the VCC pin maximum operating rating. See the <a href="#">Recommended Operation Conditions</a> .
15	EP	—	Pin is internally connected to exposed pad of the package. Connect to GND at the exposed pad to improve heat spreading.
16	NC	—	No electrical connection
17	BST	O	Bootstrap supply for the high-side gate driver. Connect to the bootstrap (boot) capacitor. The bootstrap capacitor supplies current to the high-side FET gate and must be placed as close as possible to controller. If an external bootstrap diode is used to reduce the time required to charge the bootstrap capacitor, connect the cathode of the diode to the BST pin and anode to VCC.
18	HO	P	High-side MOSFET gate drive output. Connect to the gate of the high-side MOSFET through a short, low inductance path.
19	SW	P	Switching node of the buck controller. Connect to the bootstrap capacitor, the source terminal of the high-side MOSFET, and the drain terminal of the low-side MOSFET using short, low inductance paths.
20	VIN	P	Supply voltage input for the VCC LDO regulator
—	EP	—	Exposed pad of the package. Electrically isolated. Solder to the system ground plane to reduce thermal resistance.

(1) P = Power, G = Ground, I = Input, O = Output

## 6.1 Wettable Flanks

100% automated visual inspection (AVI) post-assembly is typically required to meet requirements for high reliability and robustness. Standard quad-flat no-lead (VQFN) packages do not have solderable or exposed pins and terminals that are easily viewed. Therefore, it is difficult to visually determine whether or not the package is successfully soldered onto the printed-circuit board (PCB). The wettable-flank process was developed to resolve the issue of side-lead wetting of leadless packaging. The LM5146 is assembled using a 20-pin VQFN package with wettable flanks to provide a visual indicator of solderability, which reduces the inspection time and manufacturing costs.

## 7 Specifications

### 7.1 Absolute Maximum Ratings

Over the recommended operating junction temperature of  $-40^{\circ}\text{C}$  to  $+150^{\circ}\text{C}$  (unless otherwise noted).<sup>(1)</sup>

		MIN	MAX	UNIT
Input voltage	VIN	-0.3	100	V
	SW	-1	100	
	SW (20-ns transient)	-5	100	
	ILIM	-1	100	
	EN/UVLO	-0.3	100	
	VCC	-0.3	14	
	FB, COMP, SS/TRK, RT	-0.3	6	
	SYNCIN	-0.3	14	
Output voltage	BST	-0.3	110	V
	BST to VCC		100	
	BST to SW	-0.3	14	
	VCC to BST (20-ns transient)		7	
	LO (20-ns transient)	-3		
	PGOOD	-0.3	14	
Operating junction temperature, $T_J$			150	$^{\circ}\text{C}$
Storage temperature, $T_{stg}$		-55	150	$^{\circ}\text{C}$

- (1) Operation outside the *Absolute Maximum Ratings* may cause permanent device damage. *Absolute Maximum Ratings* do not imply functional operation of the device at these or any other conditions beyond those listed under *Recommended Operating Conditions*. If used outside the *Recommended Operating Conditions* but within the *Absolute Maximum Ratings*, the device may not be fully functional, and this may affect device reliability, functionality, performance, and shorten the device lifetime.

### 7.2 ESD Ratings

			MIN	MAX	UNIT
$V_{(ESD)}$	Electrostatic discharge	Human body model (HBM), per ANSI/ESDA/JEDEC JS-001, all pins <sup>(1)</sup>	-2000	2000	V
		Charged device model (CDM), per JEDEC specification JESD22-C101, all pins <sup>(2)</sup>	-500	500	

- (1) JEDEC document JEP155 states that 500-V HBM allows safe manufacturing with a standard ESD control process.  
 (2) JEDEC document JEP157 states that 250-V CDM allows safe manufacturing with a standard ESD control process.

## 7.3 Recommended Operating Conditions

Over the recommended operating junction temperature range of  $-40^{\circ}\text{C}$  to  $150^{\circ}\text{C}$  (unless otherwise noted). <sup>(1)</sup>

		MIN	NOM	MAX	UNIT
Input voltage	VIN	5.5		100	V
	SW	-1		100	V
	ILIM	0		100	V
	External VCC bias rail	8		13	V
	EN/UVLO	-0.3		100	V
Output voltage	BST	-0.3		110	V
	BST to VCC			100	V
	BST to SW	5		13	V
	PGOOD			13	V
I <sub>SINK</sub> , I <sub>SRC</sub>	Sink/source current SYNCOUT	-1		1	mA
I <sub>SINK</sub> , I <sub>SRC</sub>	Sink/source current PGOOD			2	mA
T <sub>J</sub>	Operating junction temperature	-40		150	$^{\circ}\text{C}$

- (1) [Recommended Operation Conditions](#) are conditions under which the device is intended to be functional. For specifications and test conditions, see [Electrical Characteristics](#).

## 7.4 Thermal Information

THERMAL METRIC <sup>(1)</sup>		LM5146	UNIT
		RGY (VQFN)	
		20 PINS	
R <sub>θJA</sub>	Junction-to-ambient thermal resistance	36.8	$^{\circ}\text{C}/\text{W}$
R <sub>θJC(top)</sub>	Junction-to-case (top) thermal resistance	28	$^{\circ}\text{C}/\text{W}$
R <sub>θJB</sub>	Junction-to-board thermal resistance	11.8	$^{\circ}\text{C}/\text{W}$
ψ <sub>JT</sub>	Junction-to-top characterization parameter	0.4	$^{\circ}\text{C}/\text{W}$
ψ <sub>JB</sub>	Junction-to-board characterization parameter	11.7	$^{\circ}\text{C}/\text{W}$
R <sub>θJC(bot)</sub>	Junction-to-case (bottom) thermal resistance	2.1	$^{\circ}\text{C}/\text{W}$

- (1) For more information about traditional and new thermal metrics, see the [Semiconductor and IC Package Thermal Metrics](#)

## 7.5 Electrical Characteristics

Typical values correspond to  $T_J = 25^\circ\text{C}$ . Minimum and maximum limits apply over the  $-40^\circ\text{C}$  to  $150^\circ\text{C}$  junction temperature range unless otherwise stated.  $V_{\text{VIN}} = 48\text{ V}$ ,  $V_{\text{EN/UVLO}} = 1.5\text{ V}$ ,  $R_{\text{RT}} = 25\text{ k}\Omega$  unless otherwise stated. (1) (2)

PARAMETER		TEST CONDITIONS	MIN	TYP	MAX	UNIT
<b>INPUT SUPPLY</b>						
$V_{\text{IN}}$	Operating input voltage range	$I_{\text{VCC}} \leq 10\text{ mA}$ at $V_{\text{IN}} = 5.5\text{ V}$	5.5		100	V
$I_{\text{Q-RUN}}$	Operating input current, not switching	$V_{\text{EN/UVLO}} = 1.5\text{ V}$ , $V_{\text{SS/TRK}} = 0\text{ V}$		1.8	2.1	mA
$I_{\text{Q-STBY}}$	Standby input current	$V_{\text{EN/UVLO}} = 1\text{ V}$		1.75	2	mA
$I_{\text{Q-SHDN}}$	Shutdown input current	$V_{\text{EN/UVLO}} = 0\text{ V}$ , $V_{\text{VCC}} < 1\text{ V}$		13.5	30	$\mu\text{A}$
<b>VCC REGULATOR</b>						
$V_{\text{VCC}}$	VCC regulation voltage	$V_{\text{SS/TRK}} = 0\text{ V}$ , $9\text{ V} \leq V_{\text{VIN}} \leq 100\text{ V}$ , $0\text{ mA} \leq I_{\text{VCC}} \leq 20\text{ mA}$	7.3	7.5	7.7	V
$V_{\text{VCC-LDO}}$	VIN to VCC dropout voltage	$V_{\text{VIN}} = 6\text{ V}$ , $V_{\text{SS/TRK}} = 0\text{ V}$ , $I_{\text{VCC}} = 20\text{ mA}$		0.25	0.72	V
$I_{\text{SC-LDO}}$	VCC short-circuit current	$V_{\text{SS/TRK}} = 0\text{ V}$ , $V_{\text{VCC}} = 0\text{ V}$	40	50	70	mA
$V_{\text{VCC-UV}}$	VCC undervoltage threshold	$V_{\text{VCC}}$ rising	4.8	4.93	5.2	V
$V_{\text{VCC-UVH}}$	VCC undervoltage hysteresis	Rising threshold – falling threshold		0.26		V
$V_{\text{VCC-EXT}}$	Minimum external bias voltage	Voltage required to disable VCC regulator	8			V
$I_{\text{VCC}}$	External VCC input current, not switching	$V_{\text{SS/TRK}} = 0\text{ V}$ , $V_{\text{VCC}} = 13\text{ V}$			2.3	mA
<b>ENABLE AND INPUT UVLO</b>						
$V_{\text{SHDN}}$	Shutdown to standby threshold	$V_{\text{EN/UVLO}}$ rising		0.42		V
$V_{\text{SHDN-HYS}}$	Shutdown threshold hysteresis	EN/UVLO Rising threshold – falling threshold		50		mV
$V_{\text{EN}}$	Standby to operating threshold	$V_{\text{EN/UVLO}}$ rising	1.164	1.2	1.236	V
$I_{\text{EN-HYS}}$	Standby to operating hysteresis current	$V_{\text{EN/UVLO}} = 1.5\text{ V}$	9	10	11	$\mu\text{A}$
<b>ERROR AMPLIFIER</b>						
$V_{\text{REF}}$	FB reference Voltage	FB connected to COMP	792	800	808	mV
$I_{\text{FB-BIAS1}}$	FB input bias current	$V_{\text{FB}} = 0.8\text{ V}$ , $-40^\circ\text{C} \leq T_J \leq 125^\circ\text{C}$	-0.1		0.1	$\mu\text{A}$
$I_{\text{FB-BIAS2}}$	FB input bias current	$V_{\text{FB}} = 0.8\text{ V}$ , $-40^\circ\text{C} \leq T_J \leq 150^\circ\text{C}$	-0.2		0.2	$\mu\text{A}$
$V_{\text{COMP-OH}}$	COMP output high voltage	$V_{\text{FB}} = 0\text{ V}$ , COMP sourcing 1 mA		5		V
$V_{\text{COMP-OL}}$	COMP output low voltage	COMP sinking 1 mA			0.3	V
AVOL	DC gain			94		dB
GBW	Unity gain bandwidth			6.5		MHz
<b>SOFT-START and VOLTAGE TRACKING</b>						
$I_{\text{SS}}$	SS/TRK capacitor charging current	$V_{\text{SS/TRK}} = 0\text{ V}$	8.5	10	12	$\mu\text{A}$
$R_{\text{SS}}$	SS/TRK discharge FET resistance	$V_{\text{EN/UVLO}} = 1\text{ V}$ , $V_{\text{SS/TRK}} = 0.1\text{ V}$		11		$\Omega$
$V_{\text{SS-FB}}$	SS/TRK to FB offset		-15	0	15	mV
$V_{\text{SS-CLAMP}}$	SS/TRK clamp voltage	$V_{\text{SS/TRK}} - V_{\text{FB}}$ , $V_{\text{FB}} = 0.8\text{ V}$		115		mV
<b>POWER GOOD INDICATOR</b>						
$\text{PG}_{\text{UTH}}$	FB upper threshold for PGOOD high to low	% of $V_{\text{REF}}$ , $V_{\text{FB}}$ rising	106%	108%	110%	
$\text{PG}_{\text{LTH}}$	FB lower threshold for PGOOD high to low	% of $V_{\text{REF}}$ , $V_{\text{FB}}$ falling	90%	92%	94%	
$\text{PG}_{\text{HYS\_U}}$	PGOOD upper threshold hysteresis	% of $V_{\text{REF}}$		3%		
$\text{PG}_{\text{HYS\_L}}$	PGOOD lower threshold hysteresis	% of $V_{\text{REF}}$		2%		
$T_{\text{PG-RISE}}$	PGOOD rising filter	FB to PGOOD rising edge		25%		$\mu\text{s}$
$T_{\text{PG-FALL}}$	PGOOD falling filter	FB to PGOOD falling edge		25%		$\mu\text{s}$
$V_{\text{PG-OL}}$	PGOOD low state output voltage	$V_{\text{FB}} = 0.9\text{ V}$ , $I_{\text{PGOOD}} = 2\text{ mA}$			150	mV



Typical values correspond to  $T_J = 25^\circ\text{C}$ . Minimum and maximum limits apply over the  $-40^\circ\text{C}$  to  $150^\circ\text{C}$  junction temperature range unless otherwise stated.  $V_{\text{VIN}} = 48\text{ V}$ ,  $V_{\text{EN/UVLO}} = 1.5\text{ V}$ ,  $R_{\text{RT}} = 25\text{ k}\Omega$  unless otherwise stated. <sup>(1)</sup> <sup>(2)</sup>

PARAMETER		TEST CONDITIONS	MIN	TYP	MAX	UNIT
$I_{\text{PG-OH}}$	PGOOD high state leakage current	$V_{\text{FB}} = 0.8\text{ V}$ , $V_{\text{PGOOD}} = 13\text{ V}$			400	nA
<b>OSCILLATOR</b>						
$F_{\text{SW1}}$	Oscillator frequency – 1	$R_{\text{RT}} = 100\text{ k}\Omega$		100		kHz
$F_{\text{SW2}}$	Oscillator frequency – 2	$R_{\text{RT}} = 25\text{ k}\Omega$	380	400	420	kHz
$F_{\text{SW3}}$	Oscillator frequency – 3	$R_{\text{RT}} = 12.5\text{ k}\Omega$		780		kHz
<b>SYNCHRONIZATION INPUT AND OUTPUT</b>						
$F_{\text{SYNC}}$	SYNCIN external clock frequency range	% of nominal frequency set by $R_{\text{RT}}$	–20%		50%	
$V_{\text{SYNC-IH}}$	SYNCIN input logic high		2			V
$V_{\text{SYNC-IL}}$	SYNCIN input logic low				0.8	V
$R_{\text{SYNC-IN}}$	SYNCIN input resistance	$V_{\text{SYNCIN}} = 3\text{ V}$		20		k $\Omega$
$T_{\text{SYNCI-PW}}$	SYNCIN input minimum pulsewidth	Minimum high state or low state duration	50			ns
$V_{\text{SYNCO-OH}}$	SYNCOOUT high-state output voltage	$I_{\text{SYNCOOUT}} = -1\text{ mA}$ (sourcing current)	3			V
$V_{\text{SYNCO-OL}}$	SYNCOOUT low-state output voltage	$I_{\text{SYNCOOUT}} = 1\text{ mA}$ (sinking current)			0.4	V
$T_{\text{SYNCOOUT}}$	Delay from HO rising to SYNCOOUT leading edge	$V_{\text{SYNCIN}} = 0\text{ V}$ , $T_S = 1/F_{\text{SW}}$ , $F_{\text{SW}}$ set by $R_{\text{RT}}$		$T_S/2 - 140$		ns
$T_{\text{SYNCIN}}$	Delay from SYNCIN rising to HO leading edge	50% to 50%		150		ns
<b>GATE DRIVERS</b>						
$R_{\text{HO-UP}}$	HO high state resistance, HO to BST	$V_{\text{BST}} - V_{\text{SW}} = 7\text{ V}$ , $I_{\text{HO}} = -100\text{ mA}$		1.5		$\Omega$
$R_{\text{HO-DOWN}}$	HO low state resistance, HO to SW	$V_{\text{BST}} - V_{\text{SW}} = 7\text{ V}$ , $I_{\text{HO}} = 100\text{ mA}$		0.9		$\Omega$
$R_{\text{LO-UP}}$	LO high state resistance, LO to VCC	$V_{\text{BST}} - V_{\text{SW}} = 7\text{ V}$ , $I_{\text{LO}} = -100\text{ mA}$		1.5		$\Omega$
$R_{\text{LO-DOWN}}$	LO low state resistance, LO to PGND	$V_{\text{BST}} - V_{\text{SW}} = 7\text{ V}$ , $I_{\text{LO}} = 100\text{ mA}$		0.9		$\Omega$
$I_{\text{HOH}}, I_{\text{LOH}}$	HO, LO source current	$V_{\text{BST}} - V_{\text{SW}} = 7\text{ V}$ , HO = SW, LO = AGND		2.3		A
$I_{\text{HOL}}, I_{\text{LOL}}$	HO, LO sink current	$V_{\text{BST}} - V_{\text{SW}} = 7\text{ V}$ , HO = BST, LO = VCC		3.5		A
<b>BOOTSTRAP DIODE AND UNDERVOLTAGE THRESHOLD</b>						
$V_{\text{BST-FWD}}$	Diode forward voltage, VCC to BST	VCC to BST, BST pin sourcing 20 mA		0.75	0.9	V
$I_{\text{Q-BST}}$	BST to SW quiescent current, not switching	$V_{\text{SS/TRK}} = 0\text{ V}$ , $V_{\text{SW}} = 48\text{ V}$ , $V_{\text{BST}} = 54\text{ V}$		80		$\mu\text{A}$
$V_{\text{BST-UV}}$	BST to SW undervoltage detection	$V_{\text{BST}} - V_{\text{SW}}$ falling		3.4		V
$V_{\text{BST-HYS}}$	BST to SW undervoltage hysteresis	$V_{\text{BST}} - V_{\text{SW}}$ rising		0.42		V
<b>PWM CONTROL</b>						
$t_{\text{ON(min)}}$	Minimum controllable on-time	$V_{\text{BST}} - V_{\text{SW}} = 7\text{ V}$ , HO 50% to 50%		40	60	ns
$t_{\text{OFF(min)}}$	Minimum off-time	$V_{\text{BST}} - V_{\text{SW}} = 7\text{ V}$ , HO 50% to 50%		140	200	ns
$\text{DC}_{100\text{kHz}}$	Maximum duty cycle	$F_{\text{SW}} = 100\text{ kHz}$ , $6\text{ V} \leq V_{\text{VIN}} \leq 60\text{ V}$	98	99		%
$\text{DC}_{400\text{kHz}}$		$F_{\text{SW}} = 400\text{ kHz}$ , $6\text{ V} \leq V_{\text{VIN}} \leq 60\text{ V}$	90	94		%
$V_{\text{RAMP(min)}}$	RAMP valley voltage (COMP at 0% duty cycle)			300		mV
$k_{\text{FF}}$	PWM feedforward gain ( $V_{\text{IN}} / V_{\text{RAMP}}$ )	$6\text{ V} \leq V_{\text{VIN}} \leq 100\text{ V}$		15		V/V
<b>OVER CURRENT PROTECT (OCP) – VALLEY CURRENT LIMITING</b>						
$I_{\text{RS}}$	ILIM source current, $R_{\text{SENSE}}$ mode	Low voltage detected at ILIM	90	100	110	$\mu\text{A}$
$I_{\text{RDSON}}$	ILIM source current, $R_{\text{DS-ON}}$ mode	SW voltage detected at ILIM, $T_J = 25^\circ\text{C}$	180	200	220	$\mu\text{A}$
$I_{\text{RDSONTc}}$	ILIM current tempco	$R_{\text{DS-ON}}$ mode		4500		ppm/ $^\circ\text{C}$
$I_{\text{RSTC}}$	ILIM current tempco	$R_{\text{SENSE}}$ mode		0		ppm/ $^\circ\text{C}$
$V_{\text{ILIM-TH}}$	ILIM comparator threshold at ILIM		–8	–2	3.5	mV
<b>SHORT CIRCUIT PROTECTION (SCP) – DUTY CYCLE CLAMP</b>						

## LM5146

ZHCSLJ7A – JUNE 2021 – REVISED JUNE 2021

Typical values correspond to  $T_J = 25^\circ\text{C}$ . Minimum and maximum limits apply over the  $-40^\circ\text{C}$  to  $150^\circ\text{C}$  junction temperature range unless otherwise stated.  $V_{VIN} = 48\text{ V}$ ,  $V_{EN/UVLO} = 1.5\text{ V}$ ,  $R_{RT} = 25\text{ k}\Omega$  unless otherwise stated. <sup>(1)</sup> <sup>(2)</sup>

PARAMETER		TEST CONDITIONS	MIN	TYP	MAX	UNIT
$V_{CLAMP-OS}$	Clamp offset voltage – no current limiting	COMP to duty cycle clamp voltage		$0.2 + V_{VIN}/75$		V
$V_{CLAMP-MIN}$	Minimum clamp voltage	Clamp voltage with continuous current limit		$0.3 + V_{VIN}/150$		V
<b>HICCUP MODE FAULT PROTECTION</b>						
$C_{HICC-DEL}$	Hiccup mode activation delay	Clock cycles with current limiting before off-time activated		128		cycles
$C_{HICCUP}$	Hiccup mode off time after activation	Clock cycles with no switching followed by SS/TRK release		8192		cycles
<b>DIODE EMULATION / DCM OPERATION</b>						
$V_{ZCD-SS}$	Zero-cross detect (ZCD) soft-start ramp	ZCD threshold measured at SW pin 50 cycles after first HO pulse		0		mV
$V_{ZCD-DIS}$	Zero-cross detect disable threshold	ZCD threshold measured at SW pin 1000 cycles after first HO pulse		200		mV
$V_{DEM-TH}$	Diode emulation zero-cross threshold	Measured at SW with $V_{SW}$ rising	-5	0	5	mV
<b>THERMAL SHUTDOWN</b>						
$T_{SD}$	Thermal shutdown threshold	$T_J$ rising		175		$^\circ\text{C}$
$T_{SD-HYS}$	Thermal shutdown hysteresis			20		$^\circ\text{C}$

- (1) All minimum and maximum limits are specified by correlating the electrical characteristics to process and temperature variations and applied statistical process control.
- (2) The junction temperature ( $T_J$  in  $^\circ\text{C}$ ) is calculated from the ambient temperature ( $T_A$  in  $^\circ\text{C}$ ) and power dissipation ( $P_D$  in Watts) as follows:  $T_J = T_A + (P_D \times R_{\theta JA})$  where  $R_{\theta JA}$  (in  $^\circ\text{C/W}$ ) is the package thermal impedance provided in [§ 7.4](#).

## 7.6 Switching Characteristics

Typical values correspond to  $T_J = 25^\circ\text{C}$ .

PARAMETER		TEST CONDITIONS	MIN	TYP	MAX	UNIT
$T_{HO-TR}$ $T_{LO-TR}$	HO, LO rise times	$V_{BST} - V_{SW} = 7\text{ V}$ , $C_{LOAD} = 1\text{ nF}$ , 20% to 80%		7		ns
$T_{HO-TF}$ $T_{LO-TF}$	HO, LO fall times	$V_{BST} - V_{SW} = 7\text{ V}$ , $C_{LOAD} = 1\text{ nF}$ , 20% to 80%		4		ns
$T_{HO-DT}$	HO turn-on dead time	$V_{BST} - V_{SW} = 7\text{ V}$ , LO off to HO on, 50% to 50%		14		ns
$T_{LO-DT}$	LO turn-on dead time	$V_{BST} - V_{SW} = 7\text{ V}$ , HO off to LO on, 50% to 50%		14		ns

## 7.7 Typical Characteristics

$V_{IN} = 48\text{ V}$ ,  $R_{RT} = 25\text{ k}\Omega$ , SYNCIN tied to VCC, EN/UVLO tied to VIN (unless otherwise noted).

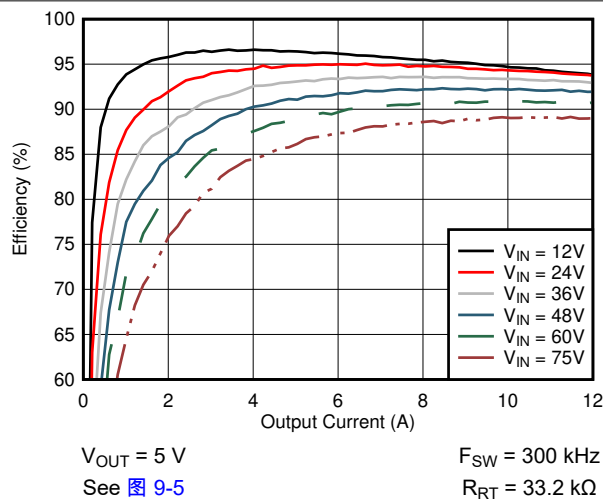


图 7-1. Efficiency vs Load, CCM

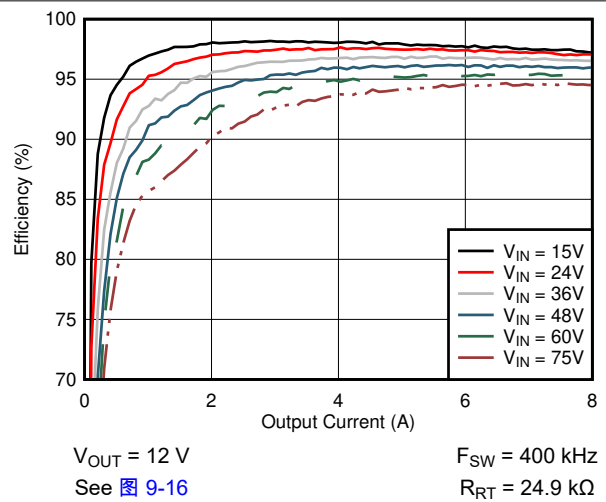


图 7-2. Efficiency vs Load, CCM

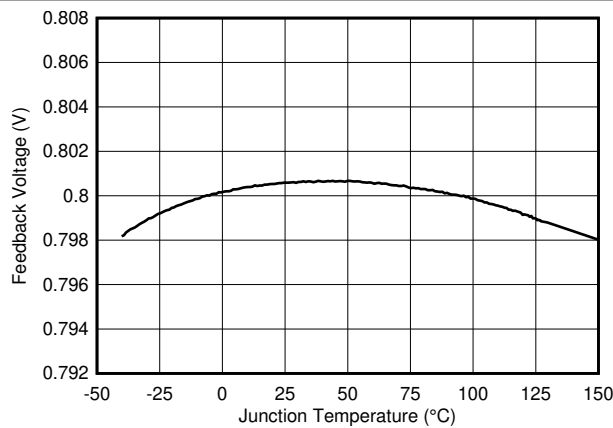


图 7-3. FB Voltage vs Junction Temperature

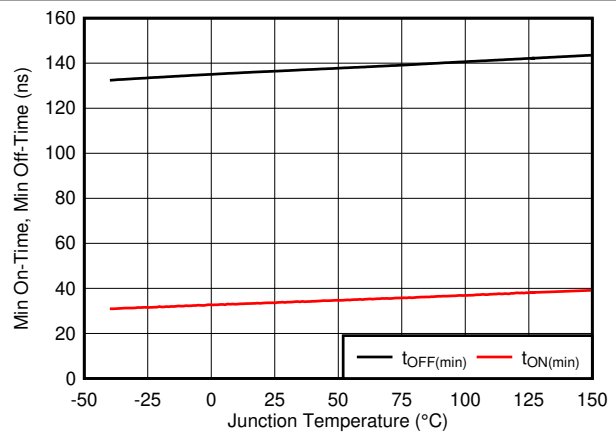


图 7-4.  $t_{ON(min)}$  and  $t_{OFF(min)}$  vs Junction Temperature

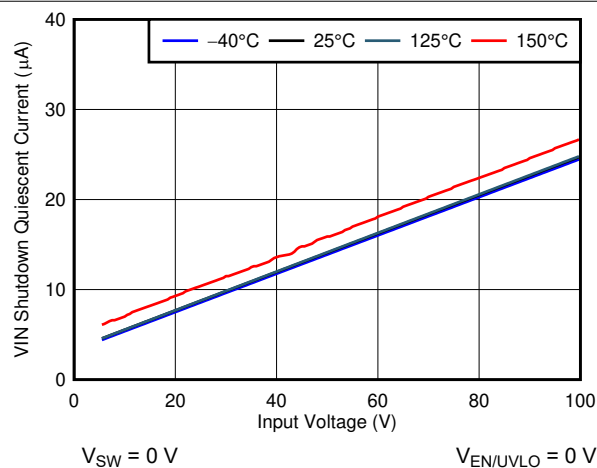


图 7-5.  $I_{Q-SHD}$  vs Input Voltage

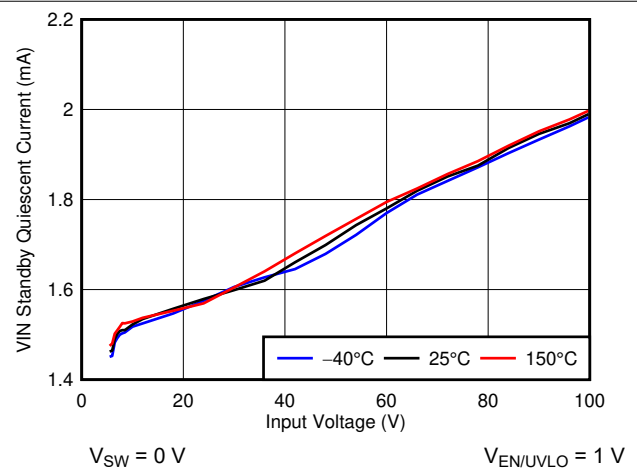


图 7-6.  $I_{Q-STANDBY}$  vs Input Voltage

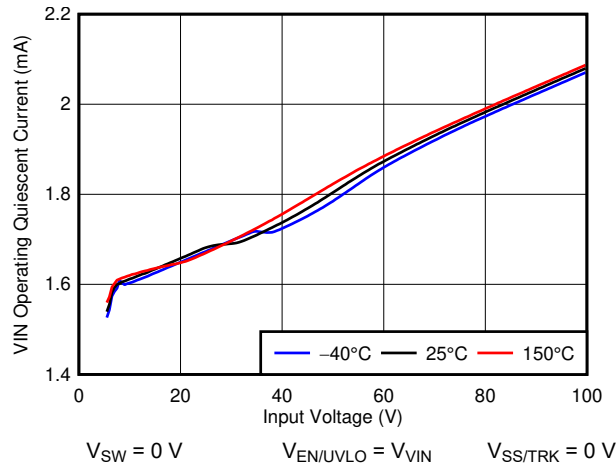
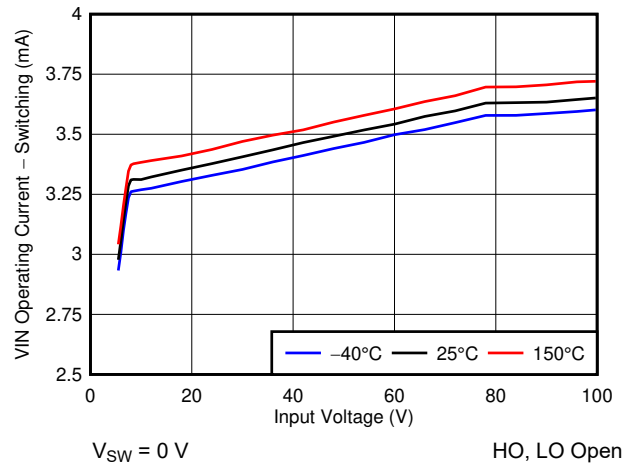
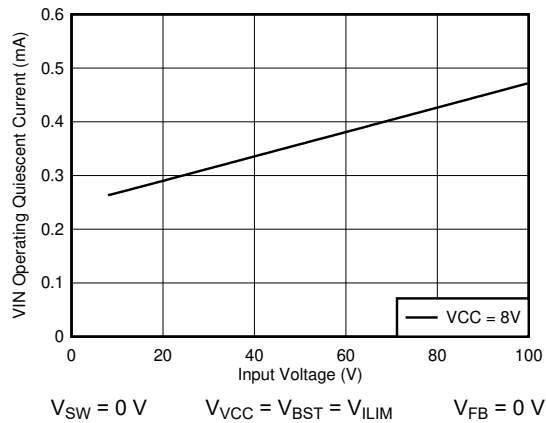
图 7-7.  $I_{Q-OPERATING}$  (Nonswitching) vs Input Voltage图 7-8.  $I_{Q-OPERATING}$  (Switching) vs Input Voltage

图 7-9. VIN Quiescent Current with External VCC Applied

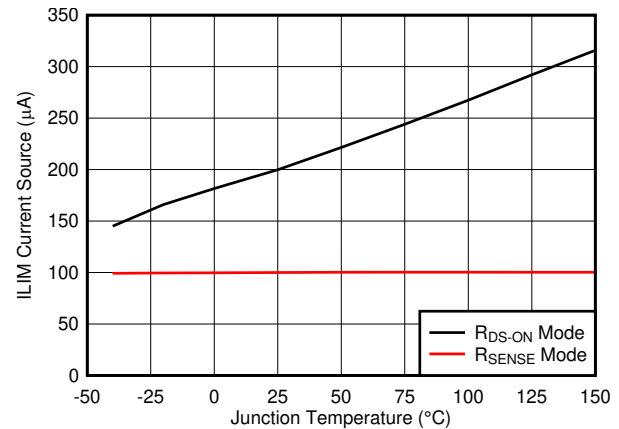


图 7-10. ILIM Current Source vs Junction Temperature

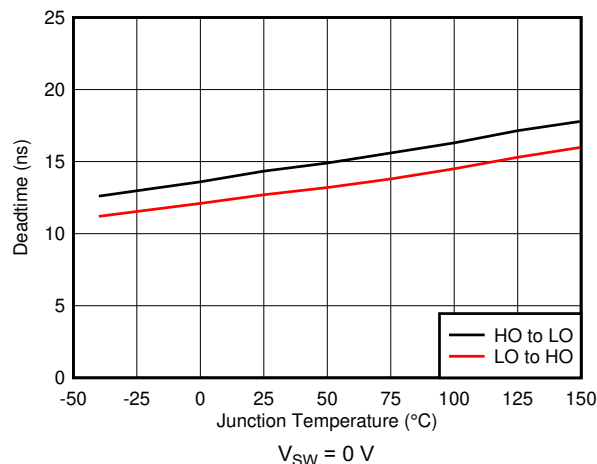


图 7-11. Deadtime vs Junction Temperature

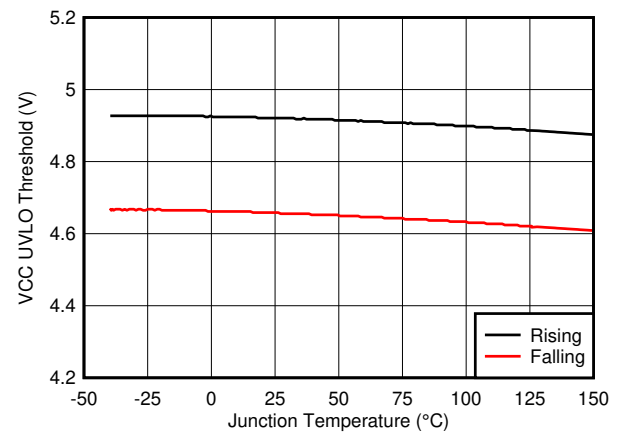
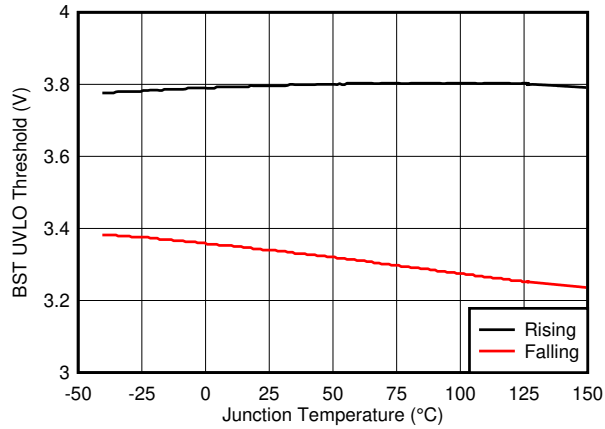
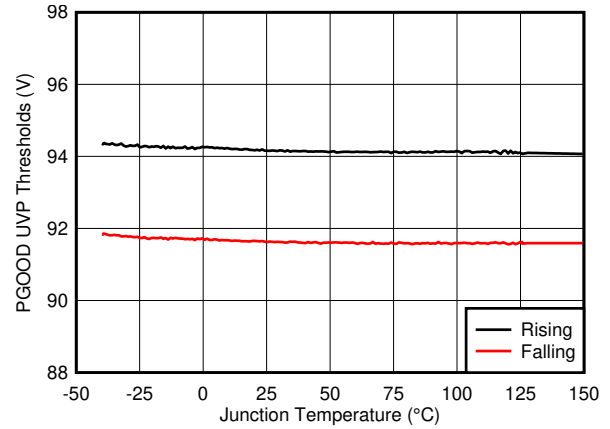


图 7-12. VCC UVLO Thresholds vs Junction Temperature



**图 7-13. BST UVLO Thresholds vs Junction Temperature**



**图 7-14. PGOOD UVP Thresholds vs Junction Temperature**

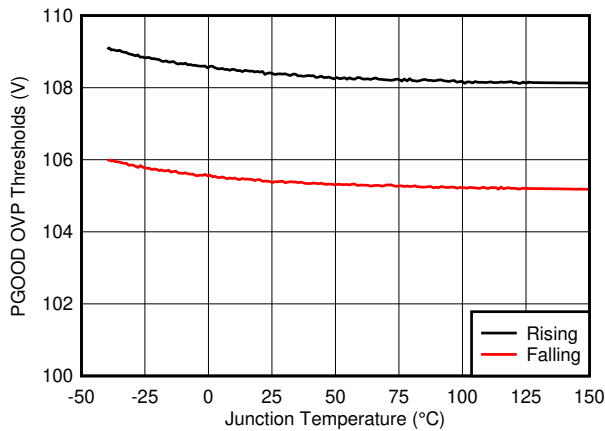


**图 7-15. PGOOD OVP Thresholds vs Junction Temperature**

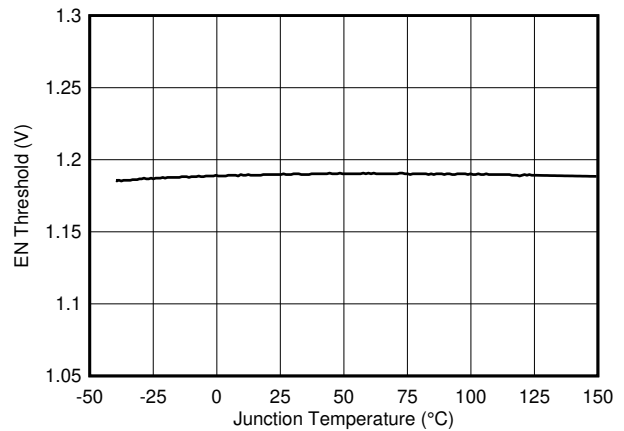


**图 7-16. EN/UVLO Threshold vs Junction Temperature**

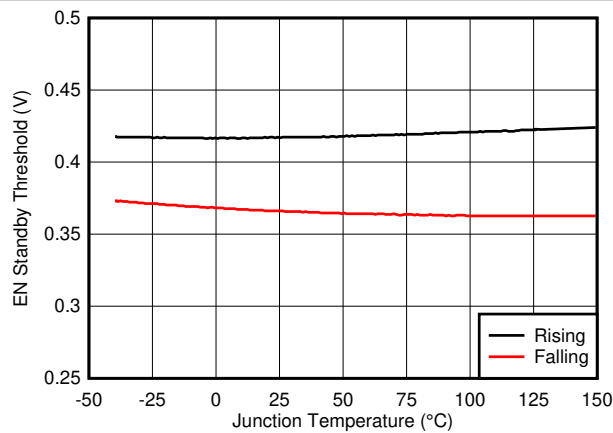


**图 7-17. EN Standby Thresholds vs Junction Temperature**

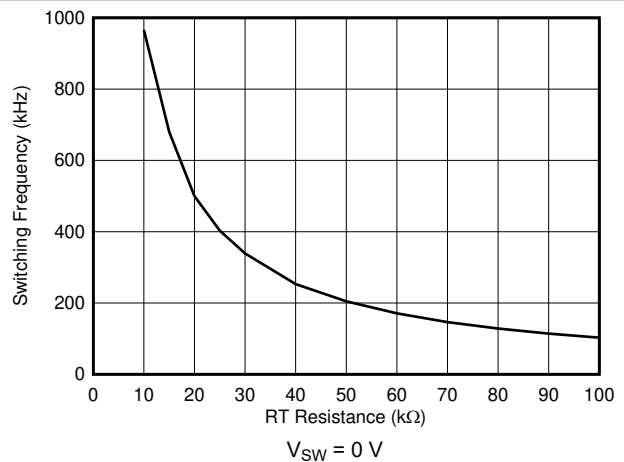


**图 7-18. Oscillator Frequency vs RT Resistance**

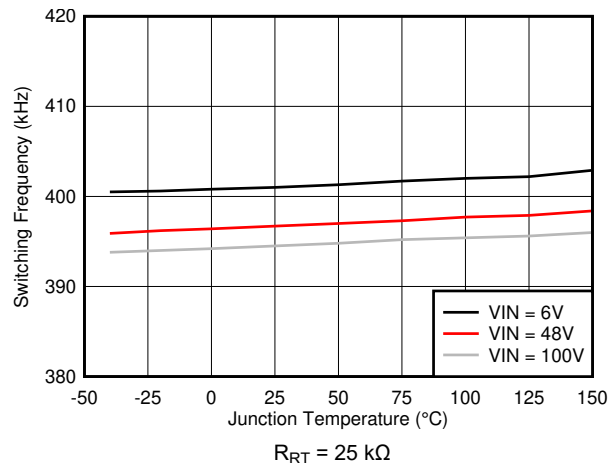


**图 7-19. Oscillator Frequency vs Junction Temperature**

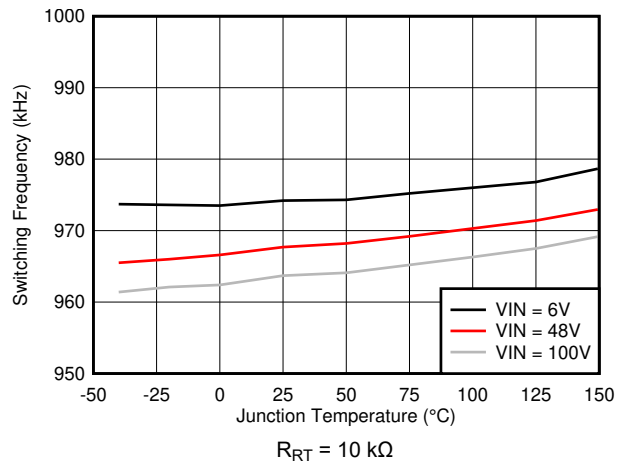


**图 7-20. Oscillator Frequency vs Junction Temperature**

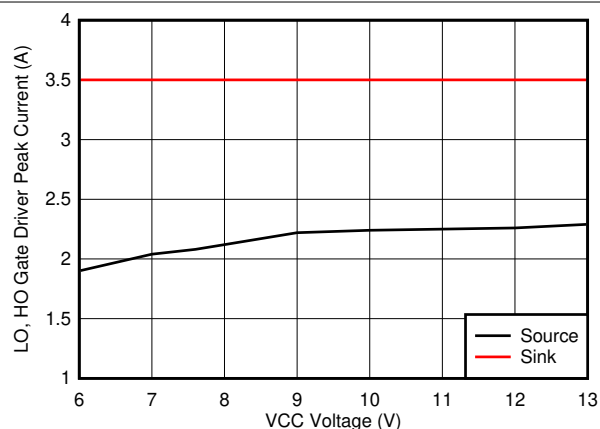


**图 7-21. Gate Driver Peak Current vs VCC Voltage**

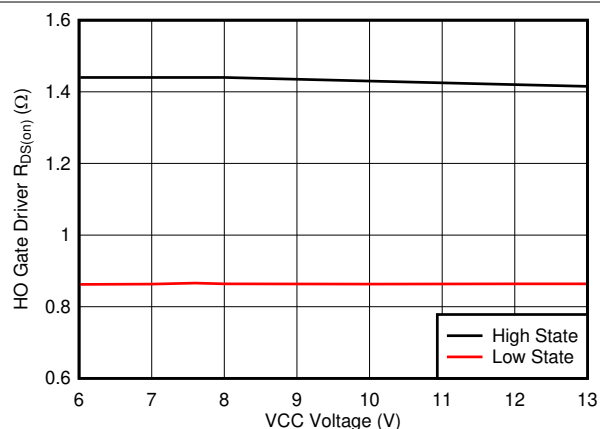


**图 7-22. HO Driver Resistance vs VCC Voltage**

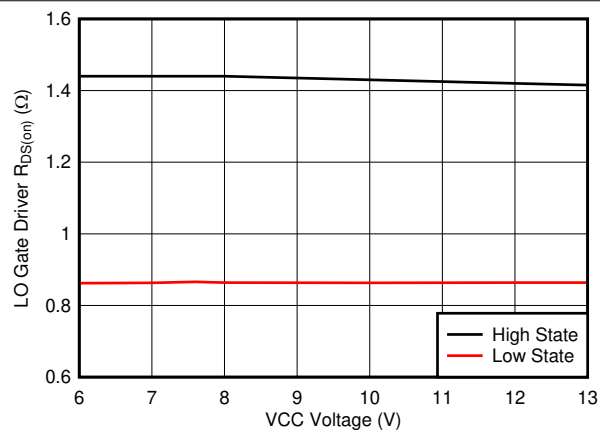


**图 7-23. LO Driver Resistance vs VCC Voltage**

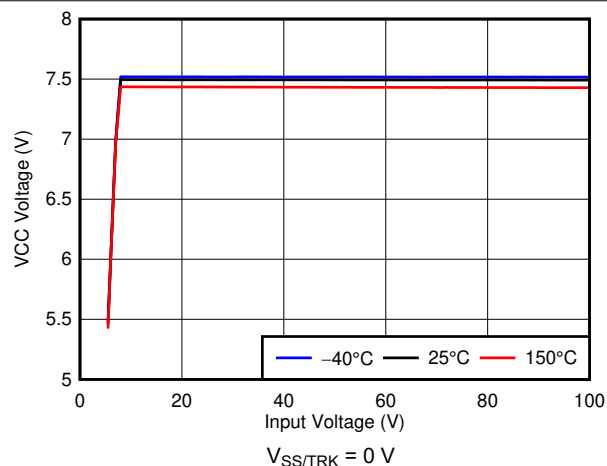


**图 7-24. VCC Voltage vs Input Voltage**

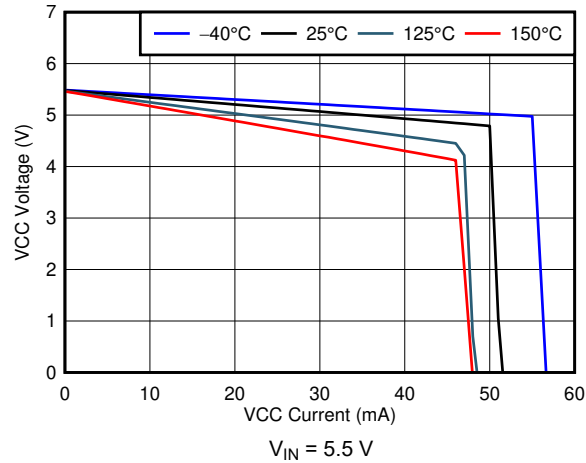


**图 7-25. VCC vs ICC Characteristic**

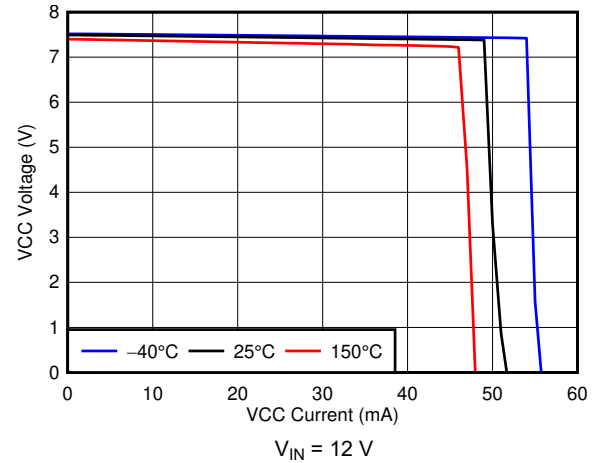


**图 7-26. VCC vs ICC Characteristic**

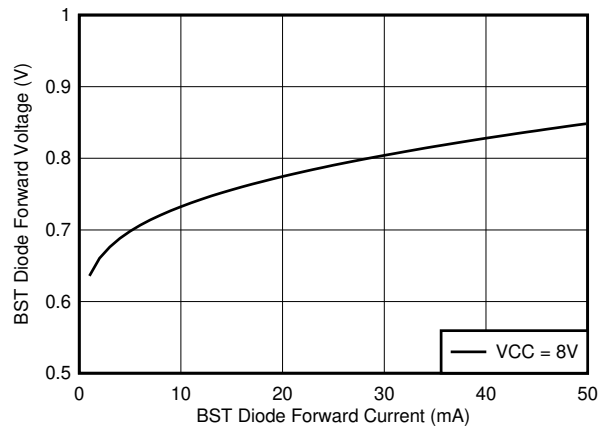


**图 7-27. BST Diode Forward Voltage vs Current**

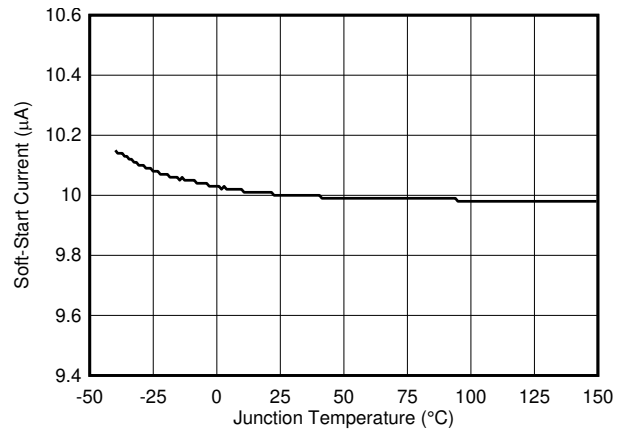


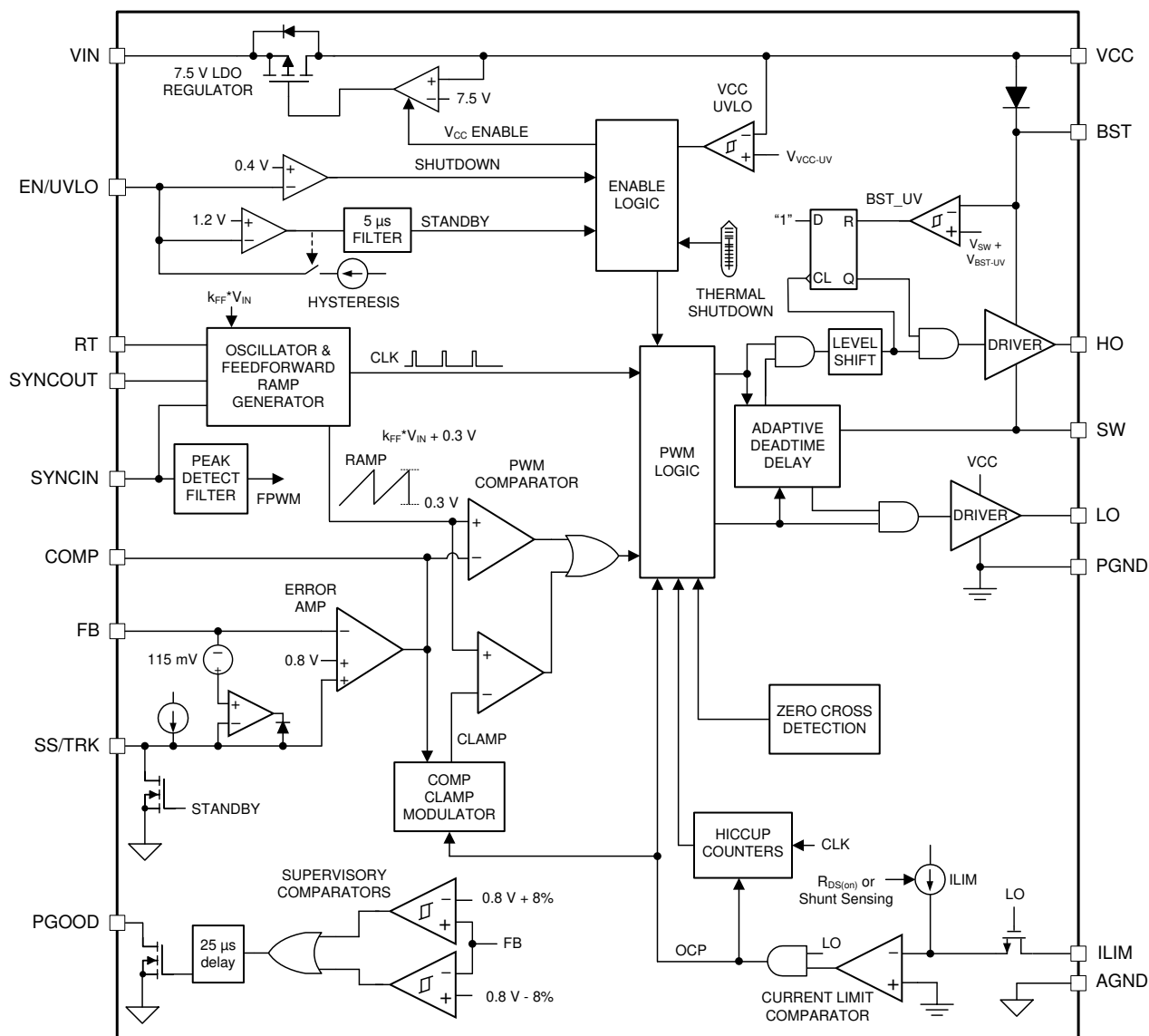
**图 7-28. SS/TRK Current Source vs Junction Temperature**

## 8 Detailed Description

### 8.1 Overview

The LM5146 is a 100-V synchronous buck controller with all of the functions necessary to implement a high-efficiency step-down power supply. The output voltage range is from 0.8 V to 60 V. The voltage-mode control architecture uses input feedforward for excellent line transient response over a wide  $V_{IN}$  range. Voltage-mode control supports the wide duty cycle range for high input voltage and low dropout applications as well as when a high-voltage conversion ratio (for example, 10-to-1) is required. Current sensing for cycle-by-cycle current limit can be implemented with either the low-side FET  $R_{DS(on)}$  or a current sense resistor. The operating frequency is programmable from 100 kHz to 1 MHz. The LM5146 drives external high-side and low-side NMOS power switches with robust 7.5-V gate drivers suitable for standard threshold MOSFETs. Adaptive dead-time control between the high-side and low-side drivers minimizes body diode conduction during switching transitions. An external bias supply can be connected to the VCC pin to improve efficiency in high-voltage applications. A user-selectable diode emulation feature enables DCM operation for improved efficiency and lower dissipation at light-load conditions.

### 8.2 Functional Block Diagram





## 8.3 Feature Description

### 8.3.1 Input Range ( $V_{IN}$ )

The LM5146 operational input voltage range is from 5.5 V to 100 V. The device is intended for step-down conversions from 12-V, 24-V, 48-V, 60-V, and 72-V unregulated, semiregulated, and fully-regulated supply rails. The application circuit in [Figure 8-1](#) shows all the necessary components to implement an LM5146-based wide- $V_{IN}$  step-down regulator using a single supply. The LM5146 uses an internal LDO subregulator to provide a 7.5-V VCC bias rail for the gate drive and control circuits (assuming the input voltage is higher than 7.5 V plus the necessary subregulator dropout specification).

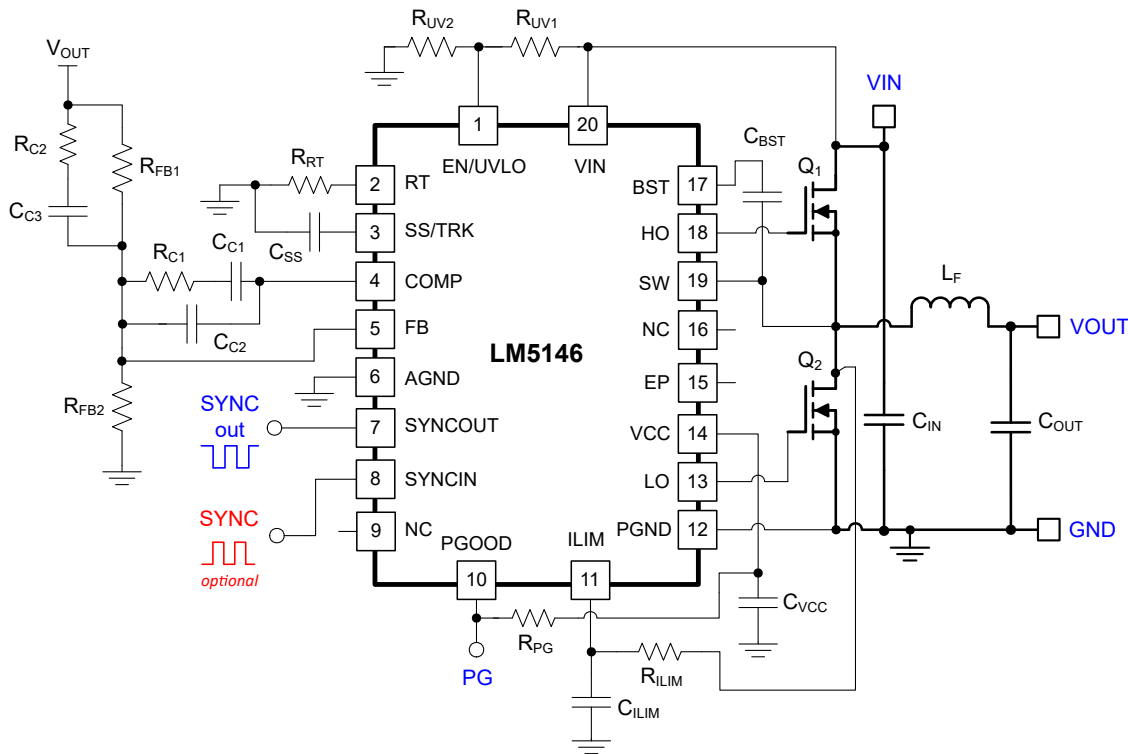


**图 8-1. Schematic Diagram for  $V_{IN}$  Operating Range of 5.5 V to 100 V**

In high-voltage applications, take extra care to ensure the VIN pin does not exceed the absolute maximum voltage rating of 100 V during line or load transient events. Voltage ringing on the VIN pin that exceeds the values in the [Absolute Maximum Ratings](#) can damage the IC. Use high-quality ceramic input capacitors to minimize ringing. An RC filter from the input rail to the VIN pin (for example, 4.7  $\Omega$  and 0.1  $\mu$ F) provides supplementary filtering at the VIN pin.

### 8.3.2 Output Voltage Setpoint and Accuracy (FB)

The reference voltage at the FB pin is set at 0.8 V with a feedback system accuracy over the full junction temperature range of  $\pm 1\%$ . Junction temperature range for the device is  $-40^{\circ}\text{C}$  to  $+150^{\circ}\text{C}$ . While dependent on switching frequency and load current requirements, the LM5146 is generally capable of providing an output voltage in the range of 0.8 V to a maximum of 60 V or slightly less than  $V_{IN}$ , whichever is lower. The DC output voltage setpoint during normal operation is set by the feedback resistor network,  $R_{FB1}$  and  $R_{FB2}$ , connected to the output.

### 8.3.3 High-Voltage Bias Supply Regulator (VCC)

The LM5146 contains an internal high-voltage VCC regulator that provides a bias supply for the PWM controller and its gate drivers for the external MOSFETs. The input pin (VIN) can be connected directly to an input voltage source up to 100 V. The output of the VCC regulator is set to 7.5 V. However, when the input voltage is below

the VCC setpoint level, the VCC output tracks  $V_{IN}$  with a small voltage drop. Connect a ceramic decoupling capacitor between 1  $\mu\text{F}$  and 5  $\mu\text{F}$  from VCC to AGND for stability.

The VCC regulator output has a current limit of 40 mA (minimum). At power up, the regulator sources current into the capacitor connected to the VCC pin. When the VCC voltage exceeds its rising UVLO threshold of 4.93 V, the output is enabled (if EN/UVLO is above 1.2 V), and the soft-start sequence begins. The output remains active until the VCC voltage falls below its falling UVLO threshold of 4.67 V (typical) or if EN/UVLO goes to a standby or shutdown state.

Internal power dissipation of the VCC regulator can be minimized by connecting the output voltage or an auxiliary bias supply rail (up to 13 V) to VCC using a diode  $D_{VCC}$  as shown in [Figure 8-2](#). A diode in series with the input prevents reverse current flow from VCC to VIN if the input voltage falls below the external VCC rail.

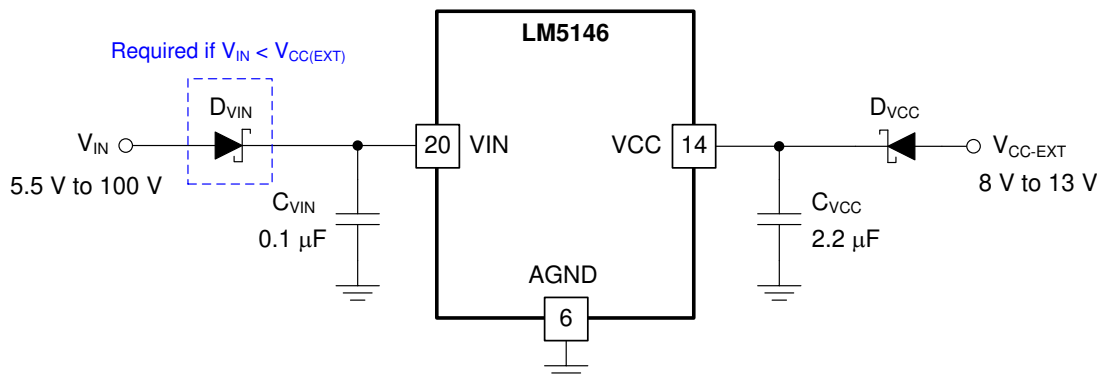


**图 8-2. VCC Bias Supply Connection From VOUT or Auxiliary Supply**

Note that a finite bias supply regulator dropout voltage exists and is manifested to a larger extent when driving high gate charge ( $Q_G$ ) power MOSFETs at elevated switching frequencies. For example, at  $V_{IN} = 6\text{ V}$ , the VCC voltage is 5.8 V with a DC operating current,  $I_{VCC}$ , of 20 mA. Such a low gate drive voltage can be insufficient to fully enhance the power MOSFETs. At the very least, MOSFET on-state resistance,  $R_{DS(ON)}$ , can increase at such low gate drive voltage.

Here are the main considerations when operating at input voltages below 7.5 V:

- Increased MOSFET  $R_{DS(on)}$  at lower  $V_{GS}$ , leading to Increased conduction losses and reduced OCP setpoint
- Increased switching losses given the slower switching times when operating at lower gate voltages
- Restricted range of suitable power MOSFETs to choose from (MOSFETs with  $R_{DS(on)}$  rated at  $V_{GS} = 4.5\text{ V}$  become mandatory)

### 8.3.4 Precision Enable (EN/UVLO)

The EN/UVLO input supports adjustable input undervoltage lockout (UVLO) with hysteresis programmed by the resistor values for application specific power-up and power-down requirements. EN/UVLO connects to a comparator-based input referenced to a 1.2-V bandgap voltage. An external logic signal can be used to drive the EN/UVLO input to toggle the output ON and OFF and for system sequencing or protection. The simplest way to enable the operation of the LM5146 is to connect EN/UVLO directly to VIN. This allows self start-up of the LM5146 when  $V_{CC}$  is within its valid operating range. However, many applications benefit from using a resistor divider  $R_{UV1}$  and  $R_{UV2}$  as shown in [Figure 8-3](#) to establish a precision UVLO level.

Use [Equation 1](#) and [Equation 2](#) to calculate the UVLO resistors given the required input turn-on and turn-off voltages.

$$R_{UV1} = \frac{V_{IN(on)} - V_{IN(off)}}{I_{HYS}} \quad (1)$$

$$R_{UV2} = R_{UV1} \cdot \frac{V_{EN}}{V_{IN(on)} - V_{EN}} \quad (2)$$

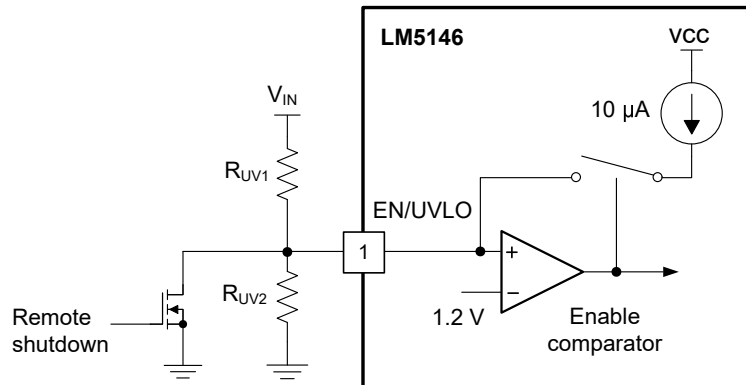


**图 8-3. Programmable Input Voltage UVLO Turn-on and Turn-off**

The LM5146 enters a low  $I_Q$  shutdown mode when EN/UVLO is pulled below approximately 0.4 V. The internal LDO regulator powers off and the internal bias supply rail collapses, shutting down the bias currents of the LM5146. The LM5146 operates in standby mode when the EN/UVLO voltage is between the hard shutdown and precision enable (standby) thresholds.

### 8.3.5 Power Good Monitor (PGOOD)

The LM5146 provides a PGOOD flag pin to indicate when the output voltage is within a regulation window. Use the PGOOD signal as shown in 图 8-4 for start-up sequencing of downstream converters, fault protection, and output monitoring. PGOOD is an open-drain output that requires a pullup resistor to a DC supply not greater than 13 V. The typical range of pullup resistance is 10 kΩ to 100 kΩ. If necessary, use a resistor divider to decrease the voltage from a higher voltage pullup rail.

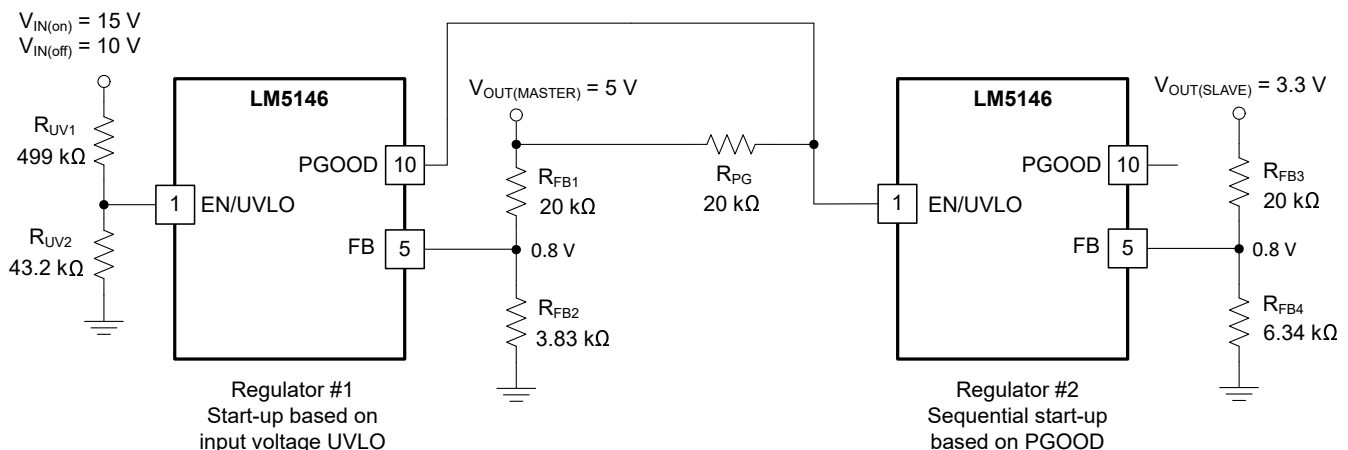


**图 8-4. Master-Slave Sequencing Implementation Using PGOOD and EN/UVLO**

When the FB voltage exceeds 94% of the internal reference  $V_{REF}$ , the internal PGOOD switch turns off and PGOOD can be pulled high by the external pullup. If the FB voltage falls below 92% of  $V_{REF}$ , the internal PGOOD switch turns on, and PGOOD is pulled low to indicate that the output voltage is out of regulation. Similarly, when the FB voltage exceeds 108% of  $V_{REF}$ , the internal PGOOD switch turns on, pulling PGOOD low. If the FB voltage subsequently falls below 105% of  $V_{REF}$ , the PGOOD switch is turned off and PGOOD is pulled high. PGOOD has a built-in deglitch delay of 25 μs.

### 8.3.6 Switching Frequency (RT, SYNCIN)

There are two options for setting the switching frequency,  $F_{SW}$ , of the LM5146, thus providing a power supply designer with a level of flexibility when choosing external components for various applications. To adjust the frequency, use a resistor from the RT pin to AGND, or synchronize the LM5146 to an external clock signal through the SYNCIN pin.

#### 8.3.6.1 Frequency Adjust

Adjust the free-running switching frequency by using a resistor from the RT pin to AGND. The switching frequency range is from 100 kHz to 1 MHz. The frequency set resistance,  $R_{RT}$ , is governed by Equation 3. E96 standard-value resistors for common switching frequencies are given in 表 8-1.

$$R_{RT} [k\Omega] = \frac{10^4}{F_{SW} [kHz]} \quad (3)$$

表 8-1. Frequency Set Resistors

SWITCHING FREQUENCY (kHz)	FREQUENCY SET RESISTANCE (kΩ)
100	100
200	49.9
250	40.2
300	33.2
400	24.9
500	20
750	13.3
1000	10

#### 8.3.6.2 Clock Synchronization

Apply an external clock synchronization signal to the LM5146 to synchronize switching in both frequency and phase. Requirements for the external clock SYNC signal are:

- Clock frequency range: 100 kHz to 1 MHz
- Clock frequency: –20% to +50% of the free-running frequency set by  $R_{RT}$
- Clock maximum voltage amplitude: 13 V
- Clock minimum pulse width: 50 ns

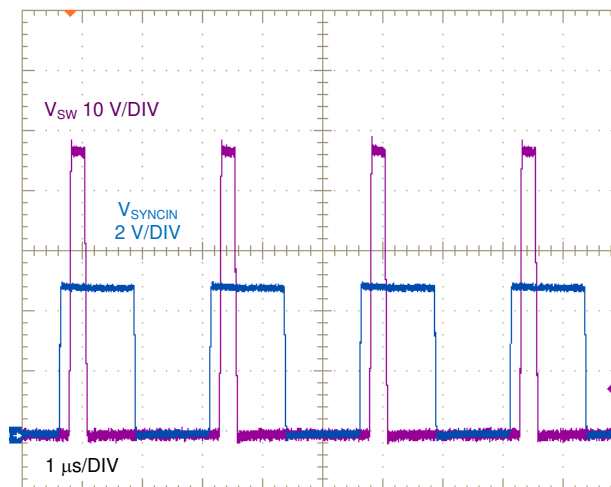


图 8-5. Typical 400-kHz SYNCIN and SW Voltage Waveforms

Figure 8-5 shows a clock signal at 400 kHz and the corresponding SW node waveform ( $V_{IN} = 48\text{ V}$ ,  $V_{OUT} = 5\text{ V}$ , free-running frequency = 280 kHz). The SW voltage waveform is synchronized with respect to the rising edge of SYNCIN. The rising edge of the SW voltage is phase delayed relative to SYNCIN by approximately 100 ns.

### 8.3.7 Configurable Soft Start (SS/TRK)

After the EN/UVLO pin exceeds its rising threshold of 1.2 V, the LM5146 begins charging the output to the DC level dictated by the feedback resistor network. The LM5146 features an adjustable soft start (set by a capacitor from the SS/TRK pin to GND) that determines the charging time of the output. A 10- $\mu\text{A}$  current source charges this soft-start capacitor. Soft start limits inrush current as a result of high output capacitance to avoid an overcurrent condition. Stress on the input supply rail is also reduced. The soft-start time,  $t_{SS}$ , for the output voltage to ramp to its nominal level is set by Equation 4.

$$t_{SS} = \frac{C_{SS} \cdot V_{REF}}{I_{SS}} \quad (4)$$

where

- $C_{SS}$  is the soft-start capacitance
- $V_{REF}$  is the 0.8-V reference
- $I_{SS}$  is the 10- $\mu\text{A}$  current sourced from the SS/TRK pin

More simply, calculate  $C_{SS}$  using Equation 5.

$$C_{SS} [\text{nF}] = 12.5 \cdot t_{SS} [\text{ms}] \quad (5)$$

The SS/TRK pin is internally clamped to  $V_{FB} + 115\text{ mV}$  to allow a soft start recovery from an overload event. The clamp circuit requires a soft-start capacitance greater than 2 nF for stability and has a current limit of approximately 2 mA.

#### 8.3.7.1 Tracking

The SS/TRK pin also doubles as a tracking pin when master-slave power-supply tracking is required. This tracking is achieved by simply dividing down the output voltage of the master with a simple resistor network. Coincident, ratiometric, and offset tracking modes are possible.

If an external voltage source is connected to the SS/TRK pin, the external soft-start capability of the LM5146 is effectively disabled. The regulated output voltage level is reached when the SS/TRK pin reaches the 0.8-V reference voltage level. It is the responsibility of the system designer to determine if an external soft-start capacitor is required to keep the device from entering current limit during a start-up event. Likewise, the system designer must also be aware of how fast the input supply ramps if the tracking feature is enabled.

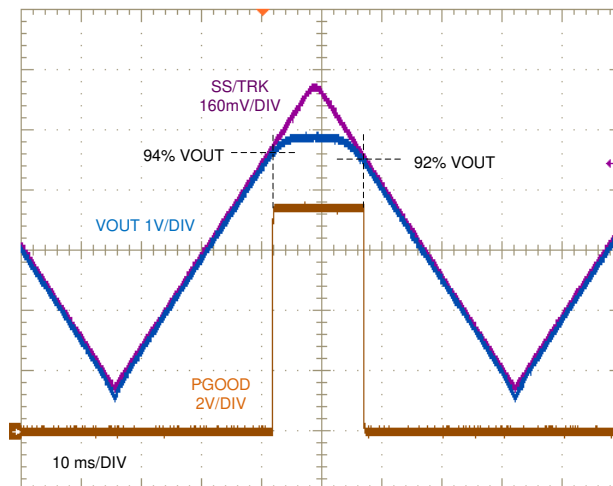


Figure 8-6. Typical Output Voltage Tracking and PGOOD Waveforms

图 8-6 shows a triangular voltage signal directly driving SS/TRK and the corresponding output voltage tracking response. Nominal output voltage here is 5 V, with oscilloscope channel scaling chosen such that the waveforms overlap during tracking. As expected, the PGOOD flag transitions at thresholds of 94% (rising) and 92% (falling) of the nominal output voltage setpoint.

Two practical tracking configurations, ratiometric and coincident, are shown in 图 8-7. The most common application is coincident tracking, used in core versus I/O voltage tracking in DSP and FPGA implementations. Coincident tracking forces the master and slave channels to have the same output voltage ramp rate until the slave output reaches its regulated setpoint. Conversely, ratiometric tracking sets the output voltage of the slave to a fraction of the output voltage of the master during start-up.

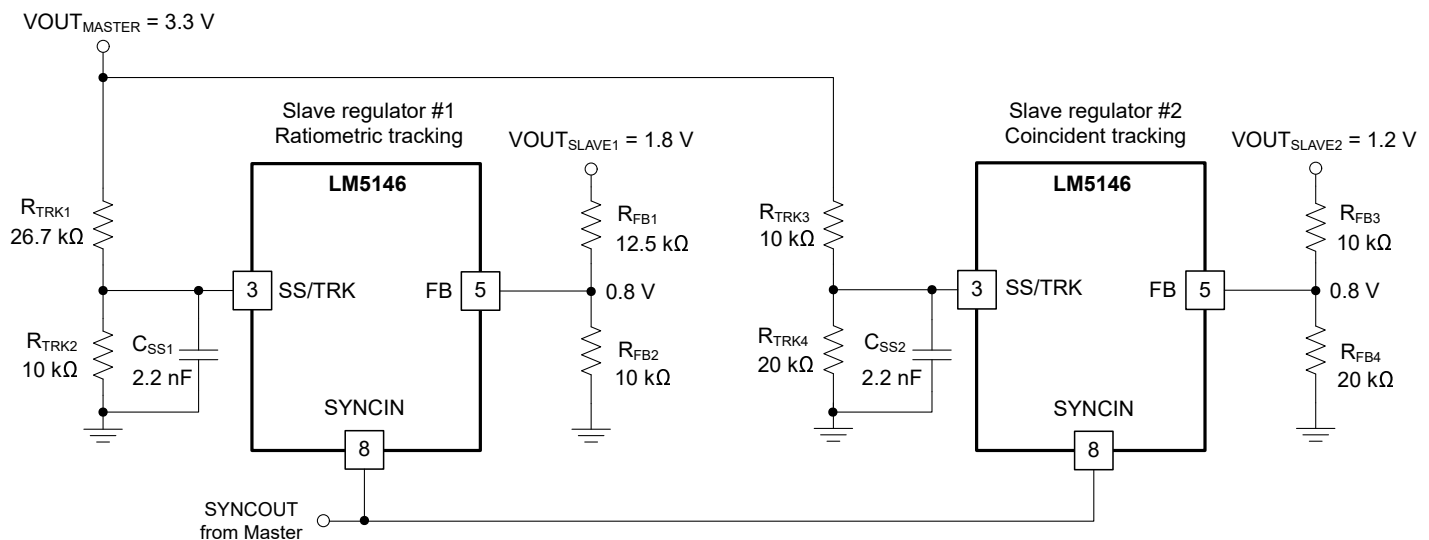


图 8-7. Tracking Implementation with Master, Ratiometric Slave, and Coincident Slave Rails

For coincident tracking, connect the SS/TRK input of the slave regulator to a resistor divider from the output voltage of the master that is the same as the divider used on the FB pin of the slave. In other words, simply select  $R_{TRK3} = R_{FB3}$  and  $R_{TRK4} = R_{FB4}$  as shown in 图 8-7. As the master voltage rises, the slave voltage rises identically (aside from the 80-mV offset from SS/TRK to FB when  $V_{FB}$  is below 0.8 V). Eventually, the slave voltage reaches its regulation voltage, at which point the internal reference takes over the regulation while the SS/TRK input continues to 115 mV above FB, and no longer controls the output voltage.

In all cases, to ensure that the output voltage accuracy is not compromised by the SS/TRK voltage being too close to the 0.8-V reference voltage, the final value of the SS/TRK voltage of the slave should be at least 100 mV above FB.

### 8.3.8 Voltage-Mode Control (COMP)

The LM5146 incorporates a voltage-mode control loop implementation with input voltage feedforward to eliminate the input voltage dependence of the PWM modulator gain. This configuration allows the controller to maintain stability throughout the entire input voltage operating range and provides optimal response to input voltage transient disturbances. The constant gain provided by the controller greatly simplifies loop compensation design because the loop characteristics remain constant as the input voltage changes, unlike a buck converter without voltage feedforward. An increase in input voltage is matched by a concomitant increase in ramp voltage amplitude to maintain constant modulator gain. The input voltage feedforward gain,  $k_{FF}$ , is 15, equivalent to the input voltage divided by the ramp amplitude,  $V_{IN}/V_{RAMP}$ . See 节 9.1.3 for more detail.

### 8.3.9 Gate Drivers (LO, HO)

The LM5146 gate driver impedances are low enough to perform effectively in high output current applications where large die-size or paralleled MOSFETs with correspondingly large gate charge,  $Q_G$ , are used. Measured at  $V_{VCC} = 7.5$  V, the low-side driver of the LM5146 has a low impedance pulldown path of  $0.9 \Omega$  to minimize the effect of  $dv/dt$  induced turn-on, particularly with low gate-threshold voltage MOSFETs. Similarly, the high-side

driver has 1.5-Ω and 0.9-Ω pullup and pulldown impedances, respectively, for faster switching transition times, lower switching loss, and greater efficiency.

The high-side gate driver works in conjunction with an integrated bootstrap diode and external bootstrap capacitor,  $C_{BST}$ . When the low-side MOSFET conducts, the SW voltage is approximately at 0 V and  $C_{BST}$  is charged from VCC through the integrated boot diode. Connect a 0.1-μF or larger ceramic capacitor close to the BST and SW pins.

Furthermore, there is a proprietary adaptive dead-time control on both switching edges to prevent shoot-through and cross-conduction, minimize body diode conduction time, and reduce body diode reverse recovery losses.

### 8.3.10 Current Sensing and Overcurrent Protection (ILIM)

The LM5146 implements a lossless current sense scheme designed to limit the inductor current during an overload or short-circuit condition. 图 8-8 portrays the popular current sense method using the on-state resistance of the low-side MOSFET. Meanwhile, 图 8-9 shows an alternative implementation with current shunt resistor,  $R_S$ . The LM5146 senses the inductor current during the PWM off-time (when LO is high).

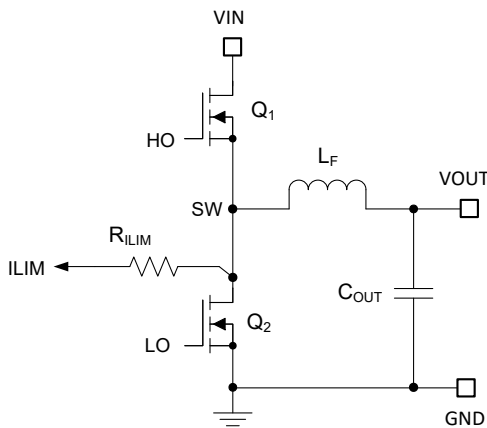


图 8-8. MOSFET  $R_{DS(on)}$  Current Sensing

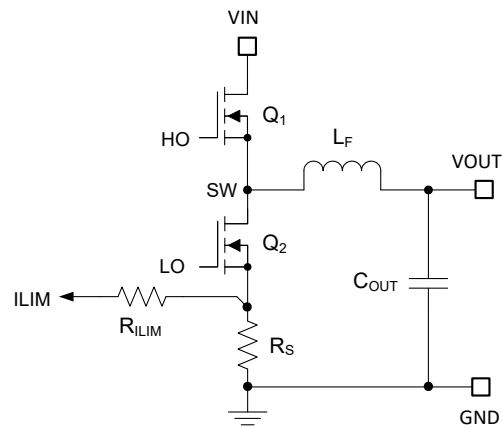


图 8-9. Shunt Resistor Current Sensing

The ILIM pin of the LM5146 sources a reference current that flows in an external resistor, designated  $R_{ILIM}$ , to program of the current limit threshold. A current limit comparator on the ILIM pin prevents further SW pulses if the ILIM pin voltage goes below GND. 图 8-10 shows the implementation.

Resistor  $R_{ILIM}$  is tied to SW to use the  $R_{DS(on)}$  of the low-side MOSFET as a sensing element (termed  $R_{DS(on)}$  mode). Alternatively,  $R_{ILIM}$  is tied to a shunt resistor connected at the source of the low-side MOSFET (termed  $R_{SENSE}$  mode). The LM5146 detects the appropriate mode at start-up and sets the source current amplitude and temperature coefficient (TC) accordingly.

The ILIM current with  $R_{DS-ON}$  sensing is 200 μA at 27°C junction temperature and incorporates a TC of +4500 ppm/°C to generally track the  $R_{DS(on)}$  temperature variation of the low-side MOSFET. Conversely, the ILIM current is a constant 100 μA in  $R_{SENSE}$  mode. This controls the valley of the inductor current during a steady-state overload at the output. Depending on the chosen mode, select the resistance of  $R_{ILIM}$  using Equation 6.

$$R_{ILIM} = \begin{cases} \frac{I_{OUT} - \Delta I_L / 2}{I_{RDS(on)}} \cdot R_{DS(on)Q2}, & R_{DS(on)} \text{ sensing} \\ \frac{I_{OUT} - \Delta I_L / 2}{I_{RS}} \cdot R_S, & \text{shunt sensing} \end{cases} \quad (6)$$

where

- $\Delta I_L$  is the peak-to-peak inductor ripple current
- $R_{DS(on)Q2}$  is the on-state resistance of the low-side MOSFET

- $I_{RDSON}$  is the ILIM pin current in  $R_{DS-ON}$  mode
- $R_S$  is the resistance of the current-sensing shunt element
- $I_{RS}$  is the ILIM pin current in  $R_{SENSE}$  mode

Given the large voltage swings of ILIM in  $R_{DS(on)}$  sensing mode, a capacitor designated  $C_{ILIM}$  connected from ILIM to PGND is essential to the operation of the valley current limit circuit. Choose this capacitance such that the time constant  $R_{ILIM} \cdot C_{ILIM}$  is approximately 6 ns.

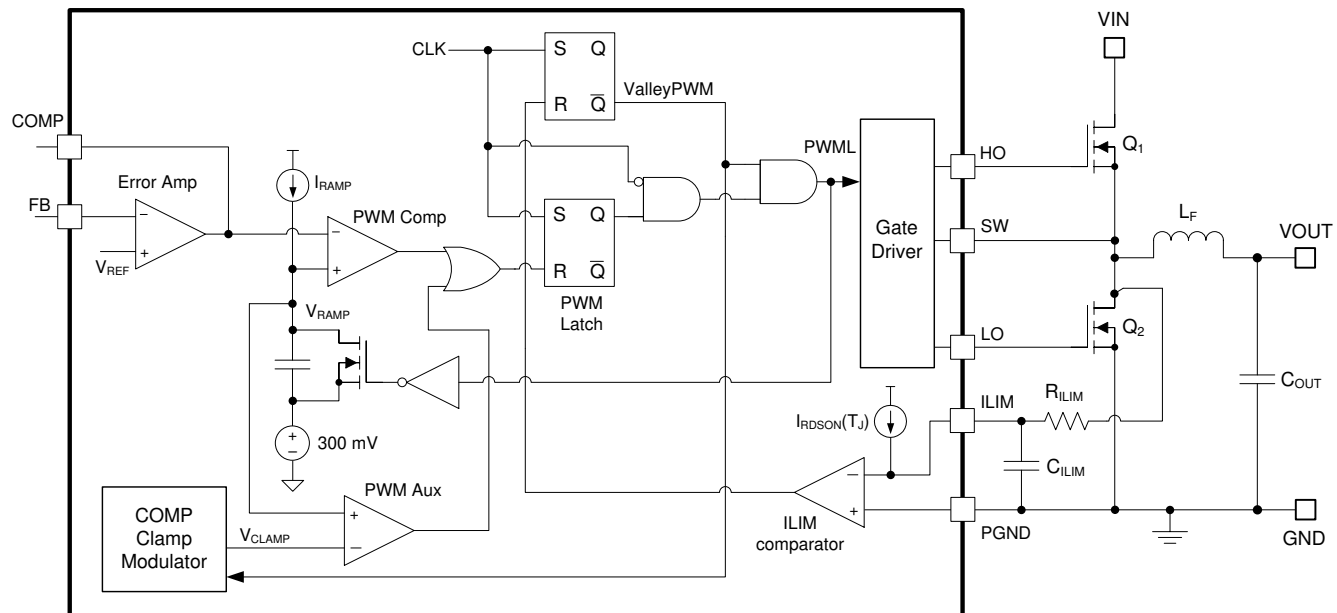


**图 8-10. OCP Setpoint Defined by Current Source  $I_{RDSON}$  and Resistor  $R_{ILIM}$  in  $R_{DS-ON}$  Mode**

Note that current sensing with a shunt component is typically implemented at lower output current levels to provide accurate overcurrent protection. Burdened by the unavoidable efficiency penalty, PCB layout, and additional cost implications, this configuration is not usually implemented in high-current applications (except where OCP setpoint accuracy and stability over the operating temperature range are critical specifications).



### 8.3.11 OCP Duty Cycle Limiter

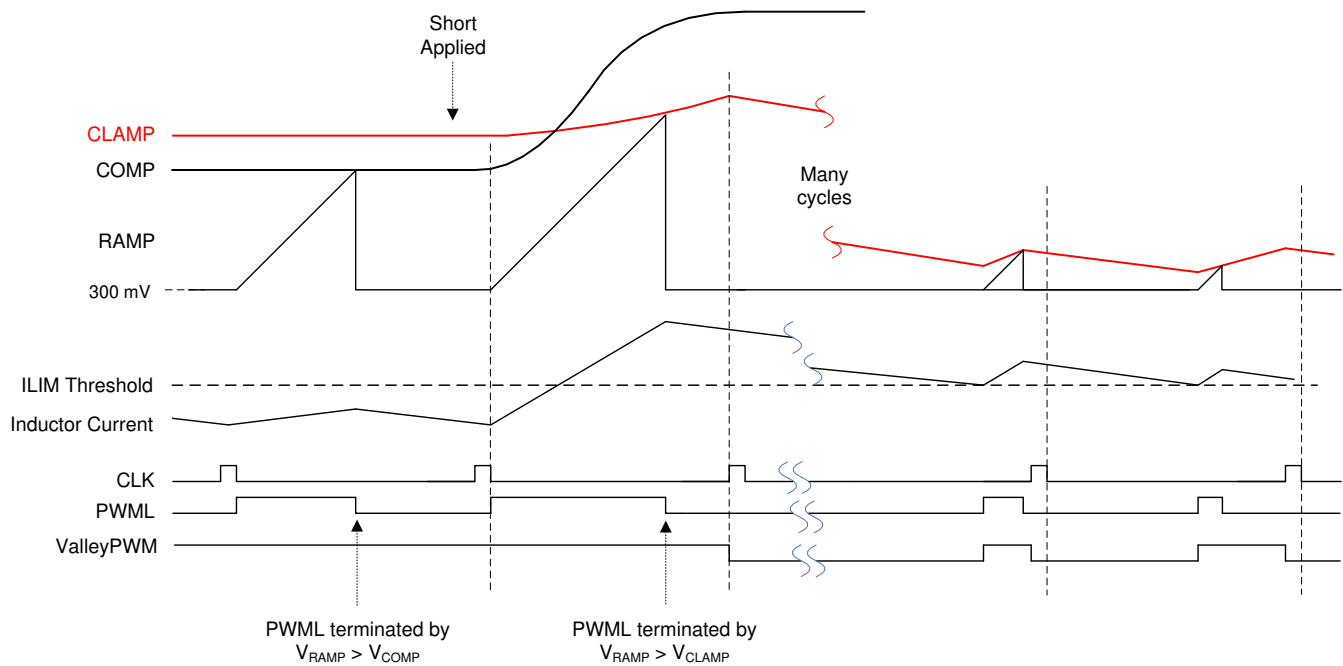


**图 8-11. OCP Duty Cycle Limiting Waveforms**

In addition to valley current limiting, the LM5146 uses a proprietary duty-cycle limiter circuit to reduce the PWM on-time during an overcurrent condition. As shown in 图 8-10, an auxiliary PWM comparator along with a modulated CLAMP voltage limits how quickly the on-time increases in response to a large step in the COMP voltage that typically occurs with a voltage-mode control loop architecture.

As depicted in 图 8-11, the CLAMP voltage,  $V_{CLAMP}$ , is normally regulated above the COMP voltage to provide adequate headroom during a response to a load-on transient. If the COMP voltage rises quickly during an overloaded or shorted output condition, the on-time pulse terminates, thereby limiting the on-time and peak inductor current. Moreover, the CLAMP voltage is reduced if additional valley current limit events occur, further reducing the average output current. If the overcurrent condition exists for 128 continuous clock cycles, a hiccup event is triggered and SS is pulled low for 8192 clock cycles before a soft-start sequence is initiated.

## 8.4 Device Functional Modes

### 8.4.1 Shutdown Mode

The EN/UVLO pin provides ON / OFF control for the LM5146. When the EN/UVLO voltage is below 0.37 V (typical), the device is in shutdown mode. Both the internal bias supply LDO and the switching regulator are off. The quiescent current in shutdown mode drops to 13.5  $\mu$ A (typical) at  $V_{IN} = 48$  V. The LM5146 also includes undervoltage protection of the internal bias LDO. If the internal bias supply voltage is below its UVLO threshold level, the switching regulator remains off.

### 8.4.2 Standby Mode

The internal bias supply LDO has a lower enable threshold than the switching regulator. When the EN/UVLO voltage exceeds 0.42 V (typical) and is below the precision enable threshold (1.2 V typically), the internal LDO is on and regulating. Switching action and output voltage regulation are disabled in standby mode.

### 8.4.3 Active Mode

The LM5146 is in active mode when the VCC voltage is above its rising UVLO threshold of 5 V and the EN/UVLO voltage is above the precision EN threshold of 1.2 V. The simplest way to enable the LM5146 is to tie EN/UVLO to VIN. This allows self start-up of the LM5146 when the input voltage exceeds the VCC threshold plus the LDO dropout voltage from VIN to VCC.

#### 8.4.4 Diode Emulation Mode

The LM5146 provides a diode emulation feature that can be enabled to prevent reverse (drain-to-source) current flow in the low-side MOSFET. When configured for diode emulation, the low-side MOSFET is switched off when reverse current flow is detected by sensing of the SW voltage using a zero-cross comparator. The benefit of this configuration is lower power loss at no-load and light-load conditions, the disadvantage being slower light-load transient response.

The diode emulation feature is configured with the SYNCIN pin. To enable diode emulation and thus achieve discontinuous conduction mode (DCM) operation at light loads, connect the SYNCIN pin to AGND or leave SYNCIN floating. If forced PWM (FPWM) continuous conduction mode (CCM) operation is desired, tie SYNCIN to VCC either directly or using a pullup resistor. Note that diode emulation mode is automatically engaged to prevent reverse current flow during a prebias start-up. A gradual change from DCM to CCM operation provides monotonic start-up performance.

#### 8.4.5 Thermal Shutdown

The LM5146 includes an internal junction temperature monitor. If the temperature exceeds 175°C (typical), thermal shutdown occurs. When entering thermal shutdown, the device:

1. Turns off the high-side and low-side MOSFETs.
2. Pulls SS/TRK and PGOOD low.
3. Turns off the VCC regulator.
4. Initiates a soft-start sequence when the die temperature decreases by the thermal shutdown hysteresis of 20°C (typical).

This is a non-latching protection, and the device will cycle into and out of thermal shutdown if the fault persists.

## 9 Application and Implementation

### Note

Information in the following applications sections is not part of the TI component specification, and TI does not warrant its accuracy or completeness. TI's customers are responsible for determining suitability of components for their purposes, as well as validating and testing their design implementation to confirm system functionality.

### 9.1 Application Information

#### 9.1.1 Design and Implementation

To expedite the process of designing of a LM5146-based regulator for a given application, use the [LM5146 Quickstart Calculator](#) available as a free download, as well as numerous LM5146 reference designs populated in [TI Designs™](#) reference design library, or the designs provided in [# 9.2](#). The LM5146 is also [WEBENCH® Designer](#) enabled.

#### 9.1.2 Power Train Components

Comprehensive knowledge and understanding of the power train components are key to successfully completing a synchronous buck regulator design.

##### 9.1.2.1 Inductor

For most applications, choose an inductance such that the inductor ripple current,  $\Delta I_L$ , is between 30% and 40% of the maximum DC output current at nominal input voltage. Choose the inductance using [Equation 7](#) based on a peak inductor current given by [Equation 8](#).

$$L_F = \frac{V_{OUT}}{V_{IN}} \cdot \left( \frac{V_{IN} - V_{OUT}}{\Delta I_L \cdot F_{SW}} \right) \quad (7)$$

$$I_{L(peak)} = I_{OUT} + \frac{\Delta I_L}{2} \quad (8)$$

Check the inductor data sheet to ensure that the saturation current of the inductor is well above the peak inductor current of a particular design. Ferrite designs have very low core loss and are preferred at high switching frequencies, so design goals can then concentrate on copper loss and preventing saturation. Low inductor core loss is evidenced by reduced no-load input current and higher light-load efficiency. However, ferrite core materials exhibit a hard saturation characteristic and the inductance collapses abruptly when the saturation current is exceeded. This results in an abrupt increase in inductor ripple current, higher output voltage ripple, not to mention reduced efficiency and compromised reliability. Note that the saturation current of an inductor generally decreases as its core temperature increases. Of course, accurate overcurrent protection is key to avoiding inductor saturation.

##### 9.1.2.2 Output Capacitors

Ordinarily, the output capacitor energy store of the regulator combined with the control loop response are prescribed to maintain the integrity of the output voltage within the dynamic (transient) tolerance specifications. The usual boundaries restricting the output capacitor in power management applications are driven by finite available PCB area, component footprint and profile, and cost. The capacitor parasitics—equivalent series resistance (ESR) and equivalent series inductance (ESL)—take greater precedence in shaping the load transient response of the regulator as the load step amplitude and slew rate increase.

The output capacitor,  $C_{OUT}$ , filters the inductor ripple current and provides a reservoir of charge for step-load transient events. Typically, ceramic capacitors provide extremely low ESR to reduce the output voltage ripple and noise spikes, while tantalum and electrolytic capacitors provide a large bulk capacitance in a relatively compact footprint for transient loading events.

Based on the static specification of peak-to-peak output voltage ripple denoted by  $\Delta V_{OUT}$ , choose an output capacitance that is larger than that given by Equation 9.

$$C_{OUT} \geq \frac{\Delta I_L}{8 \cdot F_{SW} \sqrt{\Delta V_{OUT}^2 - (R_{ESR} \cdot \Delta I_L)^2}} \quad (9)$$

图 9-1 conceptually illustrates the relevant current waveforms during both load step-up and step-down transitions. As shown, the large-signal slew rate of the inductor current is limited as the inductor current ramps to match the new load-current level following a load transient. This slew-rate limiting exacerbates the deficit of charge in the output capacitor, which must be replenished as rapidly as possible during and after the load step-up transient. Similarly, during and after a load step-down transient, the slew rate limiting of the inductor current adds to the surplus of charge in the output capacitor that must be depleted as quickly as possible.

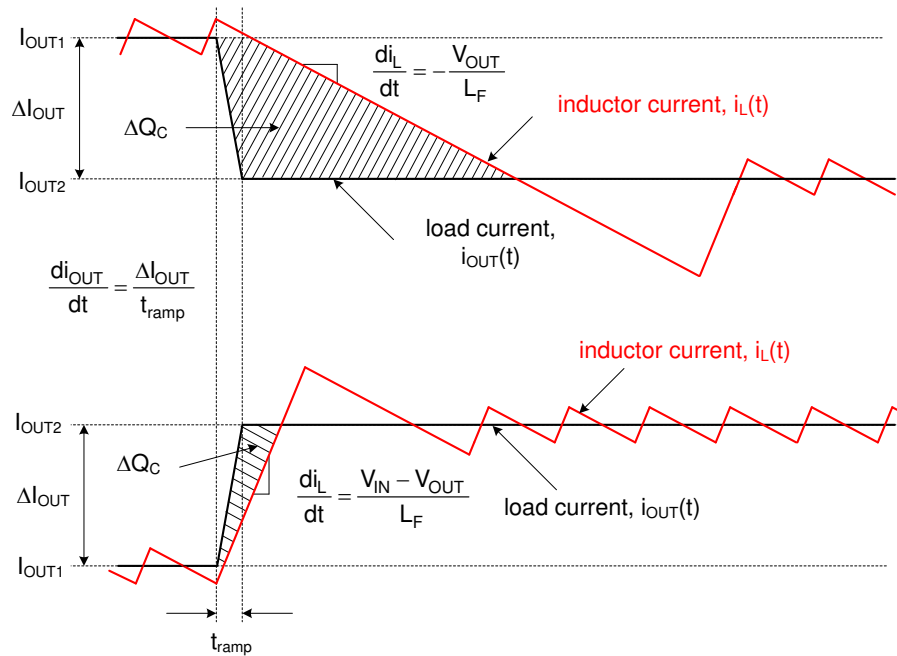


图 9-1. Load Transient Response Representation Showing  $C_{OUT}$  Charge Surplus or Deficit

In a typical regulator application of 48-V input to low output voltage (for example, 5 V), the load-off transient represents the worst case in terms of output voltage transient deviation. In that conversion ratio application, the steady-state duty cycle is approximately 10% and the large-signal inductor current slew rate when the duty cycle collapses to zero is approximately  $-V_{OUT}/L$ . Compared to a load-on transient, the inductor current takes much longer to transition to the required level. The surplus of charge in the output capacitor causes the output voltage to significantly overshoot. In fact, to deplete this excess charge from the output capacitor as quickly as possible, the inductor current must ramp below its nominal level following the load step. In this scenario, a large output capacitance can be advantageously employed to absorb the excess charge and limit the voltage overshoot.

To meet the dynamic specification of output voltage overshoot during such a load-off transient (denoted as  $\Delta V_{OVERSHOOT}$  with step reduction in output current given by  $\Delta I_{OUT}$ ), the output capacitance should be larger than

$$C_{OUT} \geq \frac{L_F \cdot \Delta I_{OUT}^2}{(V_{OUT} + \Delta V_{OVERSHOOT})^2 - V_{OUT}^2} \quad (10)$$

The ESR of a capacitor is provided in the manufacturer's data sheet either explicitly as a specification or implicitly in the impedance vs. frequency curve. Depending on type, size and construction, electrolytic capacitors have significant ESR, 5 mΩ and above, and relatively large ESL, 5 nH to 20 nH. PCB traces contribute some parasitic resistance and inductance as well. Ceramic output capacitors, on the other hand, have low ESR and

ESL contributions at the switching frequency, and the capacitive impedance component dominates. However, depending on package and voltage rating of the ceramic capacitor, the effective capacitance can drop quite significantly with applied DC voltage and operating temperature.

Ignoring the ESR term in Equation 9 gives a quick estimation of the minimum ceramic capacitance necessary to meet the output ripple specification. One to four 47-μF, 10-V, X7R capacitors in 1206 or 1210 footprint is a common choice. Use Equation 10 to determine if additional capacitance is necessary to meet the load-off transient overshoot specification.

A composite implementation of ceramic and electrolytic capacitors highlights the rationale for paralleling capacitors of dissimilar chemistries yet complementary performance. The frequency response of each capacitor is accretive in that each capacitor provides desirable performance over a certain portion of the frequency range. While the ceramic provides excellent mid- and high-frequency decoupling characteristics with its low ESR and ESL to minimize the switching frequency output ripple, the electrolytic device with its large bulk capacitance provides low-frequency energy storage to cope with load transient demands.

### 9.1.2.3 Input Capacitors

Input capacitors are necessary to limit the input ripple voltage to the buck power stage due to switching-frequency AC currents. TI recommends using X5R or X7R dielectric ceramic capacitors to provide low impedance and high RMS current rating over a wide temperature range. To minimize the parasitic inductance in the switching loop, position the input capacitors as close as possible to the drain of the high-side MOSFET and the source of the low-side MOSFET. The input capacitor RMS current is given by Equation 11.

$$I_{CIN,rms} = \sqrt{D \cdot \left( I_{OUT}^2 \cdot (1-D) + \frac{\Delta I_L^2}{12} \right)} \quad (11)$$

The highest input capacitor RMS current occurs at  $D = 0.5$ , at which point the RMS current rating of the capacitors should be greater than half the output current.

Ideally, the DC component of input current is provided by the input voltage source and the AC component by the input filter capacitors. Neglecting inductor ripple current, the input capacitors source current of amplitude  $(I_{OUT} - I_{IN})$  during the  $D$  interval and sinks  $I_{IN}$  during the  $1-D$  interval. Thus, the input capacitors conduct a square-wave current of peak-to-peak amplitude equal to the output current. It follows that the resultant capacitive component of AC ripple voltage is a triangular waveform. Together with the ESR-related ripple component, the peak-to-peak ripple voltage amplitude is given by Equation 12.

$$\Delta V_{IN} = \frac{I_{OUT} \cdot D \cdot (1-D)}{F_{SW} \cdot C_{IN}} + I_{OUT} \cdot R_{ESR} \quad (12)$$

The input capacitance required for a particular load current, based on an input voltage ripple specification of  $\Delta V_{IN}$ , is given by Equation 13.

$$C_{IN} \geq \frac{D \cdot (1-D) \cdot I_{OUT}}{F_{SW} \cdot (\Delta V_{IN} - R_{ESR} \cdot I_{OUT})} \quad (13)$$

Low-ESR ceramic capacitors can be placed in parallel with higher valued bulk capacitance to provide optimized input filtering for the regulator and damping to mitigate the effects of input parasitic inductance resonating with high-Q ceramics. One bulk capacitor of sufficiently high current rating and two or three 2.2-μF 100-V X7R ceramic decoupling capacitors are usually sufficient. Select the input bulk capacitor based on its ripple current rating and operating temperature.

### 9.1.2.4 Power MOSFETs

The choice of power MOSFETs has significant impact on DC/DC regulator performance. A MOSFET with low on-state resistance,  $R_{DS(on)}$ , reduces conduction loss, whereas low parasitic capacitances enable faster

transition times and reduced switching loss. Normally, the lower the  $R_{DS(on)}$  of a MOSFET, the higher the gate charge and output charge ( $Q_G$  and  $Q_{OSS}$  respectively), and vice versa. As a result, the product  $R_{DS(on)} \times Q_G$  is commonly specified as a MOSFET figure-of-merit. Low thermal resistance ensures that the MOSFET power dissipation does not result in excessive MOSFET die temperature.

The main parameters affecting power MOSFET selection in a LM5146 application are as follows:

- $R_{DS(on)}$  at  $V_{GS} = 7.5\text{ V}$
- Drain-source voltage rating,  $BV_{DSS}$ , typically 60 V, 80 V, or 100 V, depending on maximum input voltage
- Gate charge parameters at  $V_{GS} = 7.5\text{ V}$
- Output charge,  $Q_{OSS}$ , at the relevant input voltage
- Body diode reverse recovery charge,  $Q_{RR}$
- Gate threshold voltage,  $V_{GS(th)}$ , derived from the Miller plateau evident in the  $Q_G$  versus  $V_{GS}$  plot in the MOSFET data sheet. With a Miller plateau voltage typically in the range of 2 V to 5 V, the 7.5-V gate drive amplitude of the LM5146 provides an adequately-enhanced MOSFET when on and a margin against  $Cdv/dt$  shoot-through when off.

The MOSFET-related power losses are summarized by the equations presented in 表 9-1, where suffixes 1 and 2 represent high-side and low-side MOSFET parameters, respectively. While the influence of inductor ripple current is considered, second-order loss modes, such as those related to parasitic inductances and SW node ringing, are not included. Consult the [LM5146 Quickstart Calculator](#) to assist with power loss calculations.

**表 9-1. Buck Regulator MOSFET Power Losses**

POWER LOSS MODE	HIGH-SIDE MOSFET	LOW-SIDE MOSFET
MOSFET conduction <sup>(2)</sup> (3)	$P_{cond1} = D \cdot \left( I_{OUT}^2 + \frac{\Delta I_L^2}{12} \right) \cdot R_{DS(on)1}$	$P_{cond2} = D' \cdot \left( I_{OUT}^2 + \frac{\Delta I_L^2}{12} \right) \cdot R_{DS(on)2}$
MOSFET switching	$P_{sw1} = \frac{V_{IN} \cdot F_{SW}}{2} \left[ \left( I_{OUT} - \frac{\Delta I_L}{2} \right) \cdot t_R + \left( I_{OUT} + \frac{\Delta I_L}{2} \right) \cdot t_F \right]$	Negligible
MOSFET gate drive <sup>(1)</sup>	$P_{Gate1} = V_{CC} \cdot F_{SW} \cdot Q_{G1}$	$P_{Gate2} = V_{CC} \cdot F_{SW} \cdot Q_{G2}$
MOSFET output charge <sup>(4)</sup>	$P_{Coss} = F_{SW} \cdot (V_{IN} \cdot Q_{OSS2} + E_{OSS1} - E_{OSS2})$	
Body diode conduction	N/A	$P_{condbo} = V_F \cdot F_{SW} \left[ \left( I_{OUT} + \frac{\Delta I_L}{2} \right) \cdot t_{dt1} + \left( I_{OUT} - \frac{\Delta I_L}{2} \right) \cdot t_{dt2} \right]$
Body diode reverse recovery <sup>(5)</sup>	$P_{RR} = V_{IN} \cdot F_{SW} \cdot Q_{RR2}$	

- (1) Gate drive loss is apportioned based on the internal gate resistance of the MOSFET, externally-added series gate resistance and the relevant gate driver resistance of the LM5146.
- (2) MOSFET  $R_{DS(on)}$  has a positive temperature coefficient of approximately 4500 ppm/°C. The MOSFET junction temperature,  $T_J$ , and its rise over ambient temperature is dependent upon the device total power dissipation and its thermal impedance. When operating at or near minimum input voltage, ensure that the MOSFET  $R_{DS(on)}$  is rated at  $V_{GS} = 4.5\text{ V}$ .
- (3)  $D' = 1 - D$  is the duty cycle complement.
- (4) MOSFET output capacitances,  $C_{OSS1}$  and  $C_{OSS2}$ , are highly non-linear with voltage. These capacitances are charged losslessly by the inductor current at high-side MOSFET turn-off. During turn-on, however, a current flows from the input to charge  $C_{OSS2}$  of the low-side MOSFET.  $E_{OSS1}$ , the energy of  $C_{OSS1}$ , is dissipated at turnon, but this is offset by the stored energy  $E_{OSS2}$  on  $C_{OSS2}$ .
- (5) MOSFET body diode reverse recovery charge,  $Q_{RR}$ , depends on many parameters, particularly forward current, current transition speed, and temperature.

The high-side (control) MOSFET carries the inductor current during the PWM on-time (or D interval) and typically incurs most of the switching losses. It is therefore imperative to choose a high-side MOSFET that balances conduction and switching loss contributions. The total power dissipation in the high-side MOSFET is the sum of the losses due to conduction, switching (voltage-current overlap), output charge, and typically two-thirds of the net loss attributed to body diode reverse recovery.

The low-side (synchronous) MOSFET carries the inductor current when the high-side MOSFET is off (or 1–D interval). The low-side MOSFET switching loss is negligible as it is switched at zero voltage – current just commutates from the channel to the body diode or vice versa during the transition deadtimes. The LM5146, with

its adaptive gate drive timing, minimizes body diode conduction losses when both MOSFETs are off. Such losses scale directly with switching frequency.

In high step-down ratio applications, the low-side MOSFET carries the current for a large portion of the switching period. Therefore, to attain high efficiency, it is critical to optimize the low-side MOSFET for low  $R_{DS(on)}$ . In cases where the conduction loss is too high or the target  $R_{DS(on)}$  is lower than available in a single MOSFET, connect two low-side MOSFETs in parallel. The total power dissipation of the low-side MOSFET is the sum of the losses due to channel conduction, body diode conduction, and typically one-third of the net loss attributed to body diode reverse recovery. The LM5146 is well suited to drive TI's portfolio of NexFET™ power MOSFETs.

### 9.1.3 Control Loop Compensation

The poles and zeros inherent to the power stage and compensator are respectively illustrated by red and blue dashed rings in the schematic embedded in 表 9-2. The compensation network typically employed with voltage-mode control is a Type-III circuit with three poles and two zeros. One compensator pole is located at the origin to realize high DC gain. The normal compensation strategy uses two compensator zeros to counteract the LC double pole, one compensator pole located to nullify the output capacitor ESR zero, with the remaining compensator pole located at one-half switching frequency to attenuate high frequency noise. The resistor divider network to FB determines the desired output voltage. Note that the lower feedback resistor,  $R_{FB2}$ , has no impact on the control loop from an AC standpoint because the FB node is the input to an error amplifier and is effectively at AC ground. Hence, the control loop is designed irrespective of output voltage level. The proviso here is the necessary output capacitance derating with bias voltage and temperature.

**表 9-2. Buck Regulator Poles and Zeros**

POWER STAGE POLES	POWER STAGE ZEROS	COMPENSATOR POLES	COMPENSATOR ZEROS
$\omega_o = \frac{1}{\sqrt{L_F \cdot C_{OUT} \left( \frac{1 + R_{ESR}/R_L}{1 + R_{ESR}/R_{DAMP}} \right)}}$ $\cong \frac{1}{\sqrt{L_F \cdot C_{OUT}}}$ <p>(1) (2)</p>	$\omega_{ESR} = \frac{1}{R_{ESR} \cdot C_{OUT}}$ $\omega_L = \frac{L_F}{R_{DAMP}}$	$\omega_{p1} = \frac{1}{R_{C1} \cdot (C_{C1} \parallel C_{C2})} \cong \frac{1}{R_{C1} \cdot C_{C2}}$ $\omega_{p2} = \frac{1}{R_{C2} \cdot C_{C3}}$	$\omega_{z1} = \frac{1}{R_{C1} \cdot C_{C1}}$ $\omega_{z2} = \frac{1}{(R_{FB1} + R_{C2}) \cdot C_{C3}}$

(1)  $R_{ESR}$  represents the ESR of the output capacitor  $C_{OUT}$ .

(2)  $R_{DAMP} = D \cdot R_{DS(on)high-side} + (1-D) \cdot R_{DS(on)low-side} + R_{DCR}$ , shown as a lumped element in the schematic, represents the effective series damping resistance.

The small-signal open-loop response of a buck regulator is the product of modulator, power train and compensator transfer functions. The power stage transfer function can be represented as a complex pole pair



associated with the output LC filter and a zero related to the ESR of the output capacitor. The DC (and low frequency) gain of the modulator and power stage is  $V_{IN}/V_{RAMP}$ . The gain from COMP to the average voltage at the input of the LC filter is held essentially constant by the PWM line feedforward feature of the LM5146 (15 V/V or 23.5 dB).

Complete expressions for small-signal frequency analysis are presented in 表 9-3. The transfer functions are denoted in normalized form. While the loop gain is of primary importance, a regulator is not specified directly by its loop gain but by its performance related characteristics, namely closed-loop output impedance and audio susceptibility.

**表 9-3. Buck Regulator Small-Signal Analysis**

TRANSFER FUNCTION	EXPRESSION
Open-loop transfer function	$T_V(s) = \frac{\hat{v}_{comp}(s)}{\hat{v}_o(s)} \cdot \frac{\hat{v}_o(s)}{\hat{d}(s)} \cdot \frac{\hat{d}(s)}{\hat{v}_{comp}(s)} = G_c(s) \cdot G_{vd}(s) \cdot F_M$
Duty-cycle-to-output transfer function	$G_{vd}(s) = \frac{\hat{v}_o(s)}{\hat{d}(s)} \bigg _{\substack{\hat{v}_{in}(s)=0 \\ \hat{i}_o(s)=0}} = V_{IN} \frac{1 + \frac{s}{\omega_{ESR}}}{1 + \frac{s}{Q_o \omega_o} + \frac{s^2}{\omega_o^2}}$
Compensator transfer function <sup>(1)</sup>	$G_c(s) = \frac{\hat{v}_{comp}(s)}{\hat{v}_o(s)} = K_{mid} \frac{\left(1 + \frac{\omega_{z1}}{s}\right) \left(1 + \frac{s}{\omega_{z2}}\right)}{\left(1 + \frac{s}{\omega_{p1}}\right) \left(1 + \frac{s}{\omega_{p2}}\right)}$
Modulator transfer function	$F_M = \frac{\hat{d}(s)}{\hat{v}_{comp}(s)} = \frac{1}{V_{RAMP}}$

(1)  $K_{mid} = R_{C1}/R_{FB1}$  is the mid-band gain of the compensator. By expressing one of the compensator zeros in inverted zero format, the mid-band gain is denoted explicitly.

图 9-2 shows the open-loop response gain and phase. The poles and zeros of the system are marked with x and o symbols, respectively, and a + symbol indicates the crossover frequency. When plotted on a log (dB) scale, the open-loop gain is effectively the sum of the individual gain components from the modulator, power stage, and compensator (see 图 9-3). The open-loop response of the system is measured experimentally by breaking the loop, injecting a variable-frequency oscillator signal, and recording the ensuing frequency response using a network analyzer setup.

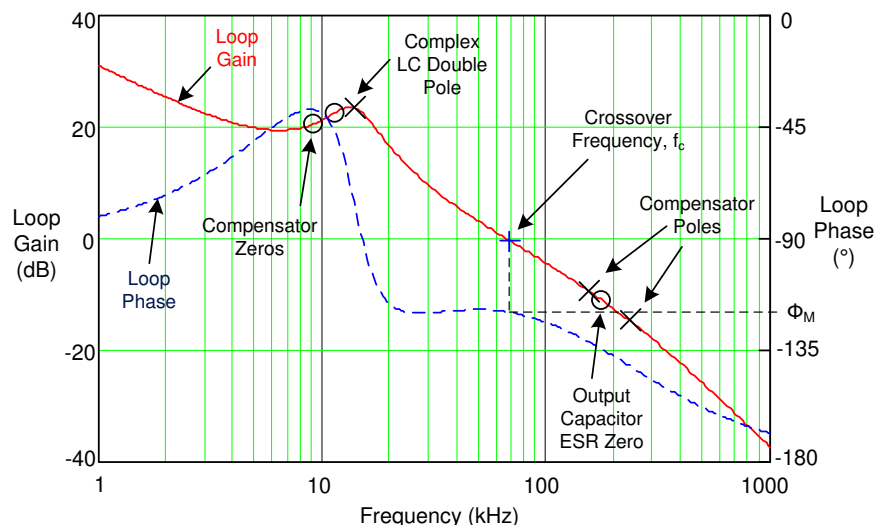


**图 9-2. Typical Buck Regulator Loop Gain and Phase With Voltage-Mode Control**



If the pole located at  $\omega_{p1}$  cancels the zero located at  $\omega_{ESR}$  and the pole at  $\omega_{p2}$  is located well above crossover, the expression for the loop gain,  $T_v(s)$  in 表 9-3, can be manipulated to yield the simplified expression given in Equation 14.

$$T_v(s) = R_{C1} \cdot C_{C3} \cdot \frac{V_{IN}}{V_{RAMP}} \cdot \frac{\omega_o^2}{s} \quad (14)$$

Essentially, a multi-order system is reduced to a single-order approximation by judicious choice of compensator components. A simple solution for the crossover frequency (denoted as  $f_c$  in 图 9-2) with Type-III voltage-mode compensation is derived as shown in Equation 15 and Equation 16.

$$\omega_c = 2\pi \cdot f_c = \omega_o \cdot K_{mid} \cdot \frac{V_{IN}}{V_{RAMP}} \quad (15)$$

$$K_{mid} = \frac{f_c}{f_o} \cdot \frac{1}{k_{FF}} = \frac{R_{C1}}{R_{FB1}} \quad (16)$$

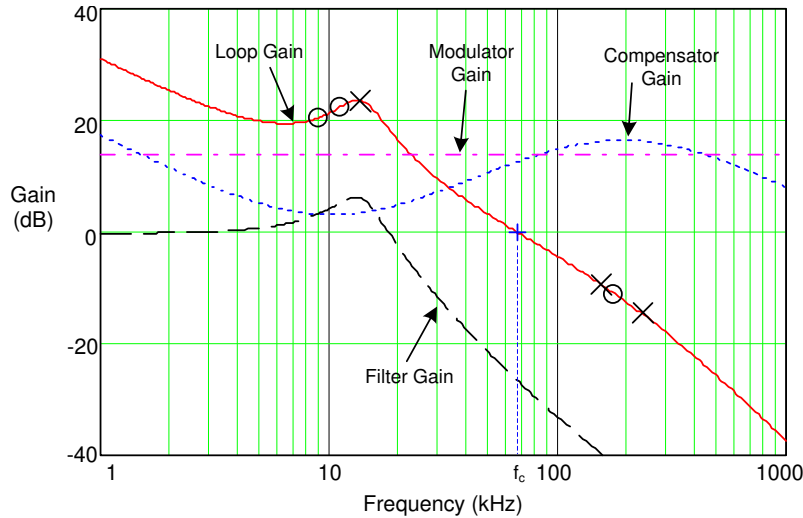


**图 9-3. Buck Regulator Constituent Gain Components**

The loop crossover frequency is usually selected between one-tenth to one-fifth of switching frequency. Inserting an appropriate crossover frequency into Equation 16 gives a target for the mid-band gain of the compensator,  $K_{mid}$ . Given an initial value for  $R_{FB1}$ ,  $R_{FB2}$  is then selected based on the desired output voltage. Values for  $R_{C1}$ ,  $R_{C2}$ ,  $C_{C1}$ ,  $C_{C2}$ , and  $C_{C3}$  are calculated from the design expressions listed in 表 9-4, with the premise that the compensator poles and zeros are set as follows:  $\omega_{z1} = 0.5 \cdot \omega_o$ ,  $\omega_{z2} = \omega_o$ ,  $\omega_{p1} = \omega_{SW}/2$ , and  $\omega_{p2} = \omega_{ESR}$ .

**表 9-4. Compensation Component Selection**

RESISTORS	CAPACITORS
$R_{FB2} = \frac{R_{FB1}}{(V_{OUT}/V_{REF}) - 1}$	$C_{C1} = \frac{1}{\omega_{z1} \cdot R_{C1}}$
$R_{C1} = K_{mid} \cdot R_{FB1}$	$C_{C2} = \frac{1}{\omega_{p1} \cdot R_{C1}}$
$R_{C2} = \frac{1}{\omega_{p2} \cdot C_{C3}}$	$C_{C3} = \frac{1}{\omega_{z2} \cdot R_{FB1}}$

Referring to the bode plot in 图 9-2, the phase margin, indicated as  $\phi_M$ , is the difference between the loop phase and  $-180^\circ$  at crossover. A target of  $50^\circ$  to  $70^\circ$  for this parameter is considered ideal. Additional phase boost is dialed in by locating the compensator zeros at a frequency lower than the LC double pole. This helps mitigate the phase dip associated with the LC filter, particularly at light loads when the Q-factor is higher and the phase dip becomes especially prominent. The ramification of low phase in the frequency domain is an under-damped transient response in the time domain.

The power supply designer now has all the necessary expressions to optimally position the loop crossover frequency while maintaining adequate phase margin over the required line, load and temperature operating ranges. The [LM5146 Quickstart Calculator](#) is available to expedite these calculations and to adjust the bode plot as needed.

### 9.1.4 EMI Filter Design

Switching regulators exhibit negative input impedance, which is lowest at the minimum input voltage. An underdamped LC filter exhibits a high output impedance at the resonant frequency of the filter. For stability, the filter output impedance must be less than the absolute value of the converter input impedance.

$$Z_{IN} = \left| -\frac{V_{IN(min)}^2}{P_{IN}} \right| \quad (17)$$

The EMI filter design steps are as follows:

- Calculate the required attenuation of the EMI filter at the switching frequency, where  $C_{IN}$  represents the existing capacitance at the input of the switching converter.
- Input filter inductor  $L_{IN}$  is usually selected between  $1\ \mu\text{H}$  and  $10\ \mu\text{H}$ , but it can be lower to reduce losses in a high current design.
- Calculate input filter capacitor  $C_F$ .

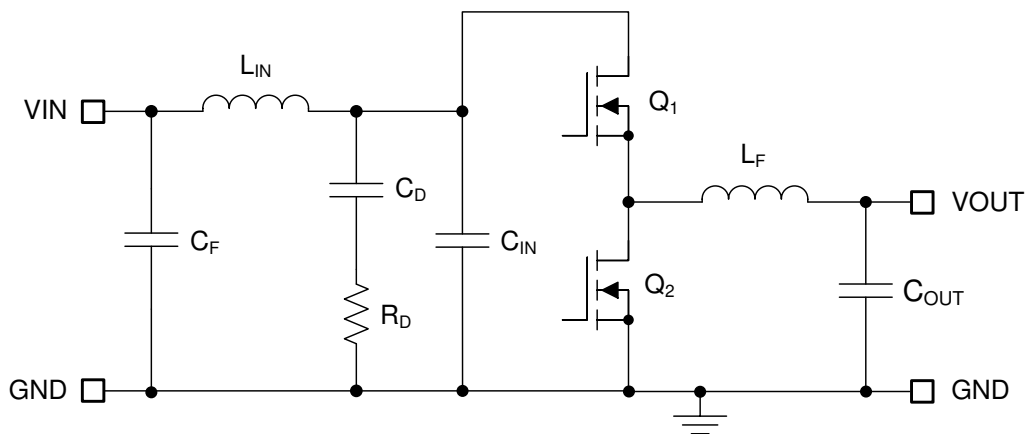


图 9-4. Buck Regulator With  $\pi$ -Stage EMI Filter

By calculating the first harmonic current from the Fourier series of the input current waveform and multiplying it by the input impedance (the impedance is defined by the existing input capacitor  $C_{IN}$ ), a formula is derived to obtain the required attenuation as shown by Equation 18.

$$\text{Attn} = 20\log\left(\frac{I_{L(PEAK)}}{\pi^2 \cdot F_{SW} \cdot C_{IN}} \cdot \sin(\pi \cdot D_{MAX}) \cdot \frac{1}{1\ \mu\text{V}}\right) - V_{MAX} \quad (18)$$

where

- $V_{MAX}$  is the noise specification in dB $\mu\text{V}$  from the applicable EMI standard, for example CISPR 32 Class B
- $C_{IN}$  is the existing input capacitance of the buck regulator

- $D_{MAX}$  is the maximum duty cycle
- $I_{PEAK}$  is the peak inductor current

For filter design purposes, the current at the input can be modeled as a square-wave. Determine the EMI filter capacitance  $C_F$  from [Equation 19](#).

$$C_F = \frac{1}{L_{IN}} \left( \frac{10^{\frac{|Att_n|}{40}}}{2\pi \cdot F_{SW}} \right)^2 \quad (19)$$

Adding an input filter to a switching regulator modifies the control-to-output transfer function. The output impedance of the filter must be sufficiently small such that the input filter does not significantly affect the loop gain of the buck converter. The impedance peaks at the filter resonant frequency. The resonant frequency of the filter is given by [Equation 20](#).

$$f_{res} = \frac{1}{2\pi \cdot \sqrt{L_{IN} \cdot C_F}} \quad (20)$$

The purpose of  $R_D$  is to reduce the peak output impedance of the filter at the resonant frequency. Capacitor  $C_D$  blocks the DC component of the input voltage to avoid excessive power dissipation in  $R_D$ . Capacitor  $C_D$  must have lower impedance than  $R_D$  at the resonant frequency with a capacitance value greater than that of the input capacitor  $C_{IN}$ . This prevents  $C_{IN}$  from interfering with the cutoff frequency of the main filter. Added damping is needed when the output impedance of the filter is high at the resonant frequency (Q of filter formed by  $L_{IN}$  and  $C_{IN}$  is too high). An electrolytic capacitor  $C_D$  can be used for damping with a value given by [Equation 21](#).

$$C_D \geq 4 \cdot C_{IN} \quad (21)$$

Select the damping resistor  $R_D$  using [Equation 22](#).

$$R_D = \sqrt{\frac{L_{IN}}{C_{IN}}} \quad (22)$$

## 9.2 Typical Applications

For step-by-step design procedure, circuit schematics, bill of materials, PCB files, simulation and test results of an LM5146-powered implementation, see [TI Designs](#) reference design library.

### 9.2.1 Design 1 – 12-A High-Efficiency Synchronous Buck DC/DC Regulator

Figure 9-5 shows the schematic diagram of a 5-V, 12-A buck regulator with a switching frequency of 300 kHz. In this example, the target efficiencies are 94% and 92% at input voltages of 24 V and 48 V, respectively. The input UVLO is set to turn on and off at 8 V and 7 V, respectively. The switching frequency is set by means of a synchronization input signal at 300 kHz, and the free-running switching frequency (in the event that the synchronization signal is removed) is set at 250 kHz by resistor  $R_{RT}$ . In terms of control loop performance, the target loop crossover frequency is 40 kHz with a phase margin greater than 50°. The output voltage soft-start time is 6 ms.

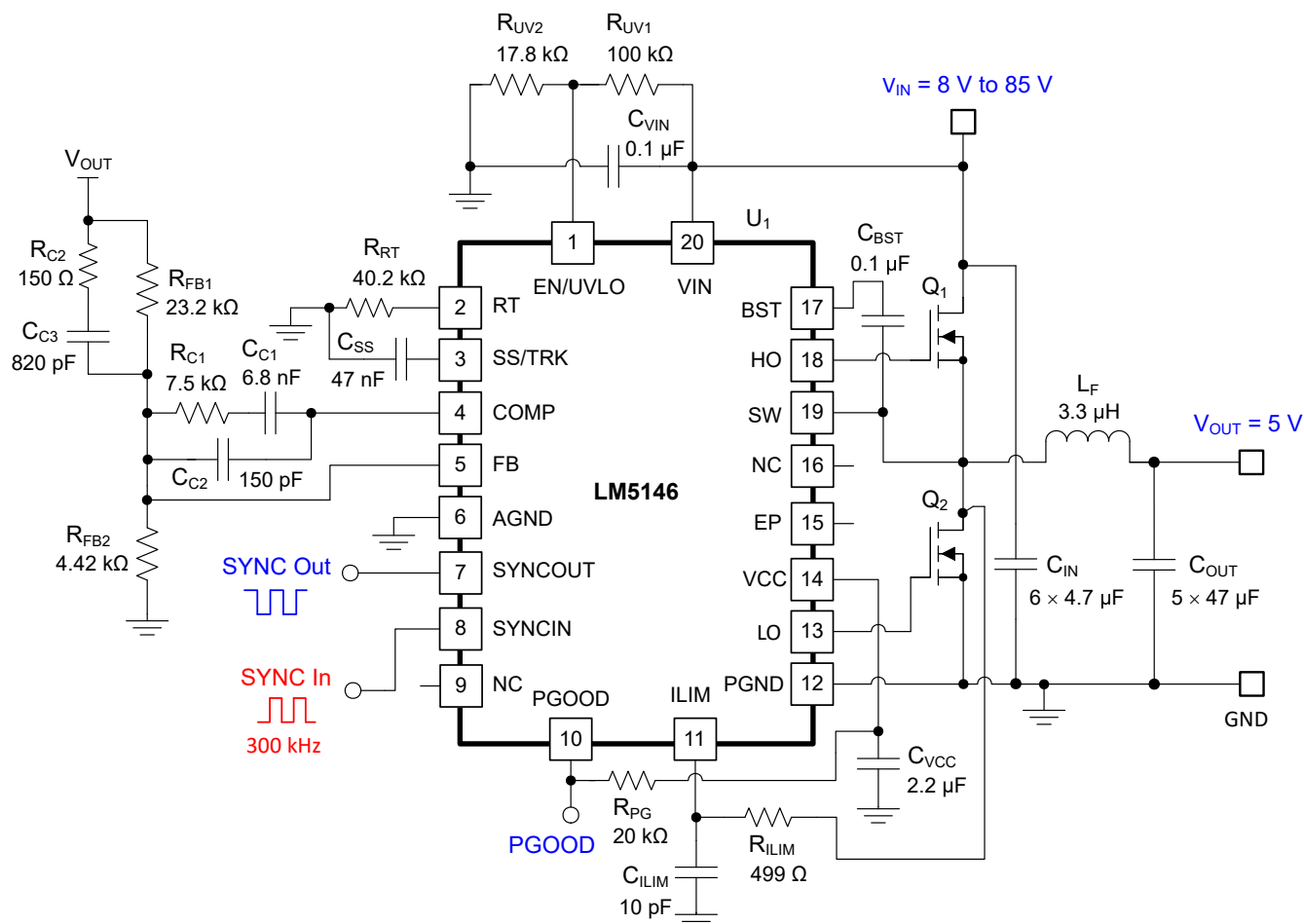


图 9-5. Application Circuit 1 With LM5146 48-V to 5-V, 12-A Buck Regulator at 300 kHz

#### Note

This and subsequent design examples are provided herein to showcase the LM5146 controller in several different applications. Depending on the source impedance of the input supply bus, an electrolytic capacitor may be required at the input to ensure stability, particularly at low input voltage and high output current operating conditions. See [节 10](#) for more detail.

### 9.2.1.1 Design Requirements

The intended input, output, and performance-related parameters pertinent to this design example are shown in 表 9-5.

**表 9-5. Design Parameters**

DESIGN PARAMETER	VALUE
Input voltage range (steady state)	8 V to 85 V
Input transient voltage (peak)	95 V
Output voltage and current	5 V, 12 A
Input voltage UVLO thresholds	8 V on, 7 V off
Switching frequency (SYNC in)	300 kHz
Output voltage regulation	±1%
Load transient peak voltage deviation	< 100 mV

### 9.2.1.2 Detailed Design Procedure

The design procedure for an LM5146 based regulator for a given application is streamlined by using the [LM5146 Quickstart Calculator](#) available as a free download, or by availing of TI's [WEBENCH® Power Designer](#). Such tools are complemented by the availability of LM5145 and LM5146-Q1 evaluation module (EVM) designs, numerous PSPICE models, as well as several LM5146 reference designs populated in the [TI Designs](#) reference design library.

The selected buck converter powertrain components are cited in 表 9-6, and many of the components are available from multiple vendors. The MOSFETs in particular are chosen for both lowest conduction and switching power loss, as discussed in detail in 节 9.1.2.4.

The current limit setpoint in this design is set at 19 A based on the resistor  $R_{ILIM}$  and the 6-mΩ  $R_{DS(on)}$  of the low-side MOSFET (typical at  $T_J = 25^\circ\text{C}$  and  $V_{GS} = 7.5\text{ V}$ ). This design uses a low-DCR, metal-powder inductor, and all-ceramic output capacitor implementation.

**表 9-6. List of Materials for Application Circuit 1**

REFERENCE DESIGNATOR	QTY	SPECIFICATION	MANUFACTURER	PART NUMBER
$C_{IN}$	6	4.7 $\mu\text{F}$ , 100 V, X7S, 1210, ceramic	TDK	CGA6M3X7S2A475K200
			Murata	GCM32DC72A475KE02L
			Taiyo Yuden	HMK325C7475MMHPE
$C_{OUT}$	5	47 $\mu\text{F}$ , 6.3 V, X7R, 1210, ceramic	Murata	GCM32ER70J476KE19L
			Taiyo Yuden	JMK325B7476KMHTR
		47 $\mu\text{F}$ , 6.3 V, X7S, 1210, ceramic	TDK	CGA6P1X7S0J476M
$L_F$	1	3.3 $\mu\text{H}$ , 6.25 mΩ, 19 A, 10.85 × 10.0 × 5.2 mm	Cyntec	VCHA105D-3R3M
		3.3 $\mu\text{H}$ , 5.8 mΩ, 28.6 A, 10.5 × 10.0 × 6.5 mm	TDK	SPM10065VTT-3R3M-D
		3.3 $\mu\text{H}$ , 6.0 mΩ, 17 A, 10.9 × 10.0 × 6.0 mm	Panasonic	ETQP6M3R3YLC
$Q_1$	1	100 V, 22 mΩ, MOSFET, SON 5 × 6	Onsemi	NVMFS6B25NL
$Q_2$	1	100 V, 6 mΩ, MOSFET, SON 5 × 6	Onsemi	FDWS86068-F085
$U_1$	1	Wide $V_{IN}$ synchronous buck controller	Texas Instruments	LM5146RGYR

### 9.2.1.3 Custom Design With WEBENCH® Tools

[Click here](#) to create a custom design using the LM5146 device with the WEBENCH® Power Designer.

1. Start by entering the input voltage ( $V_{IN}$ ), output voltage ( $V_{OUT}$ ), and output current ( $I_{OUT}$ ) requirements.
2. Optimize the design for key parameters such as efficiency, footprint, and cost using the optimizer dial.
3. Compare the generated design with other possible solutions from Texas Instruments.

The WEBENCH Power Designer provides a customized schematic along with a list of materials with real-time pricing and component availability.

In most cases, these actions are available:

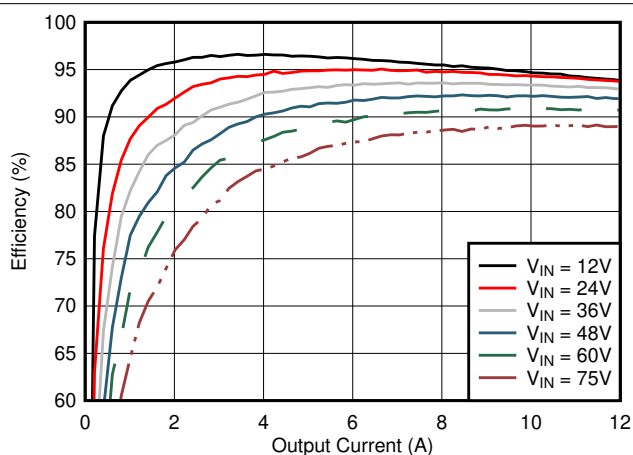
- Run electrical simulations to see important waveforms and circuit performance
- Run thermal simulations to understand board thermal performance
- Export customized schematic and layout into popular CAD formats
- Print PDF reports for the design, and share the design with colleagues

Get more information about WEBENCH tools at [www.ti.com/WEBENCH](http://www.ti.com/WEBENCH).

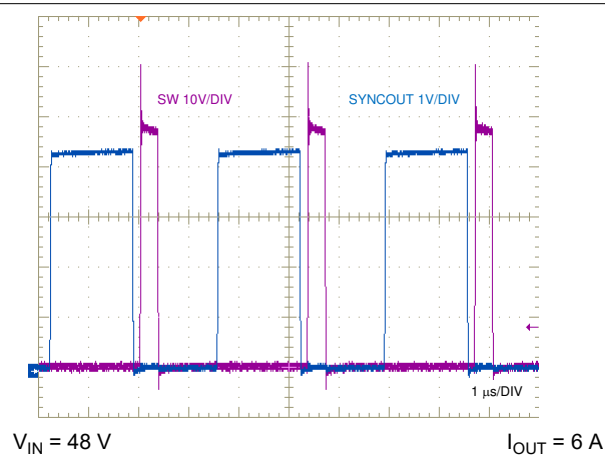
#### **9.2.1.4 Custom Design With Excel Quickstart Tool**

Select components based on the regulator specifications using the [LM5146 Quickstart Calculator](#) available for download from the product folder.

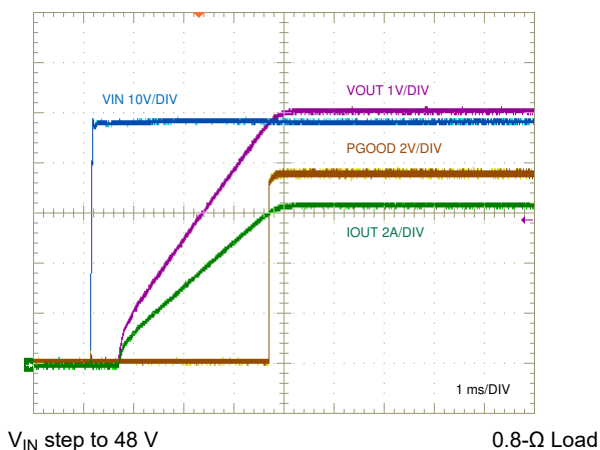
### 9.2.1.5 Application Curves



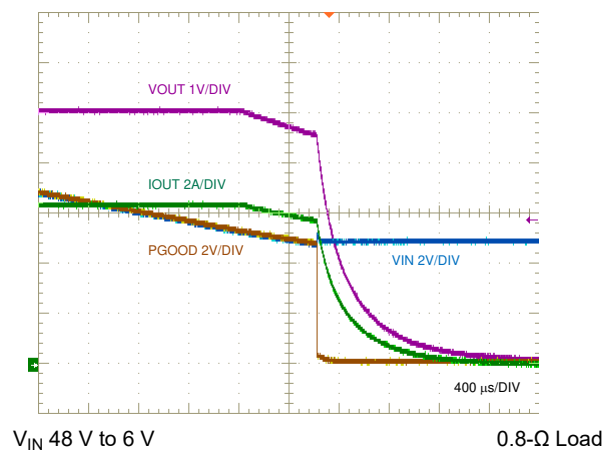
**图 9-6. Efficiency and Power Loss vs  $I_{OUT}$  and  $V_{IN}$**



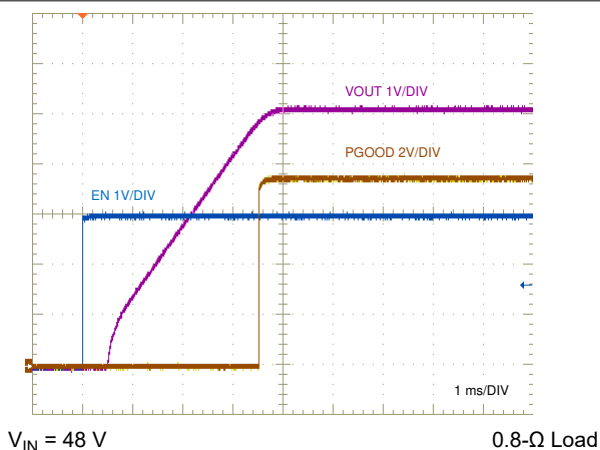
**图 9-7. SYNCOUT and SW Node Voltages**



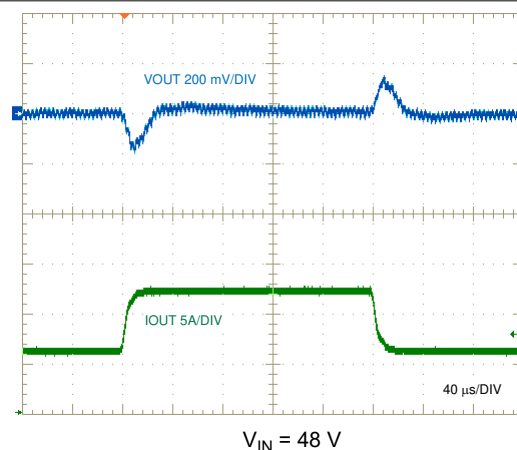
**图 9-8. Start-Up, Resistive Load**



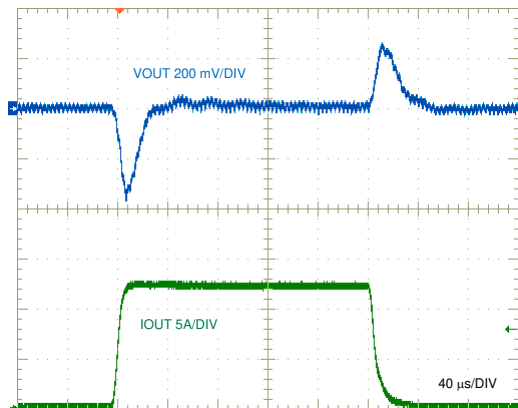
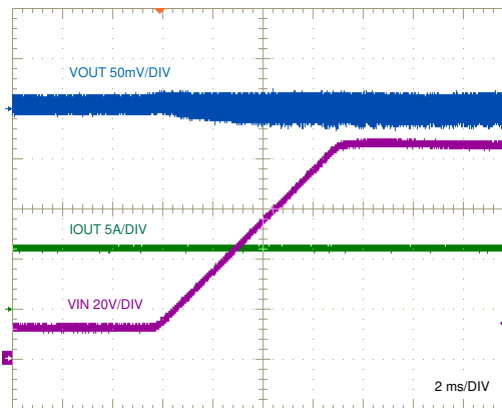
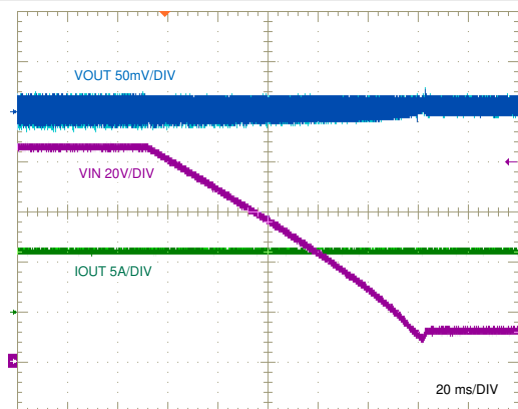
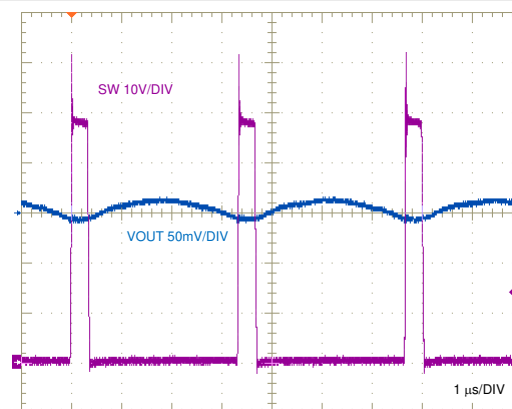
**图 9-9. Shutdown Through UVLO**



**图 9-10. ENABLE ON, Resistive Load**



**图 9-11. Load Transient Response, 6 A to 12 A to 6 A**

 $V_{IN} = 48\text{ V}$ **图 9-12. Load Transient Response, 0 A to 12 A to 0 A** $I_{OUT} = 6\text{ A}$ **图 9-13. Line Transient Response, 12 V to 85 V** $I_{OUT} = 6\text{ A}$ **图 9-14. Line Transient Response, 85 V to 12 V** $V_{IN} = 48\text{ V}$  $I_{OUT} = 0\text{ A}$ **图 9-15. SW Node and Output Ripple Voltages**



## 9.2.2 Design 2 – High Density, 12-V, 8-A Rail From 48-V Telecom Power

图 9-16 shows the schematic diagram of a 400-kHz, 12-V output, 8-A synchronous buck regulator intended for 48-V telecom applications.

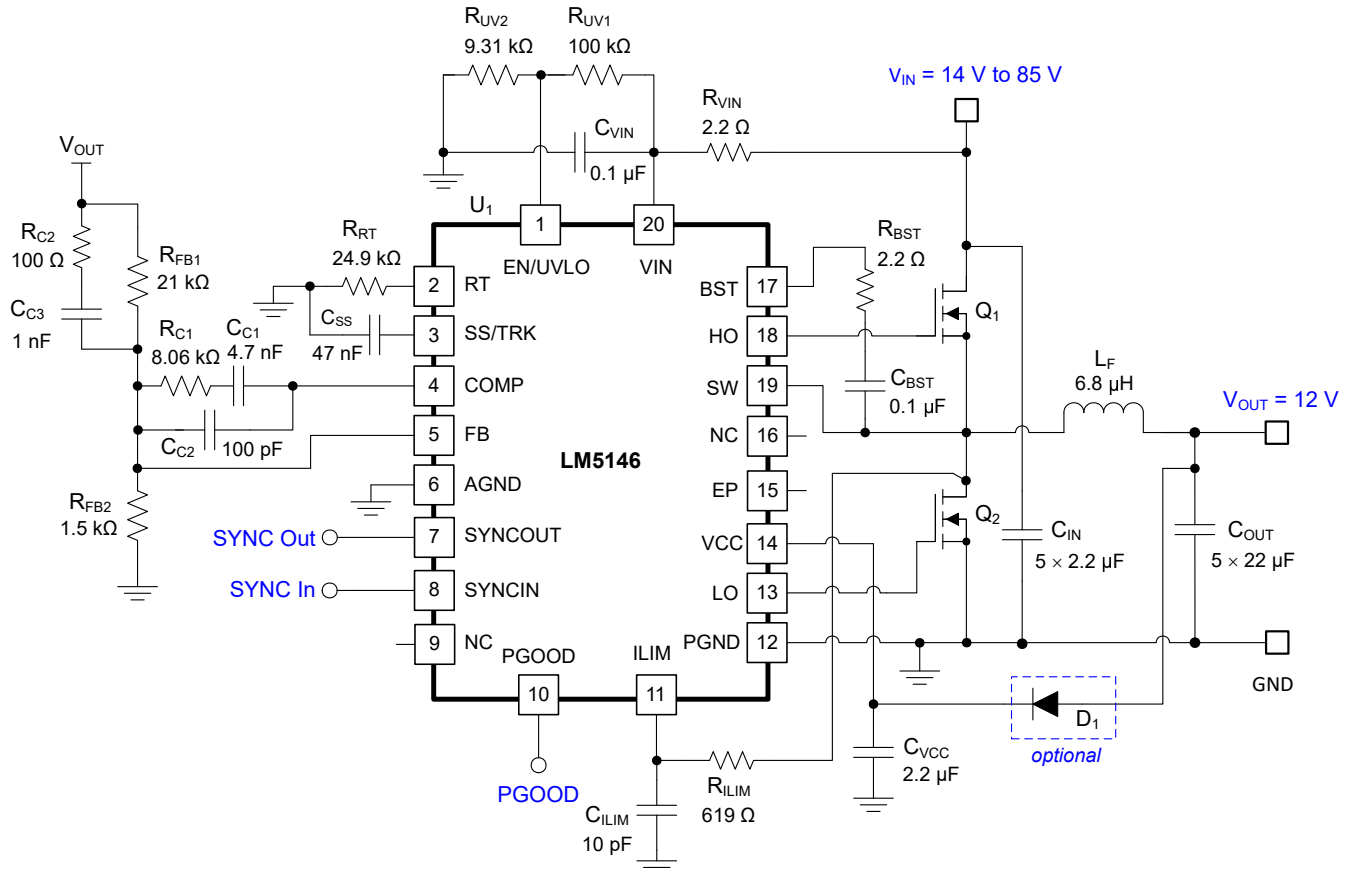


图 9-16. Application Circuit 2 With LM5146 48-V to 12-A Synchronous Buck Regulator at 400 kHz

### 9.2.2.1 Design Requirements

The required input, output, and performance parameters for this application example are shown in 表 9-7.

表 9-7. Design Parameters

DESIGN PARAMETER	VALUE
Input voltage range (steady state)	14 V to 85 V
Input transient voltage (peak)	90 V
Output voltage and current	12 V, 8 A
Input UVLO thresholds	14 V on, 13 V off
Switching frequency	400 kHz
Output voltage regulation	±1%
Load transient peak voltage deviation, 4-A load step	< 120 mV

### 9.2.2.2 Detailed Design Procedure

A high power density, high-efficiency regulator solution uses 100-V power MOSFETs in SON 5-mm × 6-mm packages, together with a low-DCR inductor and all-ceramic capacitor design. The design occupies a footprint of 30 mm × 15 mm on a single-sided PCB. The overcurrent (OC) setpoint in this design is set at 12 A based on the resistor  $R_{ILIM}$  and the 10-mΩ  $R_{DS(on)}$  of the low-side MOSFET (typical at  $T_J = 25^\circ\text{C}$  and  $V_{GS} = 10\text{ V}$ ). The 12-V output is connected to VCC through a diode, D1, to reduce IC bias power dissipation at high input voltages.

The selected buck converter powertrain components are cited in 表 9-8, including power MOSFETs, buck inductor, input and output capacitors, and ICs. Using the [LM5146 Quickstart Calculator](#), compensation components are selected based on a target loop crossover frequency of 40 kHz and phase margin greater than 55°. The output voltage soft-start time is 6 ms based on the selected soft-start capacitance,  $C_{SS}$ , of 47 nF.

**表 9-8. List of Materials for Application Circuit 2**

REFERENCE DESIGNATOR	QTY	SPECIFICATION	MANUFACTURER	PART NUMBER
$C_{IN}$	5	2.2 $\mu$ F, 100 V, X7R, 1210, ceramic	TDK	CGA6N3X7R2A225K
			Taiyo Yuden	HMK325B7225KM-P
		2.2 $\mu$ F, 100 V, X7S, 1206, ceramic	Murata	GCM31CC72A225KE02
$C_{OUT}$	5	22 $\mu$ F, 25 V, X7R, 1210, ceramic	TDK	CGA6P3X7R1E226M
			Murata	GCM32EC71E226KE36
			Taiyo Yuden	TMK325B7226KMHT
$L_F$	1	6.8 $\mu$ H, 12 m $\Omega$ , 13.3 A, 10.85 $\times$ 10.0 $\times$ 5.2 mm	Cyntec	VCHA105D-6R8MS6
		6.8 $\mu$ H, 13.3 m $\Omega$ , 21.4 A, 10.5 $\times$ 10.0 $\times$ 6.5 mm	TDK	SPM10065VT-6R8M-D
$Q_1$	1	100 V, 22 m $\Omega$ , MOSFET, SON 5 $\times$ 6	Onsemi	NVMFS6B25NLT1G
$Q_2$	1	100 V, 10 m $\Omega$ , MOSFET, SON 5 $\times$ 6	Onsemi	NVMFS6B14NLT1G
$U_1$	1	Wide $V_{IN}$ synchronous buck controller	Texas Instruments	LM5146RGYR

As shown in 图 9-16, a 2.2- $\Omega$  resistor in series with  $C_{BST}$  is used to slow the turn-on transition of the high-side MOSFET, reducing the spike amplitude and ringing of the SW node voltage and minimizing the possibility of  $C_{dv}/dt$ -induced shoot-through of the low-side MOSFET. If needed, place an RC snubber (for example, 2.2  $\Omega$  and 100 pF) close to the drain (SW node) and source (PGND) terminals of the low-side MOSFET to further attenuate any SW node voltage overshoot and/or ringing. Please refer to the application note [Reduce Buck Converter EMI and Voltage Stress by Minimizing Inductive Parasitics](#) for more detail.

### 9.2.2.3 Application Curves

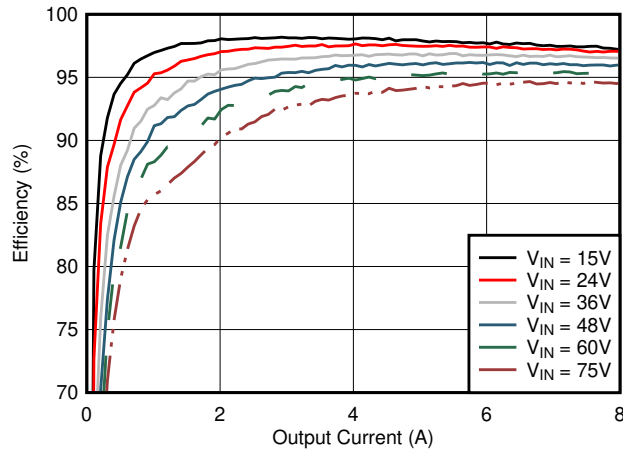


图 9-17. Efficiency vs  $I_{OUT}$  and  $V_{IN}$

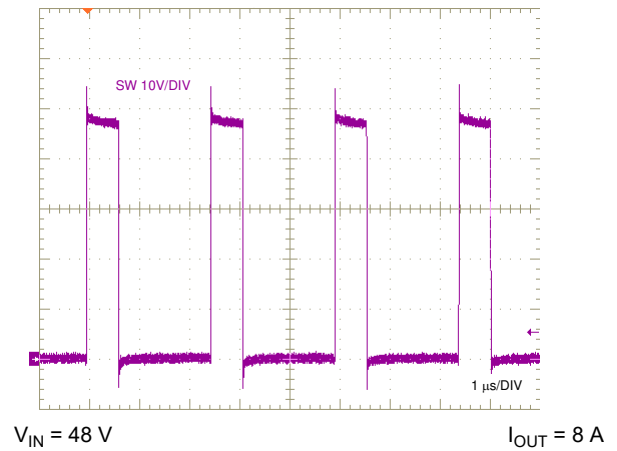


图 9-18. SW Node Voltages

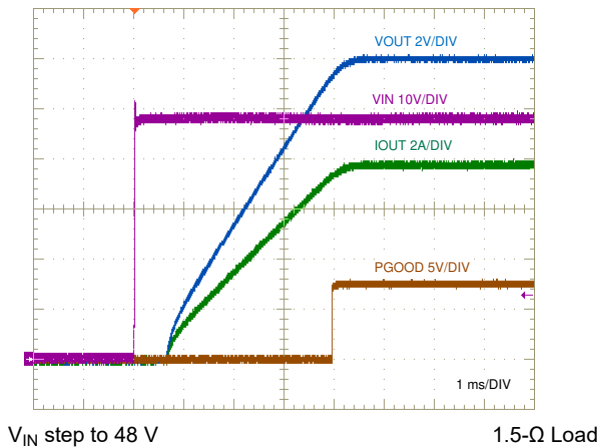


图 9-19. Start-Up, 8-A Resistive Load

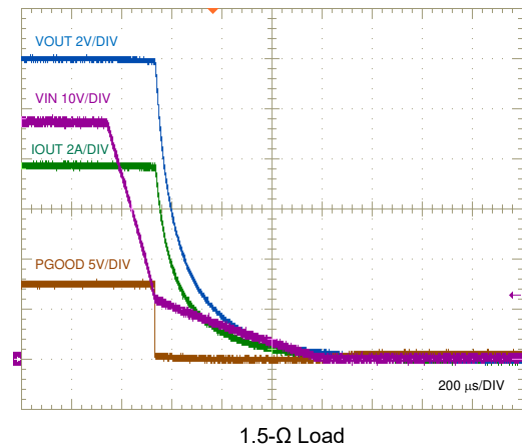


图 9-20. Shutdown By Input UVLO, 8-A Resistive Load

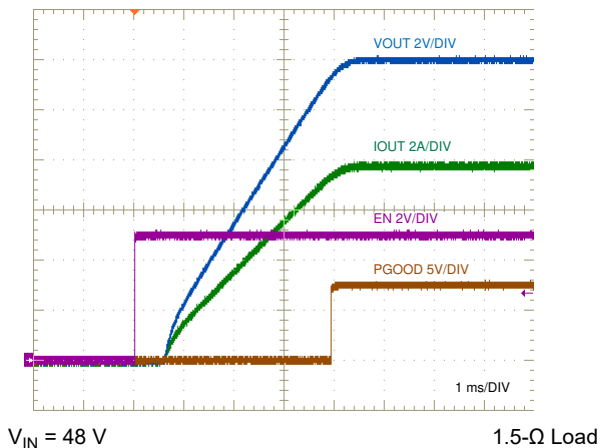


图 9-21. ENABLE ON, 10-A Resistive Load

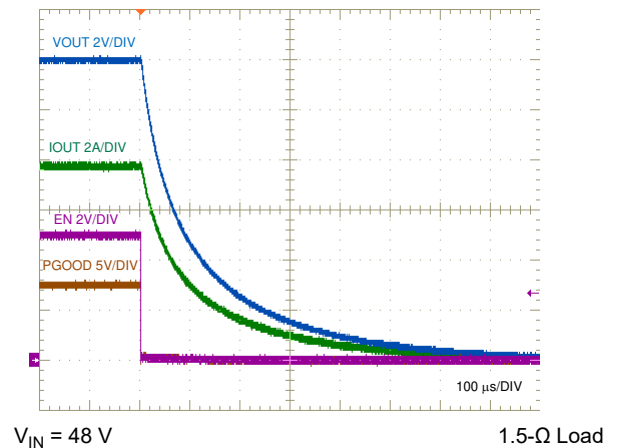


图 9-22. ENABLE OFF, 10-A Resistive Load

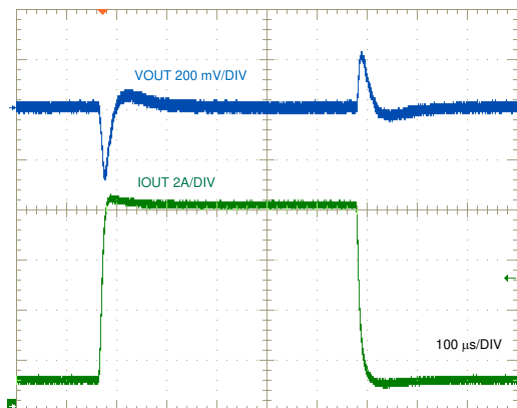
 $V_{IN} = 48\text{ V}$ 

图 9-23. Load Transient Response, 1 A to 8 A to 1 A

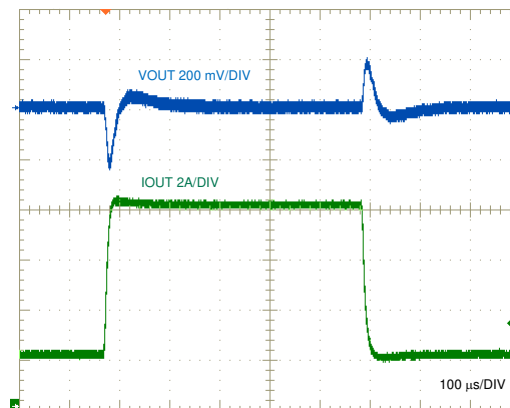
 $V_{IN} = 48\text{ V}$ 

图 9-24. Load Transient Response, 2 A to 8 A to 2 A

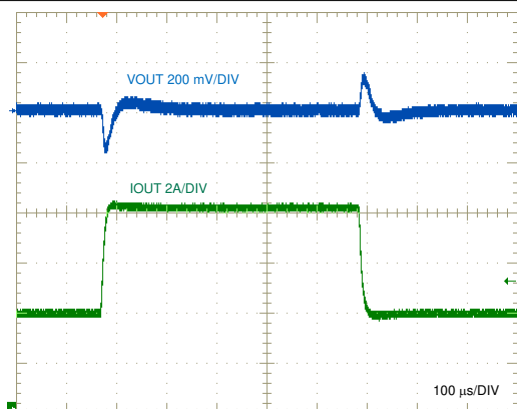
 $V_{IN} = 48\text{ V}$ 

图 9-25. Load Transient Response, 4 A to 8 A to 4 A

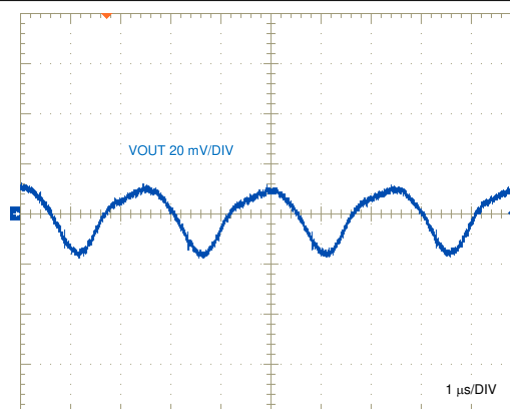
 $V_{IN} = 48\text{ V}$  $I_{OUT} = 8\text{ A}$ 

图 9-26. Output Voltage Ripple

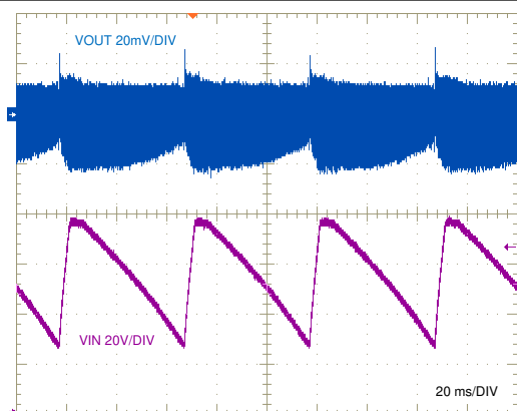
 $I_{OUT} = 4\text{ A}$ 

图 9-27. Repetitive Line Transients, 24 V to 75 V

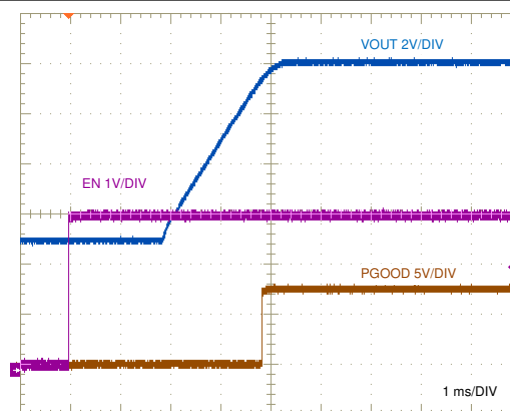
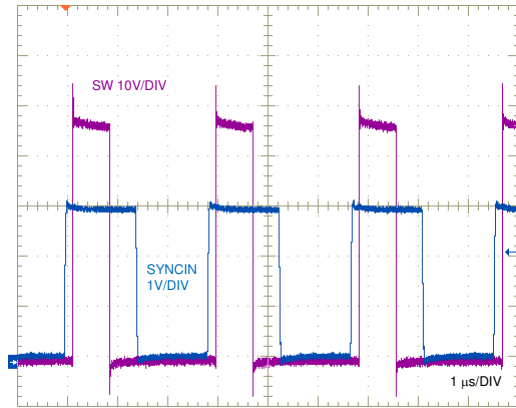
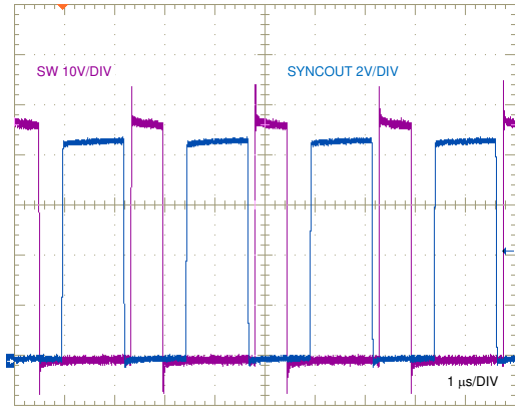
 $V_{IN} = 48\text{ V}$  $I_{OUT} = 0\text{ A}$ 

图 9-28. Pre-Biased Start-Up



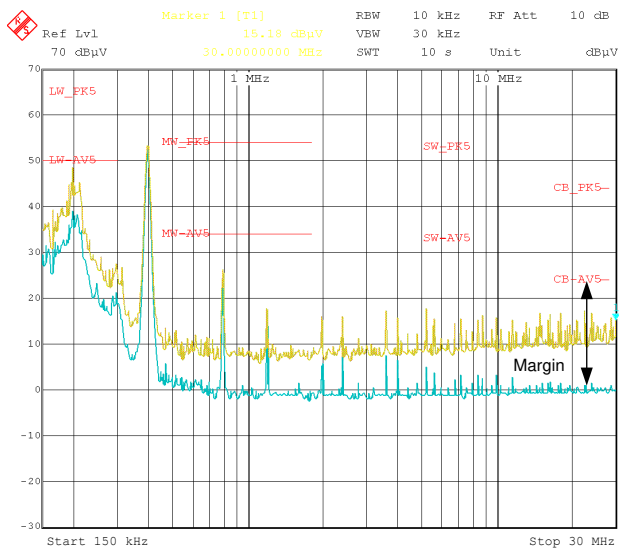
$V_{IN} = 48\text{ V}$   $F_{SW} = 350\text{ kHz}$   $I_{OUT} = 8\text{ A}$

**图 9-29. SW Node and SYNCIN Voltages**



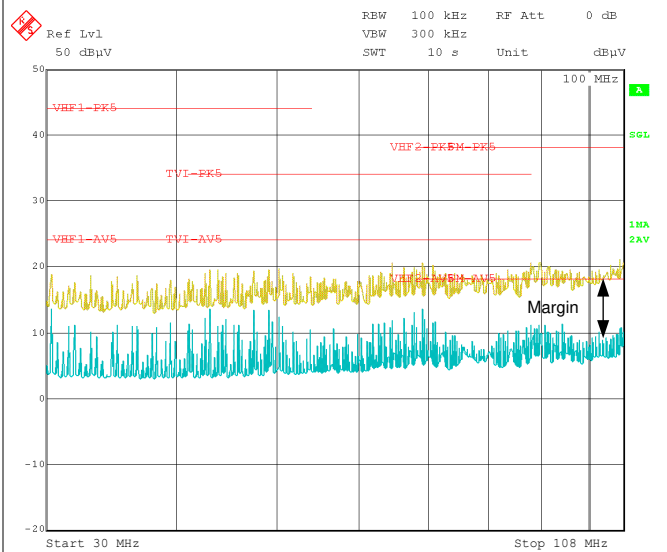
$V_{IN} = 48\text{ V}$   $I_{OUT} = 8\text{ A}$

**图 9-30. SW Node and SYNCOUT Voltages**



$V_{IN} = 48\text{ V}$   $V_{OUT} = 12\text{ V}$  6-A resistive load

**图 9-31. CISPR 25 Class 5 Conducted EMI, 150 kHz to 30 MHz**



$V_{IN} = 48\text{ V}$   $V_{OUT} = 12\text{ V}$  6-A resistive load

**图 9-32. CISPR 25 Class 5 Conducted EMI, 30 MHz to 108 MHz**

## 10 Power Supply Recommendations

The LM5146 buck controller is designed to operate from a wide input voltage range from 5.5 V to 100 V. The characteristics of the input supply must be compatible with the [Absolute Maximum Ratings](#) and [Recommended Operation Conditions](#). In addition, the input supply must be capable of delivering the required input current to the fully-loaded regulator. Estimate the average input current with [方程式 23](#).

$$I_{IN} = \frac{V_{OUT} \cdot I_{OUT}}{V_{IN} \cdot \eta} \quad (23)$$

where

- $\eta$  is the efficiency

If the converter is connected to an input supply through long wires or PCB traces with a large impedance, take special care to achieve stable performance. The parasitic inductance and resistance of the input cables may have an adverse affect on converter operation. The parasitic inductance in combination with the low-ESR ceramic input capacitors form an underdamped resonant circuit. This circuit can cause overvoltage transients at VIN each time the input supply is cycled ON and OFF. The parasitic resistance causes the input voltage to dip during a load transient. If the regulator is operating close to the minimum input voltage, this dip can cause false UVLO fault triggering and a system reset. The best way to solve such issues is to reduce the distance from the input supply to the regulator and use an aluminum or tantalum input capacitor in parallel with the ceramics. The moderate ESR of the electrolytic capacitors helps to damp the input resonant circuit and reduce any voltage overshoots. A capacitance in the range of 10  $\mu$ F to 47  $\mu$ F is usually sufficient to provide input damping and helps to hold the input voltage steady during large load transients.

An EMI input filter is often used in front of the regulator that, unless carefully designed, can lead to instability as well as some of the effects mentioned above. The application report [Simple Success with Conducted EMI for DC-DC Converters](#) (SNVA489) provides helpful suggestions when designing an input filter for any switching regulator.

## 11 Layout

### 11.1 Layout Guidelines

Proper PCB design and layout is important in a high-current, fast-switching circuits (with high current and voltage slew rates) to assure appropriate device operation and design robustness. As expected, certain issues must be considered before designing a PCB layout using the LM5146. The high-frequency power loop of the buck converter power stage is denoted by #1 in the shaded area of [图 11-1](#). The topological architecture of a buck converter means that particularly high di/dt current flows in the components of loop 1, and it becomes mandatory to reduce the parasitic inductance of this loop by minimizing its effective loop area. Also important is the gate drive loops of the low-side and high-side MOSFETs, denoted by 2 and 3, respectively, in [图 11-1](#).

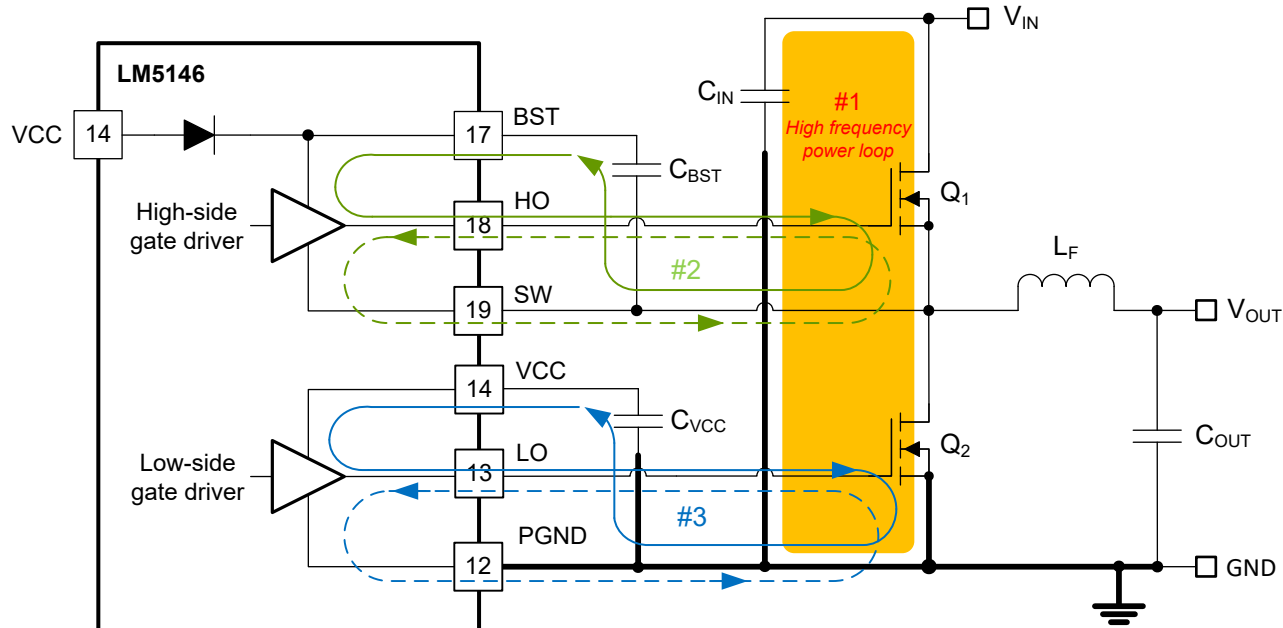


**图 11-1. DC/DC Regulator Ground System With Power Stage and Gate Drive Circuit Switching Loops**

#### 11.1.1 Power Stage Layout

1. Input capacitors, output capacitors, and MOSFETs are the constituent components of the power stage of a buck regulator and are typically placed on the top side of the PCB (solder side). The benefits of convective heat transfer are maximized because of leveraging any system-level airflow. In a two-sided PCB layout, small-signal components are typically placed on the bottom side (component side). Insert at least one inner plane, connected to ground, to shield and isolate the small-signal traces from noisy power traces and lines.
2. The DC/DC converter has several high-current loops. Minimize the area of these loops in order to suppress generated switching noise and parasitic loop inductance and optimize switching performance.
  - Loop #1: The most important loop to minimize the area of is the path from the input capacitor or capacitors through the high- and low-side MOSFETs, and back to the capacitor or capacitors through the ground connection. Connect the input capacitor or capacitors negative terminal close to the source of the low-side MOSFET (at ground). Similarly, connect the input capacitor or capacitors positive terminal close to the drain of the high-side MOSFET (at VIN). Refer to loop #1 of [图 11-1](#).
  - Another loop, not as critical though as loop #1, is the path from the low-side MOSFET through the inductor and output capacitor(s), and back to source of the low-side MOSFET through ground. Connect the source of the low-side MOSFET and negative terminal of the output capacitor or capacitors at ground as close as possible.
3. The PCB trace defined as SW node, which connects to the source of the high-side (control) MOSFET, the drain of the low-side (synchronous) MOSFET and the high-voltage side of the inductor, must be short and wide. However, the SW connection is a source of injected EMI and thus must not be too large.

4. Follow any layout considerations of the MOSFETs as recommended by the MOSFET manufacturer, including pad geometry and solder paste stencil design.
5. The SW pin connects to the switch node of the power conversion stage and acts as the return path for the high-side gate driver. The parasitic inductance inherent to loop #1 in [Figure 11-1](#) and the output capacitance ( $C_{OSS}$ ) of both power MOSFETs form a resonant circuit that induces high frequency ( $> 100$  MHz) ringing on the SW node. The voltage peak of this ringing, if not controlled, can be significantly higher than the input voltage. Ensure that the peak ringing amplitude does not exceed the absolute maximum rating limit for the SW pin. In many cases, a series resistor and capacitor snubber network connected from the SW node to GND damps the ringing and decreases the peak amplitude. Provide provisions for snubber network components in the PCB layout. If testing reveals that the ringing amplitude at the SW pin is excessive, then include snubber components as needed.

### 11.1.2 Gate Drive Layout

The LM5146 high-side and low-side gate drivers incorporate short propagation delays, adaptive dead-time control and low-impedance output stages capable of delivering large peak currents with very fast rise and fall times to facilitate rapid turnon and turnoff transitions of the power MOSFETs. Very high  $di/dt$  can cause unacceptable ringing if the trace lengths and impedances are not well controlled.

Minimization of stray or parasitic gate loop inductance is key to optimizing gate drive switching performance, whether it be series gate inductance that resonates with MOSFET gate capacitance or common source inductance (common to gate and power loops) that provides a negative feedback component opposing the gate drive command, thereby increasing MOSFET switching times. The following loops are important:

- Loop 2: high-side MOSFET,  $Q_1$ . During the high-side MOSFET turnon, high current flows from the bootstrap (boot) capacitor through the gate driver and high-side MOSFET, and back to the negative terminal of the boot capacitor through the SW connection. Conversely, to turn off the high-side MOSFET, high current flows from the gate of the high-side MOSFET through the gate driver and SW, and back to the source of the high-side MOSFET through the SW trace. Refer to loop #2 of [Figure 11-1](#).
- Loop 3: low-side MOSFET,  $Q_2$ . During the low-side MOSFET turn-on, high current flows from the VCC decoupling capacitor through the gate driver and low-side MOSFET, and back to the negative terminal of the capacitor through ground. Conversely, to turn off the low-side MOSFET, high current flows from the gate of the low-side MOSFET through the gate driver and GND, and back to the source of the low-side MOSFET through ground. Refer to loop #3 of [Figure 11-1](#).

TI strongly recommends following circuit layout guidelines when designing with high-speed MOSFET gate drive circuits.

1. Connections from gate driver outputs, HO and LO, to the respective gate of the high-side or low-side MOSFET must be as short as possible to reduce series parasitic inductance. Use 0.65 mm (25 mils) or wider traces. Use a via or vias, if necessary, of at least 0.5 mm (20 mils) diameter along these traces. Route HO and SW gate traces as a differential pair from the LM5146 to the high-side MOSFET, taking advantage of flux cancellation.
2. Minimize the current loop path from the VCC and BST pins through their respective capacitors as these provide the high instantaneous current, up to 3.5 A, to charge the MOSFET gate capacitances. Specifically, locate the bootstrap capacitor,  $C_{BST}$ , close to the BST and SW pins of the LM5146 to minimize the area of loop #2 associated with the high-side driver. Similarly, locate the VCC capacitor,  $C_{VCC}$ , close to the VCC and PGND pins of the LM5146 to minimize the area of loop #3 associated with the low-side driver.
3. Placing a 2- $\Omega$  to 10- $\Omega$  resistor in series with the boot capacitor, as shown in [Figure 9-16](#), slows down the high-side MOSFET turn-on transition, serving to reduce the voltage ringing and peak amplitude at the SW node at the expense of increased MOSFET turnon power loss.

### 11.1.3 PWM Controller Layout

With the proviso to locate the controller as close as possible to the MOSFETs to minimize gate driver trace runs, the components related to the analog and feedback signals, current limit setting, and temperature sense are considered in the following:

1. Separate power and signal traces, and use a ground plane to provide noise shielding.



2. Place all sensitive analog traces and components such as COMP, FB, RT, ILIM, and SS/TRK away from high-voltage switching nodes such as SW, HO, LO, or BST to avoid mutual coupling. Use an internal layer or layers as a ground plane or ground planes. Pay particular attention to shielding the feedback (FB) trace from power traces and components.
3. The upper feedback resistor can be connected directly to the output voltage sense point at the load device or the bulk capacitor at the converter side.
4. Connect the ILIM setting resistor from the drain of the low-side MOSFET to ILIM and make the connections as close as possible to the LM5146. The trace from the ILIM pin to the resistor must avoid coupling to a high-voltage switching net.
5. Minimize the loop area from the VCC and VIN pins through their respective decoupling capacitors to the GND pin. Locate these capacitors as close as possible to the LM5146.

#### 11.1.4 Thermal Design and Layout

The useful operating temperature range of a PWM controller with integrated gate drivers and bias supply LDO regulator is greatly affected by:

- Average gate drive current requirements of the power MOSFETs
- Switching frequency
- Operating input voltage (affecting bias regulator LDO voltage drop and hence its power dissipation)
- Thermal characteristics of the package and operating environment

For a PWM controller to be useful over a particular temperature range, the package must allow for the efficient removal of the heat produced while keeping the junction temperature within rated limits. The LM5146 controller is available in a small 3.5-mm × 4.5-mm 20-pin VQFN (RGY) PowerPAD™ package to cover a range of application requirements. The thermal metrics of this package are summarized in [节 7.4](#). The application report [Semiconductor and IC Package Thermal Metrics](#) provides detailed information regarding the thermal information table.

The 20-pin VQFN package offers a means of removing heat from the semiconductor die through the exposed thermal pad at the base of the package. While the exposed pad of the package is not directly connected to any leads of the package, it is thermally connected to the substrate of the LM5146 device (ground). This allows a significant improvement in heat sinking, and it becomes imperative that the PCB is designed with thermal lands, thermal vias, and a ground plane to complete the heat removal subsystem. The exposed pad of the LM5146 is soldered to the ground-connected copper land on the PCB directly underneath the device package, reducing the thermal resistance to a very low value. Wide traces of the copper tying in the no-connect pins of the LM5146 (pins 9 and 16) and connection to this thermal land helps to dissipate heat.

Numerous vias with a 0.3-mm diameter connected from the thermal land to the internal and solder-side ground plane(s) are vital to help dissipation. In a multi-layer PCB design, a solid ground plane is typically placed on the PCB layer below the power components. Not only does this provide a plane for the power stage currents to flow but it also represents a thermally conductive path away from the heat generating devices.

The thermal characteristics of the MOSFETs also are significant. The drain pad of the high-side MOSFET is normally connected to a VIN plane for heat sinking. The drain pad of the low-side MOSFET is tied to the SW plane, but the SW plane area is purposely kept relatively small to mitigate EMI concerns.

#### 11.1.5 Ground Plane Design

As mentioned previously, using one or more of the inner PCB layers as a solid ground plane is recommended. A ground plane offers shielding for sensitive circuits and traces and also provides a quiet reference potential for the control circuitry. Connect the PGND pin to the system ground plane using an array of vias under the exposed pad. Also connect the PGND directly to the return terminals of the input and output capacitors. The PGND net contains noise at the switching frequency and can bounce because of load current variations. The power traces for PGND, VIN and SW can be restricted to one side of the ground plane. The other side of the ground plane contains much less noise and is ideal for sensitive analog trace routes.

## 11.2 Layout Example

图 11-2 shows an example PCB layout based on the [LM5146-Q1-EVM12V](#) design. The power component connections are made on the top layer with wide, copper-filled polygon areas. The SW connection from the power MOSFETs to the inductor is purposely kept at minimum area to reduce radiated EMI. A power ground plane is placed on layer 2 with 6 mil (0.15 mm) spacing to the top layer, see 图 11-3. As a result, the buck regulator hot loop has a small effective area based on this tightly-coupled GND plane directly underneath the MOSFETs.

The LM5146 controller is located close to the gate terminals of the MOSFETs such that the gate drive traces are routed short and direct. Refer to the [LM5146-Q1-EVM12V Evaluation Module User's Guide](#) for more detail.

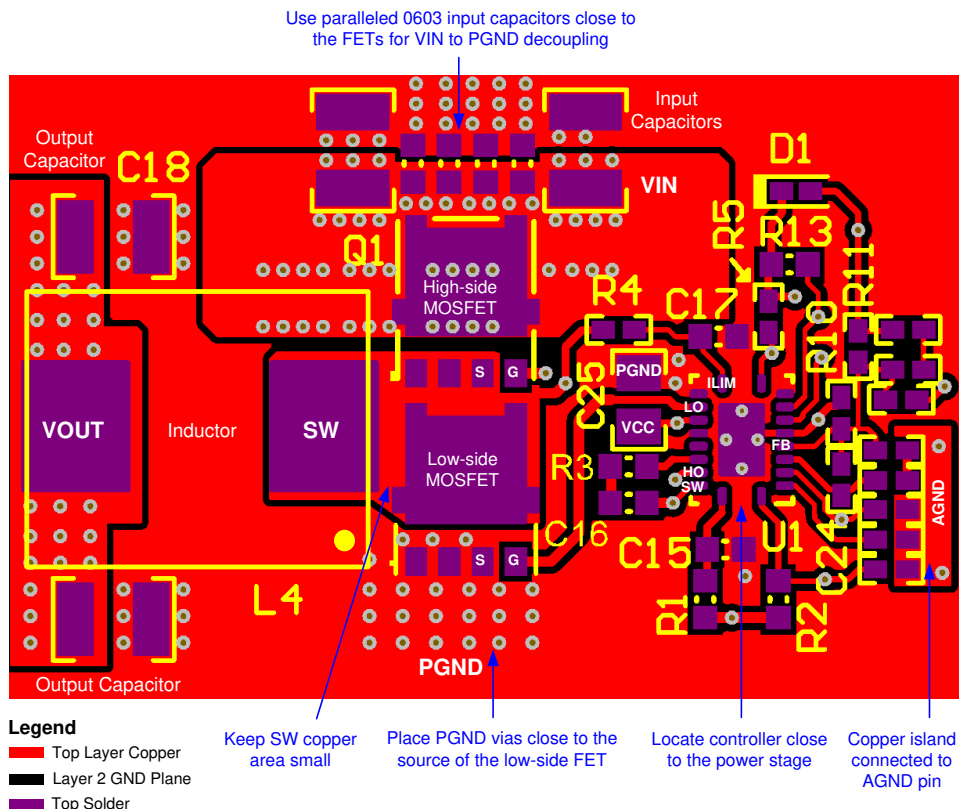
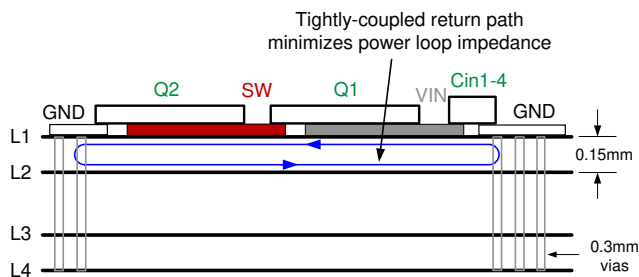


图 11-2. LM5146 Controller PCB Layout (Viewed From Top)



### Note

See the [Improve High-current DC/DC Regulator Performance for Free with Optimized Power Stage Layout](#) application report for more detail.

图 11-3. PCB Stack-up Diagram With Low L1-L2 Intra-layer Spacing

## 12 Device and Documentation Support

### 12.1 Device Support

#### 12.1.1 第三方产品免责声明

TI 发布的与第三方产品或服务有关的信息，不能构成与此类产品或服务或保修的适用性有关的认可，不能构成此类产品或服务单独或与任何 TI 产品或服务一起的表示或认可。

#### 12.1.2 Development Support

With an input operating voltage as low as 3.5 V and up to 100 V as specified in [表 12-1](#), the LM(2)514x family of synchronous buck controllers from TI provides flexibility, scalability and optimized solution size for a range of applications. These controllers enable DC/DC solutions with high density, low EMI and increased flexibility. Available EMI mitigation features include dual-random spread spectrum (DRSS) or triangular spread spectrum (TRSS), split gate driver outputs for slew rate (SR) control, and integrated active EMI filtering (AEF).

**表 12-1. Synchronous Buck DC/DC Controller Family**

DC/DC CONTROLLER	SINGLE or DUAL	V <sub>IN</sub> RANGE	CONTROL METHOD	GATE DRIVE VOLTAGE	SYNC OUTPUT	EMI MITIGATION
<a href="#">LM25148</a>	Single	3.5 V to 42 V	Peak current mode	5 V	180° phase shift	DRSS
<a href="#">LM25149</a>	Single	3.5 V to 42 V	Peak current mode	5 V	180° phase shift	AEF, DRSS
<a href="#">LM25141</a>	Single	3.8 V to 42 V	Peak current mode	5 V	N/A	SR control, TRSS
<a href="#">LM5141</a>	Single	3.8 V to 42 V	Peak current mode	5 V	N/A	SR control, TRSS
<a href="#">LM5143</a>	Dual	3.5 V to 65 V	Peak current mode	5 V	90° phase shift	SR control, TRSS
<a href="#">LM25145</a>	Single	6 V to 42 V	Voltage mode	7.5 V	180° phase shift	N/A
<a href="#">LM5145</a>	Single	6 V to 75 V	Voltage mode	7.5 V	180° phase shift	N/A
<a href="#">LM5146</a>	Single	5.5 V to 100 V	Voltage mode	7.5 V	180° phase shift	N/A

For development support see the following:

- [LM5146 Quickstart Calculator](#)
- [LM5146 simulation models](#)
- For TI's reference design library, visit [TI Designs](#)
- For TI's WEBENCH Design Environment, visit the [WEBENCH® Design Center](#)
- To design a low-EMI power supply, review TI's comprehensive [EMI Training Series](#)
- TI Reference Designs:
  - [57W output synchronous buck converter for telecom reference design](#)
  - [10-A automotive pre-regulator reference design](#)
  - [10-A automotive pre-regulator reference design with extended input voltage range for trucks](#)
  - [20-A automotive pre-regulator reference design](#)
  - [20-A automotive pre-regulator reference design with extended input voltage range for trucks](#)
- Technical Articles:
  - [High-density PCB layout of DC/DC converters](#)
  - [Synchronous buck controller solutions support wide V<sub>IN</sub> performance and flexibility](#)
  - [How to use slew rate for EMI control](#)
  - [How to reduce EMI and shrink power-supply size with an integrated active EMI filter](#)

#### 12.1.2.1 Custom Design With WEBENCH® Tools

to create a custom design using the LM5146 device with the WEBENCH® Power Designer.

1. Start by entering the input voltage (V<sub>IN</sub>), output voltage (V<sub>OUT</sub>), and output current (I<sub>OUT</sub>) requirements.
2. Optimize the design for key parameters such as efficiency, footprint, and cost using the optimizer dial.
3. Compare the generated design with other possible solutions from Texas Instruments.

The WEBENCH Power Designer provides a customized schematic along with a list of materials with real-time pricing and component availability.

In most cases, these actions are available:

- Run electrical simulations to see important waveforms and circuit performance
- Run thermal simulations to understand board thermal performance
- Export customized schematic and layout into popular CAD formats
- Print PDF reports for the design, and share the design with colleagues

Get more information about WEBENCH tools at [www.ti.com/WEBENCH](http://www.ti.com/WEBENCH).

## 12.2 Documentation Support

### 12.2.1 Related Documentation

For related documentation see the following:

- [LM5146-Q1 EVM User's Guide](#)
- [LM5145 EVM User's Guide](#)
- [LM5143-Q1 Synchronous Buck Controller EVM](#)
- [LM5143-Q1 Synchronous Buck Controller High-Density 4-Phase Design](#)
- [Reduce Buck Converter EMI and Voltage Stress by Minimizing Inductive Parasitics](#)
- [AN-2162 Simple Success with Conducted EMI from DC-DC Converters](#)
- White Papers:
  - [Valuing Wide  \$V\_{IN}\$ , Low-EMI Synchronous Buck Circuits for Cost-Effective, Demanding Applications](#)
  - [An Overview of Conducted EMI Specifications for Power Supplies](#)
  - [An Overview of Radiated EMI Specifications for Power Supplies](#)

#### 12.2.1.1 PCB Layout Resources

- [Improve High-current DC/DC Regulator Performance for Free with Optimized Power Stage Layout](#)
- [AN-1149 Layout Guidelines for Switching Power Supplies](#)
- [Constructing Your Power Supply – Layout Considerations](#)
- Technical Articles:
  - [High-Density PCB Layout of DC-DC Converters](#)

#### 12.2.1.2 Thermal Design Resources

- [AN-2020 Thermal Design by Insight, Not Hindsight](#)
- [AN-1520 A Guide to Board Layout for Best Thermal Resistance for Exposed Pad Packages](#)
- [Semiconductor and IC Package Thermal Metrics](#)
- [Thermal Design Made Simple with LM43603 and LM43602](#)
- [PowerPAD™ Thermally Enhanced Package](#)
- [PowerPAD Made Easy](#)
- [Using New Thermal Metrics](#)

## 12.3 接收文档更新通知

要接收文档更新通知，请导航至 [ti.com](http://ti.com) 上的器件产品文件夹。点击 [订阅更新](#) 进行注册，即可每周接收产品信息更改摘要。有关更改的详细信息，请查看任何已修订文档中包含的修订历史记录。

## 12.4 支持资源

**TI E2E™ 支持论坛**是工程师的重要参考资料，可直接从专家获得快速、经过验证的解答和设计帮助。搜索现有解答或提出自己的问题可获得所需的快速设计帮助。

链接的内容由各个贡献者“按原样”提供。这些内容并不构成 TI 技术规范，并且不一定反映 TI 的观点；请参阅 TI 的《[使用条款](#)》。

## 12.5 Trademarks

NexFET™, PowerPAD™, and TI E2E™ are trademarks of Texas Instruments.  
WEBENCH® is a registered trademark of Texas Instruments.  
are registered trademarks of Texas Instruments.  
所有商标均为其各自所有者的财产。

## 12.6 Electrostatic Discharge Caution



This integrated circuit can be damaged by ESD. Texas Instruments recommends that all integrated circuits be handled with appropriate precautions. Failure to observe proper handling and installation procedures can cause damage.

ESD damage can range from subtle performance degradation to complete device failure. Precision integrated circuits may be more susceptible to damage because very small parametric changes could cause the device not to meet its published specifications.

## 12.7 Glossary

[TI Glossary](#)      This glossary lists and explains terms, acronyms, and definitions.

## 13 Mechanical, Packaging, and Orderable Information

The following pages include mechanical, packaging, and orderable information. This information is the most current data available for the designated devices. This data is subject to change without notice and revision of this document. For browser-based versions of this data sheet, refer to the left-hand navigation.

## 重要声明和免责声明

TI 提供技术和可靠性数据（包括数据表）、设计资源（包括参考设计）、应用或其他设计建议、网络工具、安全信息和其他资源，不保证没有瑕疵且不做任何明示或暗示的担保，包括但不限于对适销性、某特定用途方面的适用性或不侵犯任何第三方知识产权的暗示担保。

这些资源可供使用 TI 产品进行设计的熟练开发人员使用。您将自行承担以下全部责任：(1) 针对您的应用选择合适的 TI 产品，(2) 设计、验证并测试您的应用，(3) 确保您的应用满足相应标准以及任何其他安全、安保或其他要求。这些资源如有变更，恕不另行通知。TI 授权您仅可将这些资源用于研发本资源所述的 TI 产品的应用。严禁对这些资源进行其他复制或展示。您无权使用任何其他 TI 知识产权或任何第三方知识产权。您应全额赔偿因在这些资源的使用中对 TI 及其代表造成的任何索赔、损害、成本、损失和债务，TI 对此概不负责。

TI 提供的产品受 TI 的销售条款 (<https://www.ti.com/legal/termsofsale.html>) 或 [ti.com](https://www.ti.com) 上其他适用条款/TI 产品随附的其他适用条款的约束。TI 提供这些资源并不会扩展或以其他方式更改 TI 针对 TI 产品发布的适用的担保或担保免责声明。

邮寄地址：Texas Instruments, Post Office Box 655303, Dallas, Texas 75265  
Copyright © 2021，德州仪器 (TI) 公司

## PACKAGING INFORMATION

Orderable part number	Status (1)	Material type (2)	Package   Pins	Package qty   Carrier	RoHS (3)	Lead finish/ Ball material (4)	MSL rating/ Peak reflow (5)	Op temp (°C)	Part marking (6)
<a href="#">LM5146RGYR</a>	Active	Production	VQFN (RGY)   20	3000   LARGE T&R	Yes	NIPDAU   SN	Level-2-260C-1 YEAR	-40 to 150	LM5146
LM5146RGYR.A	Active	Production	VQFN (RGY)   20	3000   LARGE T&R	Yes	NIPDAU	Level-2-260C-1 YEAR	-40 to 125	LM5146
LM5146RGYRG4	Active	Production	VQFN (RGY)   20	3000   LARGE T&R	Yes	NIPDAU	Level-2-260C-1 YEAR	-40 to 125	LM5146
LM5146RGYRG4.A	Active	Production	VQFN (RGY)   20	3000   LARGE T&R	Yes	NIPDAU	Level-2-260C-1 YEAR	-40 to 125	LM5146

<sup>(1)</sup> **Status:** For more details on status, see our [product life cycle](#).

<sup>(2)</sup> **Material type:** When designated, preproduction parts are prototypes/experimental devices, and are not yet approved or released for full production. Testing and final process, including without limitation quality assurance, reliability performance testing, and/or process qualification, may not yet be complete, and this item is subject to further changes or possible discontinuation. If available for ordering, purchases will be subject to an additional waiver at checkout, and are intended for early internal evaluation purposes only. These items are sold without warranties of any kind.

<sup>(3)</sup> **RoHS values:** Yes, No, RoHS Exempt. See the [TI RoHS Statement](#) for additional information and value definition.

<sup>(4)</sup> **Lead finish/Ball material:** Parts may have multiple material finish options. Finish options are separated by a vertical ruled line. Lead finish/Ball material values may wrap to two lines if the finish value exceeds the maximum column width.

<sup>(5)</sup> **MSL rating/Peak reflow:** The moisture sensitivity level ratings and peak solder (reflow) temperatures. In the event that a part has multiple moisture sensitivity ratings, only the lowest level per JEDEC standards is shown. Refer to the shipping label for the actual reflow temperature that will be used to mount the part to the printed circuit board.

<sup>(6)</sup> **Part marking:** There may be an additional marking, which relates to the logo, the lot trace code information, or the environmental category of the part.

Multiple part markings will be inside parentheses. Only one part marking contained in parentheses and separated by a "-" will appear on a part. If a line is indented then it is a continuation of the previous line and the two combined represent the entire part marking for that device.

**Important Information and Disclaimer:** The information provided on this page represents TI's knowledge and belief as of the date that it is provided. TI bases its knowledge and belief on information provided by third parties, and makes no representation or warranty as to the accuracy of such information. Efforts are underway to better integrate information from third parties. TI has taken and continues to take reasonable steps to provide representative and accurate information but may not have conducted destructive testing or chemical analysis on incoming materials and chemicals. TI and TI suppliers consider certain information to be proprietary, and thus CAS numbers and other limited information may not be available for release.

In no event shall TI's liability arising out of such information exceed the total purchase price of the TI part(s) at issue in this document sold by TI to Customer on an annual basis.

**OTHER QUALIFIED VERSIONS OF LM5146 :**



- Automotive : [LM5146-Q1](#)

NOTE: Qualified Version Definitions:

- Automotive - Q100 devices qualified for high-reliability automotive applications targeting zero defects

## TAPE AND REEL INFORMATION



\*All dimensions are nominal

Device	Package Type	Package Drawing	Pins	SPQ	Reel Diameter (mm)	Reel Width W1 (mm)	A0 (mm)	B0 (mm)	K0 (mm)	P1 (mm)	W (mm)	Pin1 Quadrant
LM5146RGYR	VQFN	RGY	20	3000	330.0	12.4	3.71	4.71	1.1	8.0	12.0	Q1
LM5146RGYRG4	VQFN	RGY	20	3000	330.0	12.4	3.71	4.71	1.1	8.0	12.0	Q1

## TAPE AND REEL BOX DIMENSIONS



\*All dimensions are nominal

Device	Package Type	Package Drawing	Pins	SPQ	Length (mm)	Width (mm)	Height (mm)
LM5146RGYR	VQFN	RGY	20	3000	367.0	367.0	35.0
LM5146RGYRG4	VQFN	RGY	20	3000	367.0	367.0	35.0

## GENERIC PACKAGE VIEW

**RGY 20**

**VQFN - 1 mm max height**

3.5 x 4.5, 0.5 mm pitch

PLASTIC QUAD FGLATPACK - NO LEAD

This image is a representation of the package family, actual package may vary.  
Refer to the product data sheet for package details.



4225264/A

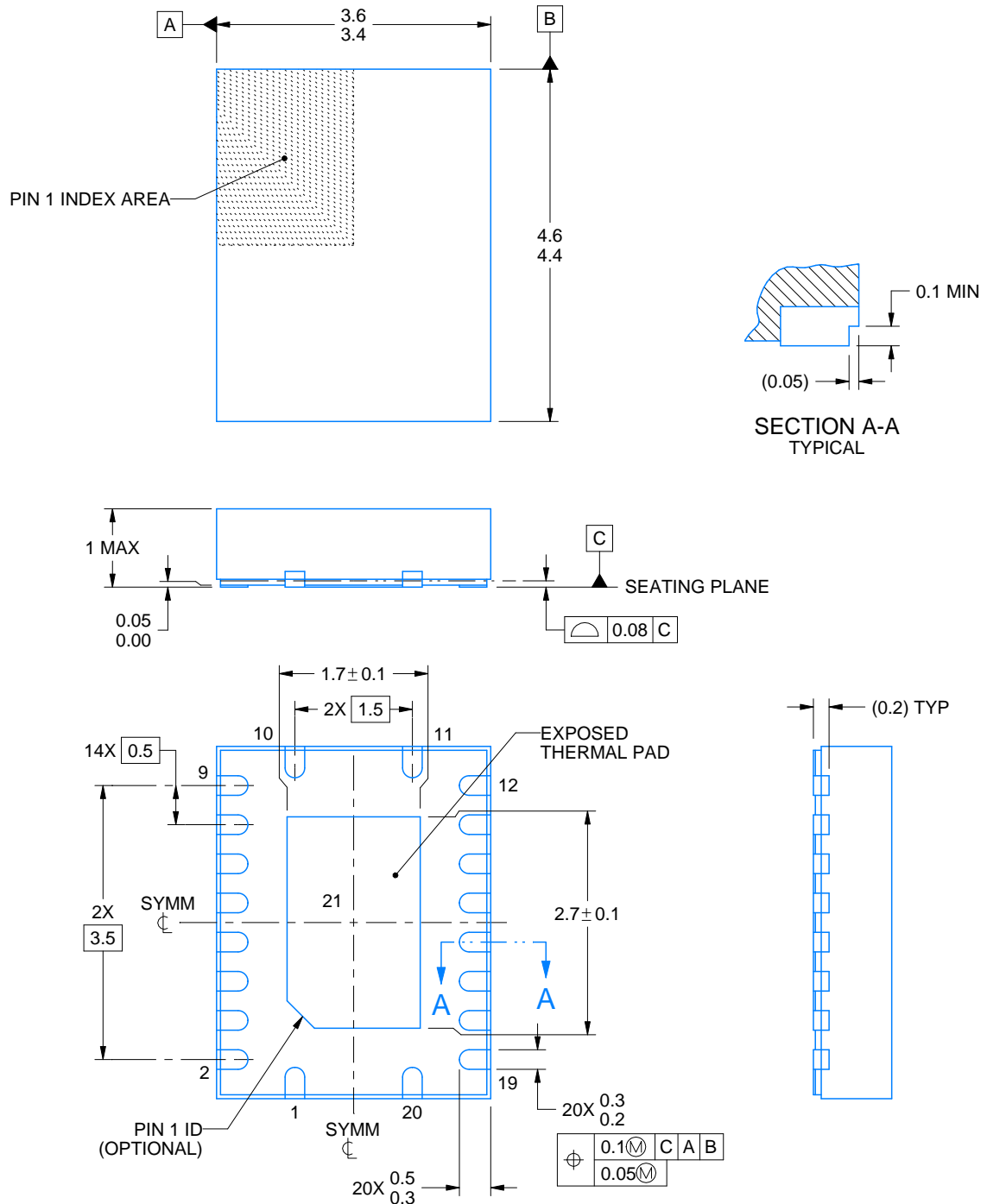
RGY0020B



## PACKAGE OUTLINE

VQFN - 1 mm max height

PLASTIC QUAD FLATPACK - NO LEAD



4222860/B 06/2017

### NOTES:

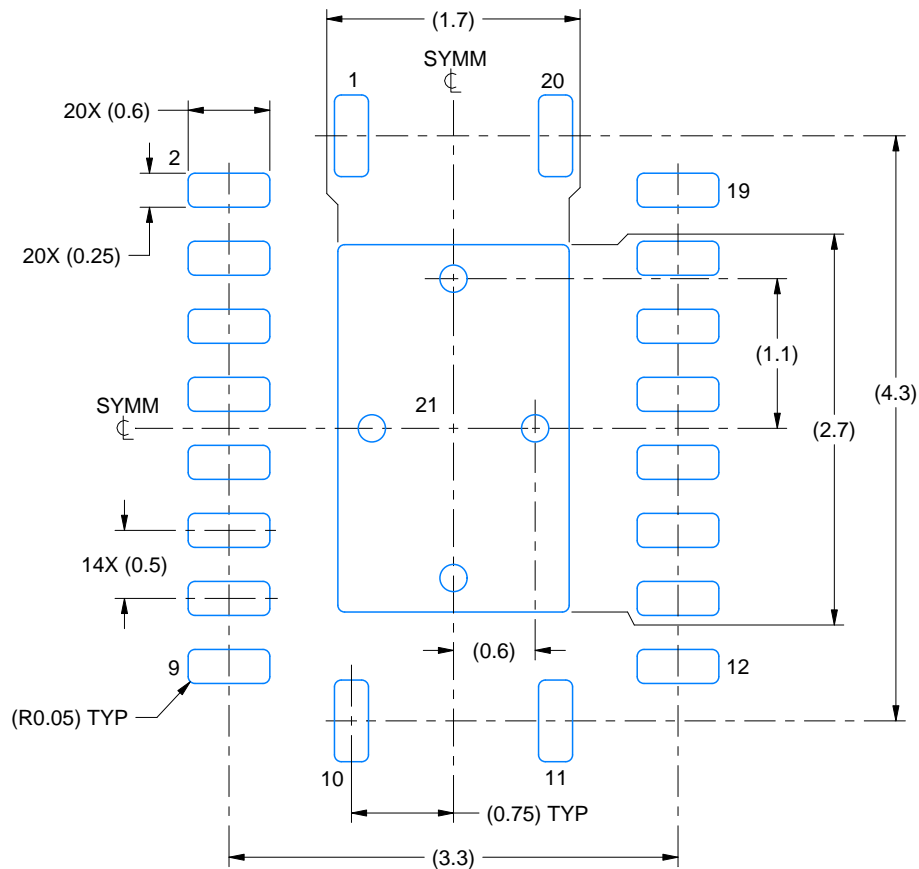
1. All linear dimensions are in millimeters. Any dimensions in parenthesis are for reference only. Dimensioning and tolerancing per ASME Y14.5M.
2. This drawing is subject to change without notice.
3. The package thermal pad must be soldered to the printed circuit board for thermal and mechanical performance.

# EXAMPLE BOARD LAYOUT

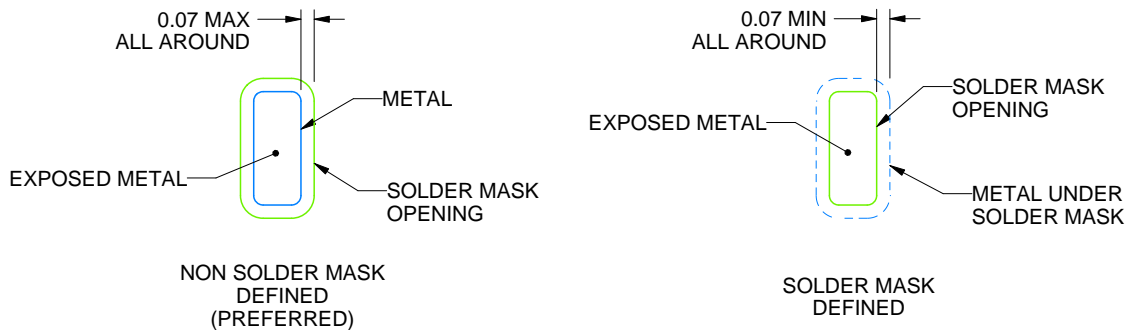
RGY0020B

VQFN - 1 mm max height

PLASTIC QUAD FLATPACK - NO LEAD



LAND PATTERN EXAMPLE  
EXPOSED METAL SHOWN  
SCALE:18X



SOLDER MASK DETAILS

4222860/B 06/2017

NOTES: (continued)

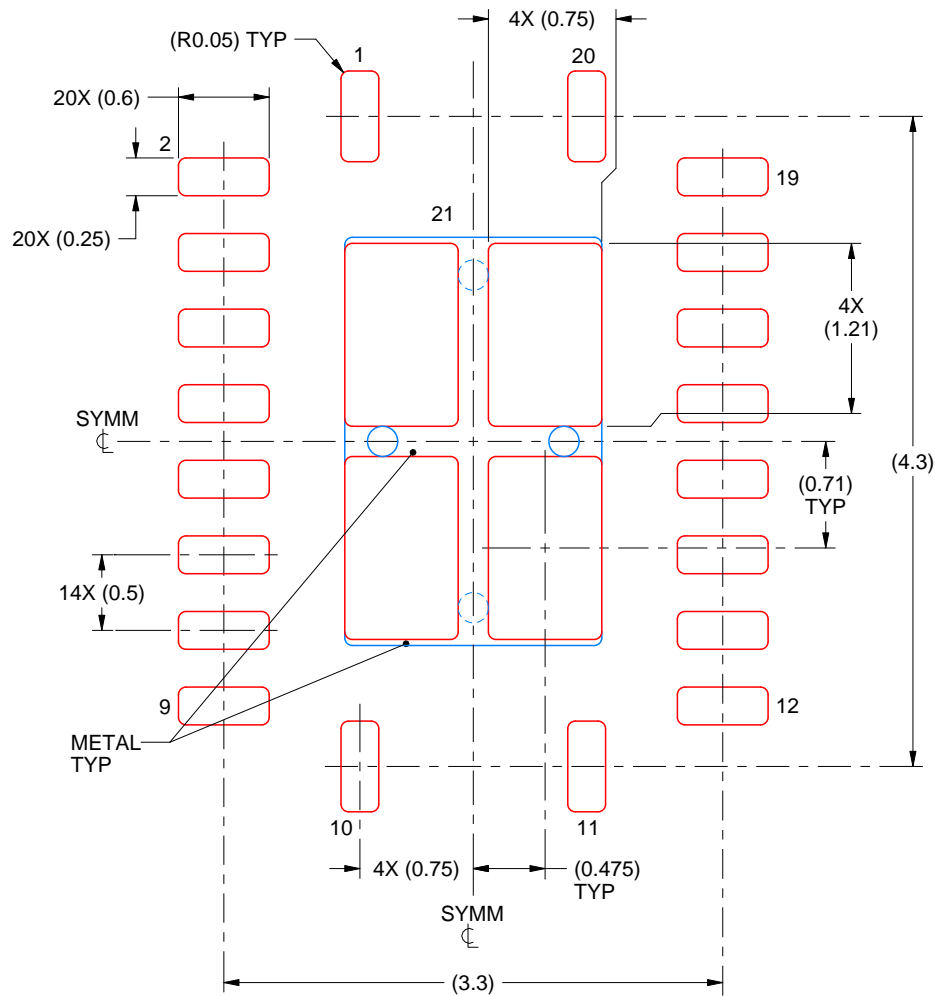
4. This package is designed to be soldered to a thermal pad on the board. For more information, see Texas Instruments literature number SLUA271 ([www.ti.com/lit/sluea271](http://www.ti.com/lit/sluea271)).
5. Vias are optional depending on application, refer to device data sheet. If any vias are implemented, refer to their locations shown on this view. It is recommended that vias under paste be filled, plugged or tented.

# EXAMPLE STENCIL DESIGN

RGY0020B

VQFN - 1 mm max height

PLASTIC QUAD FLATPACK - NO LEAD



**SOLDER PASTE EXAMPLE**  
BASED ON 0.125 mm THICK STENCIL

EXPOSED PAD 21  
80% PRINTED SOLDER COVERAGE BY AREA UNDER PACKAGE  
SCALE:20X

4222860/B 06/2017

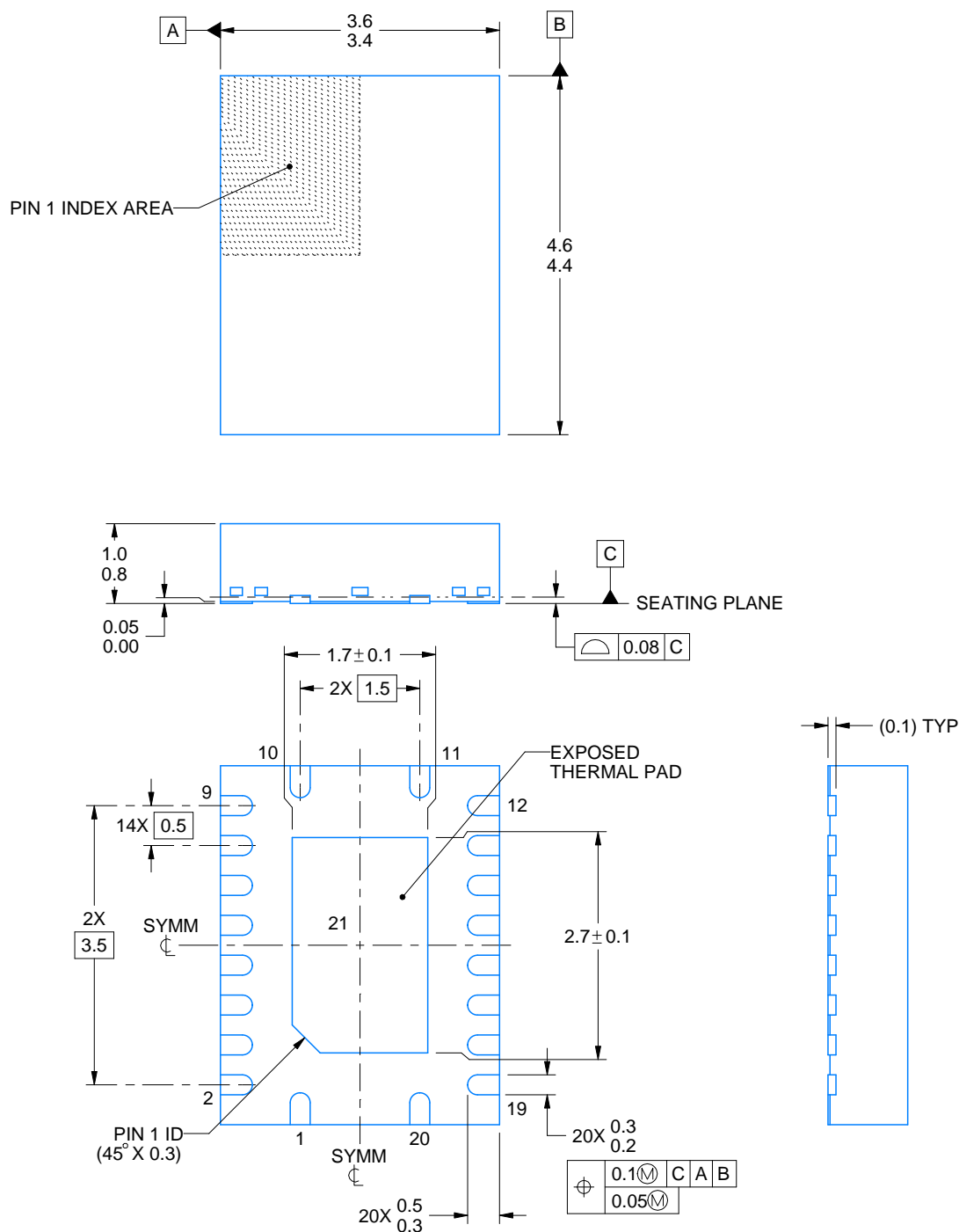
NOTES: (continued)

6. Laser cutting apertures with trapezoidal walls and rounded corners may offer better paste release. IPC-7525 may have alternate design recommendations.



### VQFN - 1 mm max height

PLASTIC QUAD FLATPACK - NO LEAD



4229343/A 01/2023

NOTES:

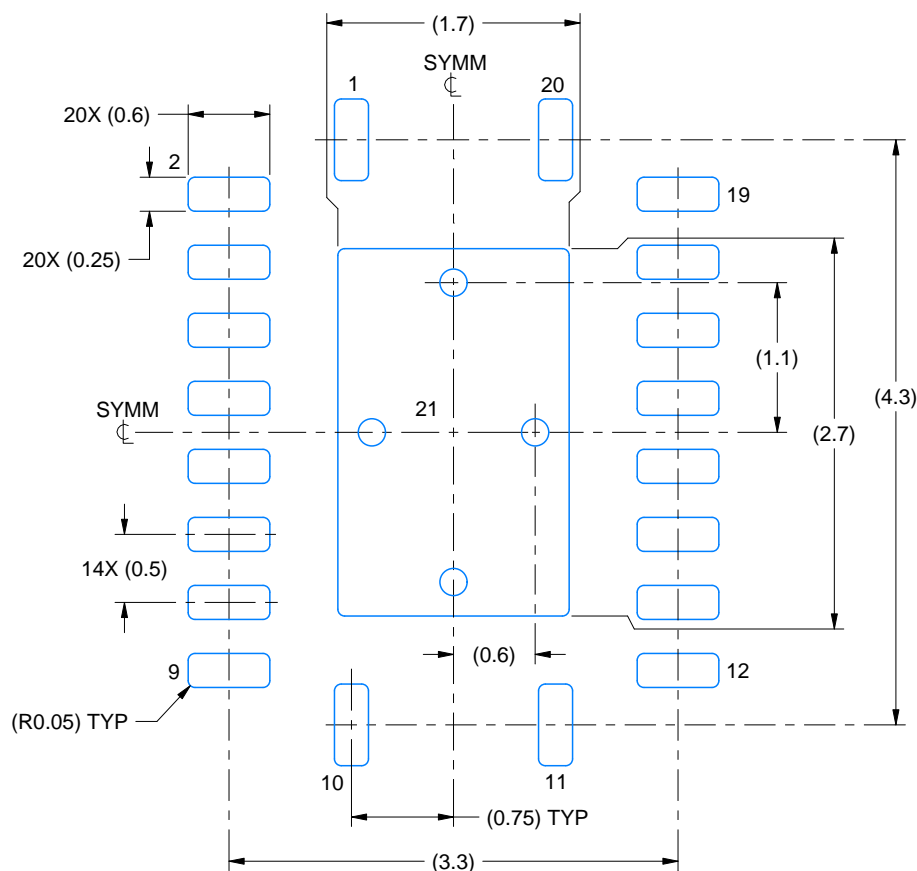
1. All linear dimensions are in millimeters. Any dimensions in parenthesis are for reference only. Dimensioning and tolerancing per ASME Y14.5M.
2. This drawing is subject to change without notice.
3. The package thermal pad must be soldered to the printed circuit board for thermal and mechanical performance.



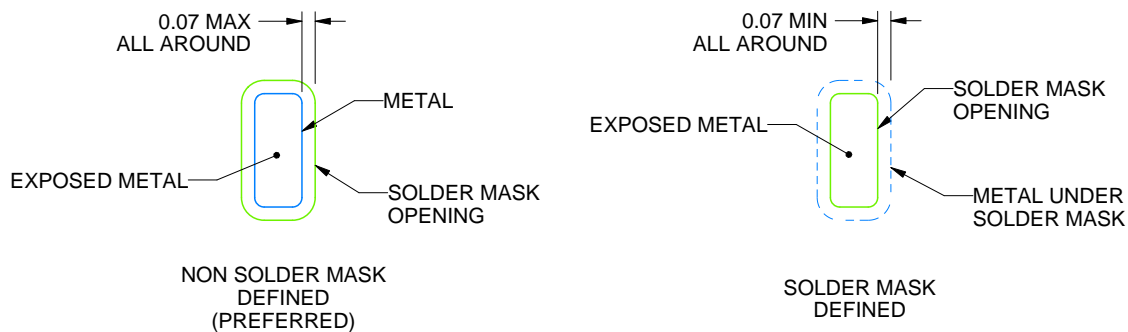
# RGY0020G

## VQFN - 1 mm max height

PLASTIC QUAD FLATPACK - NO LEAD



LAND PATTERN EXAMPLE  
EXPOSED METAL SHOWN  
SCALE:18X



## SOLDER MASK DETAILS

4229343/A 01/2023

NOTES: (continued)

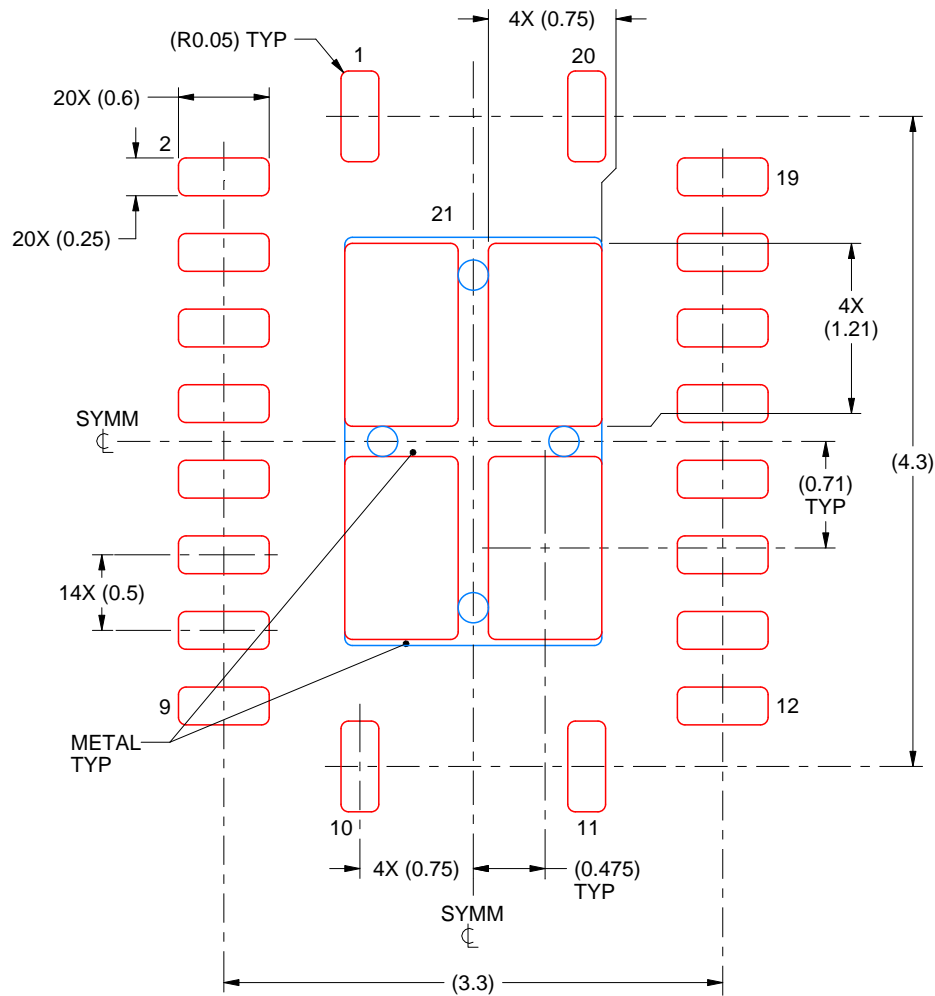
4. This package is designed to be soldered to a thermal pad on the board. For more information, see Texas Instruments literature number SLUA271 ([www.ti.com/lit/sluea271](http://www.ti.com/lit/sluea271)).
5. Vias are optional depending on application, refer to device data sheet. If any vias are implemented, refer to their locations shown on this view. It is recommended that vias under paste be filled, plugged or tented.

# EXAMPLE STENCIL DESIGN

RGY0020G

VQFN - 1 mm max height

PLASTIC QUAD FLATPACK - NO LEAD



**SOLDER PASTE EXAMPLE**  
BASED ON 0.125 mm THICK STENCIL

EXPOSED PAD 21  
80% PRINTED SOLDER COVERAGE BY AREA UNDER PACKAGE  
SCALE:20X

4229343/A 01/2023

NOTES: (continued)

6. Laser cutting apertures with trapezoidal walls and rounded corners may offer better paste release. IPC-7525 may have alternate design recommendations.

## 重要通知和免责声明

TI“按原样”提供技术和可靠性数据（包括数据表）、设计资源（包括参考设计）、应用或其他设计建议、网络工具、安全信息和其他资源，不保证没有瑕疵且不做任何明示或暗示的担保，包括但不限于对适销性、某特定用途方面的适用性或不侵犯任何第三方知识产权的暗示担保。

这些资源可供使用 TI 产品进行设计的熟练开发人员使用。您将自行承担以下全部责任：(1) 针对您的应用选择合适的 TI 产品，(2) 设计、验证并测试您的应用，(3) 确保您的应用满足相应标准以及任何其他功能安全、信息安全、监管或其他要求。

这些资源如有变更，恕不另行通知。TI 授权您仅可将这些资源用于研发本资源所述的 TI 产品的相关应用。严禁以其他方式对这些资源进行复制或展示。您无权使用任何其他 TI 知识产权或任何第三方知识产权。您应全额赔偿因在这些资源的使用中对 TI 及其代表造成的任何索赔、损害、成本、损失和债务，TI 对此概不负责。

TI 提供的产品受 [TI 的销售条款](#) 或 [ti.com](#) 上其他适用条款/TI 产品随附的其他适用条款的约束。TI 提供这些资源并不会扩展或以其他方式更改 TI 针对 TI 产品发布的适用的担保或担保免责声明。

TI 反对并拒绝您可能提出的任何其他或不同的条款。

邮寄地址：Texas Instruments, Post Office Box 655303, Dallas, Texas 75265  
版权所有 © 2025，德州仪器 (TI) 公司